

INFORMATION TO USERS

This manuscript has been reproduced from the microfilm master. UMI films the text directly from the original or copy submitted. Thus, some thesis and dissertation copies are in typewriter face, while others may be from any type of computer printer.

The quality of this reproduction is dependent upon the quality of the copy submitted. Broken or indistinct print, colored or poor quality illustrations and photographs, print bleedthrough, substandard margins, and improper alignment can adversely affect reproduction.

In the unlikely event that the author did not send UMI a complete manuscript and there are missing pages, these will be noted. Also, if unauthorized copyright material had to be removed, a note will indicate the deletion.

Oversize materials (e.g., maps, drawings, charts) are reproduced by sectioning the original, beginning at the upper left-hand corner and continuing from left to right in equal sections with small overlaps. Each original is also photographed in one exposure and is included in reduced form at the back of the book.

Photographs included in the original manuscript have been reproduced xerographically in this copy. Higher quality 6" x 9" black and white photographic prints are available for any photographs or illustrations appearing in this copy for an additional charge. Contact UMI directly to order.

UMI

A Bell & Howell Information Company
300 North Zeeb Road, Ann Arbor MI 48106-1346 USA
313/761-4700 800/521-0600

NOTE TO USERS

The original manuscript received by UMI contains pages with indistinct and slanted print. Pages were microfilmed as received.

This reproduction is the best copy available

UMI

STUDY OF THE *CRYPTOSPORIDIUM*
PARVUM DHFR-TS IN THE MODEL SYSTEM
SACCHAROMYCES CEREVISIAE

by

Victoria Hertle Brophy

A dissertation submitted in partial fulfillment of the
requirements for the degree of

Doctor of Philosophy

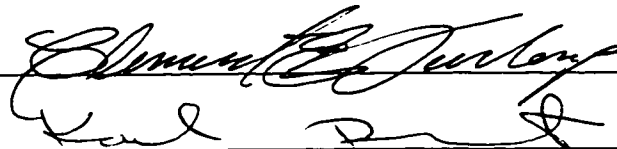
University of Washington

1998

Approved by



Chairperson of Supervisory Committee



Program Authorized
to Offer Degree

Genetics

Date

August 6, 1998

UMI Number: 9907885

UMI Microform 9907885
Copyright 1998, by UMI Company. All rights reserved.
This microform edition is protected against unauthorized
copying under Title 17, United States Code.

UMI
300 North Zeeb Road
Ann Arbor, MI 48103

Doctoral Dissertation

In presenting this dissertation in partial fulfillment of the requirements for the Doctoral degree at the University of Washington, I agree that the Library shall make its copies freely available for inspection. I further agree that extensive copying of this dissertation is allowable only for scholarly purposes, consistent with "fair use" as prescribed in the U.S. Copyright Law. Requests for copying or reproduction of this dissertation may be referred to University Microfilms, 1490 Eisenhower Place, P.O. Box 975, Ann Arbor, MI 48106, to whom the author has granted "the right to reproduce and sell (a) copies of the manuscript in microform and/or (b) printed copies of the manuscript made from microform."

Signature Victoria Hebble Bryson

Date August 6, 1998

University of Washington

Abstract

STUDY OF THE *CRYPTOSPORIDIUM*
PARVUM DHFR-TS IN THE MODEL
SYSTEM *SACCHAROMYCES CEREVISIAE*

by Victoria Hertle Brophy

Chairperson of the Supervisory Committee: Professor Carol Hopkins Sibley,
Department of Genetics

Cryptosporidium parvum is a ubiquitous protozoan that causes severe gastrointestinal disease. The severe diarrhea that results can be life-threatening, particularly for the very young, old, and immune-compromised. Currently there is no approved therapy for cryptosporidiosis. We have developed a method using the model organism *Saccharomyces cerevisiae* to rapidly screen for compounds effective against the *C. parvum* dihydrofolate reductase (DHFR) enzyme. The DHFR enzyme is essential and an effective drug target in other organisms. The yeast screening method has identified several compounds that are effective inhibitors of the *C. parvum* DHFR but also inhibit the human enzyme. Three related compounds have been identified in the yeast system that selectively inhibit the protozoal DHFR and not the human enzyme but are not extremely effective.

The yeast system was also used to investigate the functional differences between the native *C. parvum* bifunctional DHFR-TS (dihydrofolate reductase-

thymidylate synthase) enzyme and an engineered monofunctional DHFR domain alone. Yeast reliant on the DHFR-TS form show the expected synergy between trimetrexate, a DHFR inhibitor, and sulfanilamide, an inhibitor of dihydropteroate synthase (DHPS), another enzyme in the folate pathway. Yeast reliant on the *C. parvum* DHFR domain alone, however, did not show synergy between the two drugs. *In vitro* assays on purified enzyme revealed that the DHFR domain alone has a lower affinity than the DHFR-TS for trimetrexate and for the cofactor, NADPH. The DHFR domain alone also is much less stable and is a less efficient enzyme than its bifunctional counterpart.

TABLE OF CONTENTS

LIST OF FIGURES	iii
LIST OF TABLES	v
LIST OF ABBREVIATIONS	vii
INTRODUCTION	1
CHAPTER 1: SCREENING DHFR INHIBITORS FOR <i>CRYPTOSPORIDIUM</i>	
<i>PARVUM</i> SPECIFICITY USING <i>SACCHAROMYCES CEREVISIAE</i>	14
CHAPTER SECTION: INTRODUCTION	14
CHAPTER SECTION: EXPRESSION OF HETEROLOGOUS DHFR	
SEQUENCES IN <i>SACCHAROMYCES CEREVISIAE</i>	17
CHAPTER SECTION: OPTIMIZATION OF DRUG SENSITIVITY ASSAY....	26
CHAPTER SECTION: SCREENING OF POTENTIAL INHIBITORS OF <i>C.</i>	
<i>PARVUM</i> DHFR-TS	42
CHAPTER SECTION: DISCUSSION	50
CHAPTER 2: COMPARISON OF THE <i>CRYPTOSPORIDIUM PARVUM</i>	
BIFUNCTIONAL DHFR-TS TO THE ENGINEERED MONOFUNCTIONAL	
DHFR	59
CHAPTER SECTION: INTRODUCTION	59
CHAPTER SECTION: DIFFERENCES BETWEEN <i>C. PARVUM</i> DHFR AND	
DHFR-TS EXPRESSED IN YEAST	62
CHAPTER SECTION: PURIFICATION OF <i>C. PARVUM</i> DHFR AND DHFR-TS ..	68
CHAPTER SECTION: <i>IN VITRO</i> ASSAYS OF PURIFIED <i>C. PARVUM</i> DHFR	
AND DHFR-TS	75
CHAPTER SECTION: DISCUSSION	81
CHAPTER 3: CONCLUSIONS	89

CHAPTER 4: MATERIALS AND METHODS.....	93
CHAPTER SECTION: BACTERIAL AND YEAST CULTURE	93
Chapter subsection: strains	93
Chapter subsection: transformations	94
Chapter subsection: plasmid construction	94
Chapter subsection: promoter mutagenesis	99
Chapter subsection: sequence analysis	101
Chapter subsection: plasmid recovery	103
Chapter subsection: compounds	103
Chapter subsection: spoke assay	104
Chapter subsection: IC ₅₀ assay	104
Chapter subsection: complementation tests.....	106
CHAPTER SECTION: IN VITRO ASSAYS	107
Chapter subsection: yeast protein extracts.....	107
Chapter subsection: western analysis	107
Chapter subsection: <i>E. coli</i> overexpression and protein extracts	108
Chapter subsection: <i>in vitro</i> DHFR activity assays	109
Chapter subsection: optimization of enzyme activity in extracts	111
Chapter subsection: methotrexate affinity column purification	112
BIBLIOGRAPHY	114
APPENDIX A: CHEMICAL STRUCTURES OF TEST COMPOUNDS.....	125
APPENDIX B: EXPRESSION OF CD14 CORRECTS THE SLOW RESPONSE TO LIPOPOLYSACCHARIDE IN THE 1B8 MUTANT OF THE B CELL LYMPHOMA 70Z/3	130

LIST OF FIGURES

<i>Number</i>	<i>Page</i>
Figure 1: Life cycle of <i>Cryptosporidium parvum</i>	2
Figure 2: <i>Cryptosporidium parvum</i> morphological features.	4
Figure 3: Key enzymes and intermediates in the folate pathway.....	9
Figure 4: <i>Saccharomyces cerevisiae</i> strains.....	15
Figure 5: Complementation of the <i>dfr1</i> disruption by the <i>C. parvum</i> DHFR.....	22
Figure 6: Chemical structures.....	27
Figure 7: IC ₅₀ assay with trimetrexate.....	29
Figure 8: Western blot probed with an antibody directed against the <i>P. f.</i> DHFR....	31
Figure 9: IC ₅₀ assay with trimetrexate and the Cyc1 promoter.....	32
Figure 10: IC ₅₀ assay with trimetrexate and the truncated promoter.....	34
Figure 11: Promoter sequence.....	35
Figure 12: IC ₅₀ assay with various mutagenized promoters.....	36
Figure 13: Spoke assay on defined media lacking one C1 metabolite.....	38
Figure 14: Synergism between TMX and sulfanilamide.....	40
Figure 15: IC ₅₀ assay using sulfanilamide in the media.....	41
Figure 16: IC ₅₀ assays with NCI compounds 121146 and 112421.....	45
Figure 17: Sensitivity to NCI 106568/trimethoprim.....	46
Figure 18: IC ₅₀ assay with PY490.....	49
Figure 19: IC ₅₀ assay with trimethoprim analogs WR 3 and 6.....	52
Figure 20: IC ₅₀ assay with sulfanilamide.....	63
Figure 21: Isobologram diagram.....	65
Figure 22: Isobolograms for <i>C. parvum</i> DHFR and DHFR-TS.....	67
Figure 23: Isobologram for human DHFR.....	69

Figure 24: Isobologram for <i>P. falciparum</i> DHFR	70
Figure 25: Chemical structures.....	71
Figure 26: “IC ₅₀ ” assay of sulfanilamide and purified enzymes	78
Figure 27: Velocity dependence on enzyme concentration.....	82
Figure 28: Map of the yeast expression plasmid	95
Figure 29: Spoke assay diagram	105

LIST OF TABLES

<i>Number</i>	<i>Page</i>
Table 1: Comparison of amino acid changes that confer Pyrimethamine resistance in the <i>P. falciparum</i> DHFR to the analogous amino acids in the <i>C. parvum</i> DHFR.....	12
Table 2: Polymorphisms in the <i>C. parvum</i> DHFR sequence.....	16
Table 3: Confirmation of the identity of the yeast strains and complementation of the <i>dhfr1</i> disruption.	19
Table 4: Complementation of the yeast <i>dhfr1</i> disruption by the control DHFR enzymes.....	24
Table 5: Yeast strains used in this work.....	25
Table 6: Drug sensitivity to NCI compounds.....	43
Table 7: Drug sensitivity to Dana-Farber compounds.....	48
Table 8: Drug sensitivity to WRAIR trimethoprim analogs.....	51
Table 9: Sample data used for plotting isobologram..	66
Table 10: Comparison of codon preferences in <i>E. coli</i> and <i>C. parvum</i>	74
Table 11: Kinetics of the purified <i>C. parvum</i> DHFR and DHFR-TS.....	76
Table 12: Representative data of TMX and sulfanilamide <i>in vitro</i> inhibition of the <i>C. parvum</i> DHFR.....	79
Table 13: Representative data of TMX and sulfanilamide <i>in vitro</i> inhibition of the <i>C. parvum</i> DHFR-TS.....	80
Table 14: Summary of TMX and sulfanilamide interactions with the <i>C. parvum</i> DHFR and DHFR-TS	80
Table 15: Plasmids used in the yeast assays.....	93
Table 16: PCR primers.....	97

Table 17: PCR cycling conditions.....	99
Table 18: Plasmids generated during this work..	101

LIST OF ABBREVIATIONS

Ade. Adenine

Arg. Arginine

C. C yeast media; synthetic, defined, and complete

C.p. *Cryptosporidium parvum*

CDC. Centers for Disease Control

D. D yeast media, rich and complete

DHF. Dihydrofolate

DHFR. Dihydrofolate reductase

DHFS. Dihydrofolate synthase

DHPS. Dihydropteroate synthase

dTMP. Deoxythymidine

DTT. Dithiothreitol

EDTA. Ethylenediaminetetraacetic Acid

His. histidine

IC₅₀. Concentration at which growth is inhibited 50%

Met. methionine

NCI. National Cancer Institute

P.c. *Pneumocystis carinii*

P.f. *Plasmodium falciparum*

pABA. Para-aminobenzoic acid

PCR. Polymerase chain reaction

PMSF. Phenylmethanysulfonyl Fluoride

PyrR. Pyrimethamine resistant

PyrS. Pyrimethamine sensitive

S.c. *Saccharomyces cerevisiae*

Ser. Serine

T.g. *Toxoplasma gondii*

THF. Tetrahydrofolate

TMP. Trimethoprim

TMX. Trimetrexate

TS. Thymidylate synthase

WRAIR. Walter Reed Army Institute for Research

ACKNOWLEDGMENTS

The author wishes to thank her advisor, Carol Hopkins Sibley, and the other members of her committee, Robert Braun, Karol Bomsztyk, Walton Fangman, Clement Furlong, Colin Manoil, and Christopher Wilson for their advice and assistance. The author also wishes to thank the present and former members of the Sibley laboratory: Matthew Breeze, Kelly Hamilton, Eleanor Hankins, Erik Jacobs, Owen Lawrence, Somnath Mookherjee, Whitney Neufeld-Kaiser, Sarah Pownder, Linda Rhodes, Greg Satvinit, and Jason Wooden for valuable advice and for making the laboratory an enjoyable place. All of the members of the Genetics Department were instrumental in the timely completion of this work. Dr. Jean Campbell also provided valuable assistance. The author also thanks her brother Mark Hertle, her parents, Joseph Hertle, Victoria McCoy, and Guy McCoy and her husband Bruce Brophy for their encouragement and support.

DEDICATION

The author wishes to dedicate this dissertation to her parents, Joseph Hertle, Victoria McCoy, and Guy McCoy for providing the education, moral support and encouragement that allowed her to complete this work. Without them, the author may not have attempted this degree.

INTRODUCTION

Protozoa of the genus *Cryptosporidium* were first described by Clarke (Clarke, 1895) and Tyzzer (Tyzzer, 1907) at the turn of the century. *Cryptosporidia* are protozoa of the phylum *Apicomplexa*, class *sporozoa* and are related to human pathogens such as *Plasmodium falciparum* (malaria) and *Toxoplasma gondii*, an opportunistic parasite (Despommier and Karapelou, 1987). *Cryptosporidium parvum* (*C.p.*) was identified as a human pathogen in 1976 (Meisel *et al.*, 1976; Nime *et al.*, 1976). This species infects not only humans but also an unusually wide variety of mammals and other animals, causing gastrointestinal disease, with the primary symptom being severe diarrhea (O'Donoghue, 1985). The disease is self-limiting in immune-competent people, but is chronic, severe, and may be lethal in the immune-deficient (Guerrant, 1997; Hoepelman, 1996). At present, there is no therapy for *C. parvum* infection beyond treating the symptoms. As monitoring for the organism improves, the widespread prevalence and potential threat to the population is becoming better recognized (Guerrant, 1997; Hellard *et al.*, 1997; Rose, 1997). The organism is difficult to culture, preventing rapid screening of potential drugs (Richard Nelson, personal communication). The work described here avoids the culture difficulties by using the model organism *Saccharomyces cerevisiae* for development of a recombinant genetic system for studying *C. parvum* enzymes. This yeast system has been designed with the goal of identifying potential inhibitors effective against the *C. parvum* enzyme dihydrofolate reductase (DHFR).

The *C. parvum* life cycle is depicted in Figure 1 (Current, 1989; O'Donoghue, 1985). Infection begins when *Cryptosporidium parvum* oocysts are ingested (Figure 1-1a, 1b). Each spherical oocyst measures 4 to 5 μm in diameter and is surrounded by five membranes. This oocyst is very durable and can survive months

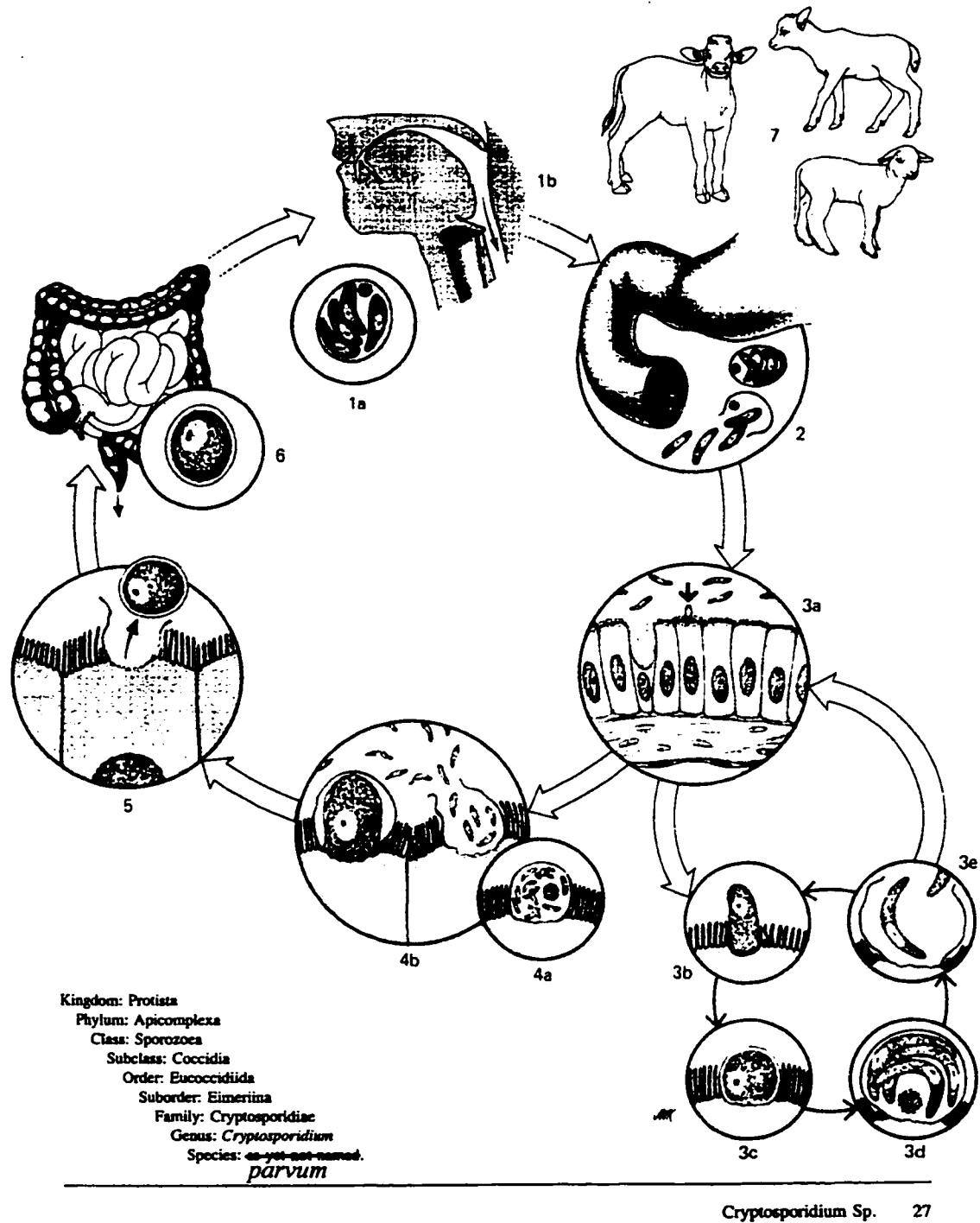


Figure 1: Life cycle of *Cryptosporidium parvum*. Stages are described in the text. From Despommier, D.D. and Karapelou, J.W., Parasite Life Cycles, Springer-Verlag, London, 1987.

in the environment and can withstand severe disinfection conditions. Within each oocyst are four haploid sporozoites, each of which can infect an intestinal epithelial cell (Figure 2). Once in the favorable environment of the small intestine, a suture on one side of the oocyst opens and the sporozoites excyst and infect the epithelial cells (Figure 1-2). Protozoal sporozoites are generally protected within a sporocyst inside of the oocyst. A distinguishing feature of *C. parvum* is that the sporozoites are naked and do not have this covering. *C. parvum* resides inside the host cells, but outside of the host cytoplasm. The host cell membrane is stimulated to reach up to envelope the parasite inside a parasitophorous vacuole, separated from the host cytoplasm by a lamella and an adhesion zone. The lamella is formed by folding of the pellicle and the adhesion zone comes from a fusion of the microvillus and plasma membranes (Figure 2). Inside the epithelial cells, the sporozoites undergo asexual replication (merogony). Each sporozoite divides to form eight type I merozoites (Figure 1-3). The merozoites burst out of the epithelial cells and infect new host cells. Type I merozoites repeat this cycle, producing eight progeny each round. Some type I merozoites produce progeny of type II; upon infecting new host cells, type II merozoites differentiate into macrogametes or microgamonts. Each microgamont divides to form 16 microgametes, which then burst out of the cell and fertilize the macrogametes (Figure 1-4). The zygote then undergoes meiosis and forms four sporozoites and an oocyst (Figure 1-5). Two types of oocysts are generated: a soft oocyst and a resistant oocyst. The soft oocysts reinfect the host, while the resistant ones leave the host in the feces and start the cycle again in another host (Figure 1-6).

Human infections usually result from contaminated drinking or recreational water although person-to-person contact transmits the parasite as well (Guerrant, 1997; Hoepelman, 1996). Contaminated fruits and vegetables have also been shown to spread the disease (Anonymous, 1997; Ortega *et al.*, 1997). Daycare centers are common sites of small outbreaks. The largest outbreak on record occurred

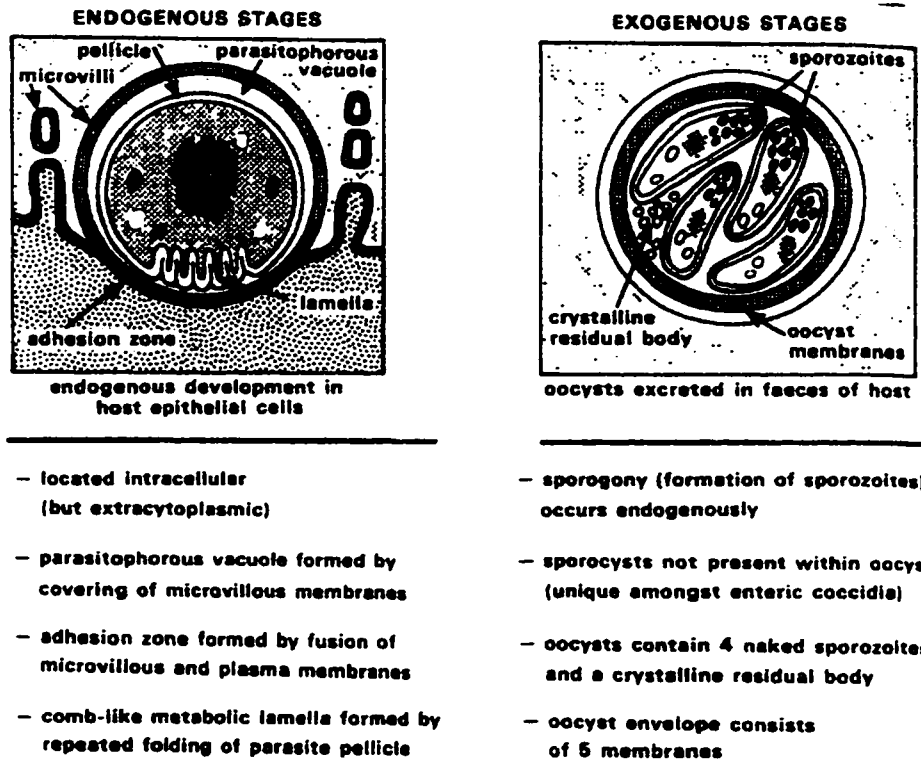


Figure 2. *Cryptosporidium parvum* morphological features. From *Cryptosporidium* infections in man, animals, birds and fish. O'Donoghue, P. J. (1985). *Cryptosporidium* infections in man, animals, birds and fish. Australian Veterinary Journal 62, 253-8.

in 1993 when 400,000 people in Milwaukee, Wisconsin (half of the population) became sick from *C. parvum* infection (MacKenzie *et al.*, 1994). Over one hundred people died as a result of this outbreak. The source of the oocysts was traced to the municipal water supply, although the reason for the high degree of contamination was never satisfactorily determined. Recently, the Centers for Disease Control (CDC) has determined that the oocysts were of human origin, not dairy cows as had been postulated (CDC, 1997).

A wide variety of animals can be infected with this parasite and shed oocysts into the environment (Dubey *et al.*, 1990). Although humans of any age may be infected, animals are primarily susceptible as neonates (O'Donoghue, 1985). Adult mice are known to be resistant to infection (Sherwood *et al.*, 1982). However, the wide host range and durability of the oocysts ensures that the organism remains widespread. The oocysts are washed into the surface water that becomes drinking water for the populations downstream. Closing watersheds offers protection from human-borne disease but not from the high frequency of animal-borne oocysts. A study that monitored 67 surface water sites in the eastern US found that 60% of the 347 samples taken were positive for *C. parvum* (LeChevallier and Moser, 1993; LeChevallier *et al.*, 1991). In addition, outbreaks have resulted from contaminated well water, indicating that the small oocysts can move through the soil. Due to the small size of the oocysts, flocculation and sand filtration, two common methods of water treatment plants to remove particulates from water, fail to completely remove *C. parvum* (Guerrant, 1997; Rose, 1997). The oocysts are extremely resistant to disinfection treatments. Standard disinfection methods such as chlorine bleach fail to inactivate the oocyst. In fact, oocysts have been found to be viable after two hours in 100% bleach. Thus, current water treatment rarely removes the organism. Treatment of the water with ozone will inactivate the oocysts and some municipalities are starting to upgrade their treatment facilities to do this. Membrane filtration will also

remove *C. parvum*, but both are expensive alternatives. Alternatively, boiling potentially contaminated water for five minutes will inactivate the oocysts.

The primary symptom of cryptosporidiosis is large amounts of watery diarrhea that can be so copious that it resembles cholera. Additional common symptoms are abdominal pain, nausea, fever and fatigue (MacKenzie et al., 1994; Marshall *et al.*, 1997). Since no therapy to eliminate the infection is available, treatments try to relieve the diarrhea, attempting to reduce dehydration and electrolyte imbalance. In individuals with a healthy immune system, the severity of disease varies widely. Many people are seropositive for *C. parvum* but are not aware that they have ever been infected, implying that symptoms were minimal or non-existent. If significant disease does result, symptoms can last from a few days up to two weeks (Jokipii and Jokipii, 1986). Fortunately, most people's immune systems are able to resolve the infection. People who have compromised immune systems, however, are defenseless against the parasite. Immune deficiency due to AIDS, transplant immune suppression and diseases such as cancer and its treatment leaves patients vulnerable to severe infection. The infection cannot be cured unless the immune function returns to sufficient levels. As the symptoms can be severe, death is often hastened as a result of *C. parvum* infection. As the number of people suffering from immune deficiency rises, the incidence of severe *Cryptosporidium* infection will rise too.

Studies of non-immunocompromised young adults in Virginia, Texas, and Wisconsin and Peace Corps volunteers before travel showed that 17 to 32% of the individuals were seropositive for *C. parvum* (Ungar *et al.*, 1989). Clearly, the prevalence of *C. parvum* in the U.S. is high enough that infection is a common occurrence. *Cryptosporidium* is an even larger problem in developing countries. In a rural area of China, more than half of the children had seroconverted by age 5. In a poor area of Brazil, more than 90% of the children are seropositive by one year of age

(Ungar *et al.*, 1988). Many of these children spend much of their first years suffering from diarrhea. As a consequence, they grow slowly and have an increased likelihood of other illnesses. Gastrointestinal illnesses are the largest single cause of death in small children worldwide. *C. parvum* is only one of many pathogens responsible, but it is clear that its impact on world health is substantial.

It is believed that incidence of *C. parvum* infection is underdiagnosed in healthy individuals, indicating that the parasite is more prevalent than previously thought. A U.S. Department of Agriculture study found that more than 90% of dairy herds were infected (Anonymous, 1993a; Anonymous, 1993b). Since human infection can result from bovine derived oocysts, these herds pose a significant risk to the water supply. In addition, since the oocysts can be passed from person to person, situations such as AIDS wards at hospitals may amplify the incidence of disease. *C. parvum* is estimated to cause 10-15% of chronic diarrhea in HIV cases in the US and 30-50% in developing countries (Colebunders *et al.*, 1987; Laughon *et al.*, 1988). In one case, 45% of workers caring for an infected AIDS patient seroconverted and thus had been exposed to the parasite (Koch *et al.*, 1985). The extreme difficulty of disinfection makes passage of the disease easier.

C. parvum is very difficult to maintain in the laboratory. It may be grown in animals, but they must be either neonates or severely immunocompromised. Even with these conditions, the animals are often not very ill and progression of disease must be monitored by counting the number of oocysts shed in the feces, a laborious process (Harp *et al.*, 1996; Lemeteil *et al.*, 1993). Cell culture systems have recently been devised, but these are imperfect as well (McDonald *et al.*, 1990; Woods *et al.*, 1995; Yang *et al.*, 1996). A monolayer of mammalian epithelial cells is incubated with oocysts that have been treated to stimulate them to excyst. The sporozoites infect the cells and divide, but in most culture systems the oocyst stage of

the life cycle cannot be produced and in all cases the infections only persist for 48 to 72 hours. Although less labor intensive than the culture in animals, the cell culture system is complex and progress is slow. The data generated on sensitivity to potential drugs tend to be difficult to quantitate. The difficulties involved in maintaining *C. parvum* in the lab have largely contributed to the lack of progress in finding therapies.

We have devised a strategy to rapidly screen for compounds effective against a *C. parvum* drug target without actually growing the parasite. In recent years, the conservation of gene sequence and function among distantly related organisms has become better recognized. Widely divergent organisms have been found to express remarkably similar proteins and the proteins often perform the same or similar functions. *Saccharomyces cerevisiae* are eukaryotic, single-celled yeast that are well-suited to experimentation. They have been well studied and myriad genetic and molecular techniques have been developed for manipulation of this organism. The entire genome has been sequenced and is available on the Internet (<http://genome-www.stanford.edu/Saccharomyces>), expanding experimental possibilities considerably. I have expressed *C. parvum* dihydrofolate reductase (DHFR) in yeast and developed a system to screen for drugs that inhibit this *C. parvum* protein. We chose this protein from *C. parvum* because it is highly functionally conserved and is an excellent drug target in other organisms.

The dihydrofolate reductase enzyme (E.C. 1.5.1.3) is an oxidoreductase in the folate synthesis pathway (Figure 3). In the folate pathway, dihydropteridine is condensed with para-aminobenzoic acid (pABA) by the enzyme dihydropteroate synthase (DHPS; E.C. 2.5.1.15) to form dihydropteroate. Dihydropteroate is then combined with L-glutamate to form dihydrofolate (DHF). In the next step of the pathway, DHFR catalyzes the transfer of two hydrogens from NADPH to DHF to form tetrahydrofolate (THF) and NADP. THF is modified in one of several ways by

Folate Pathway

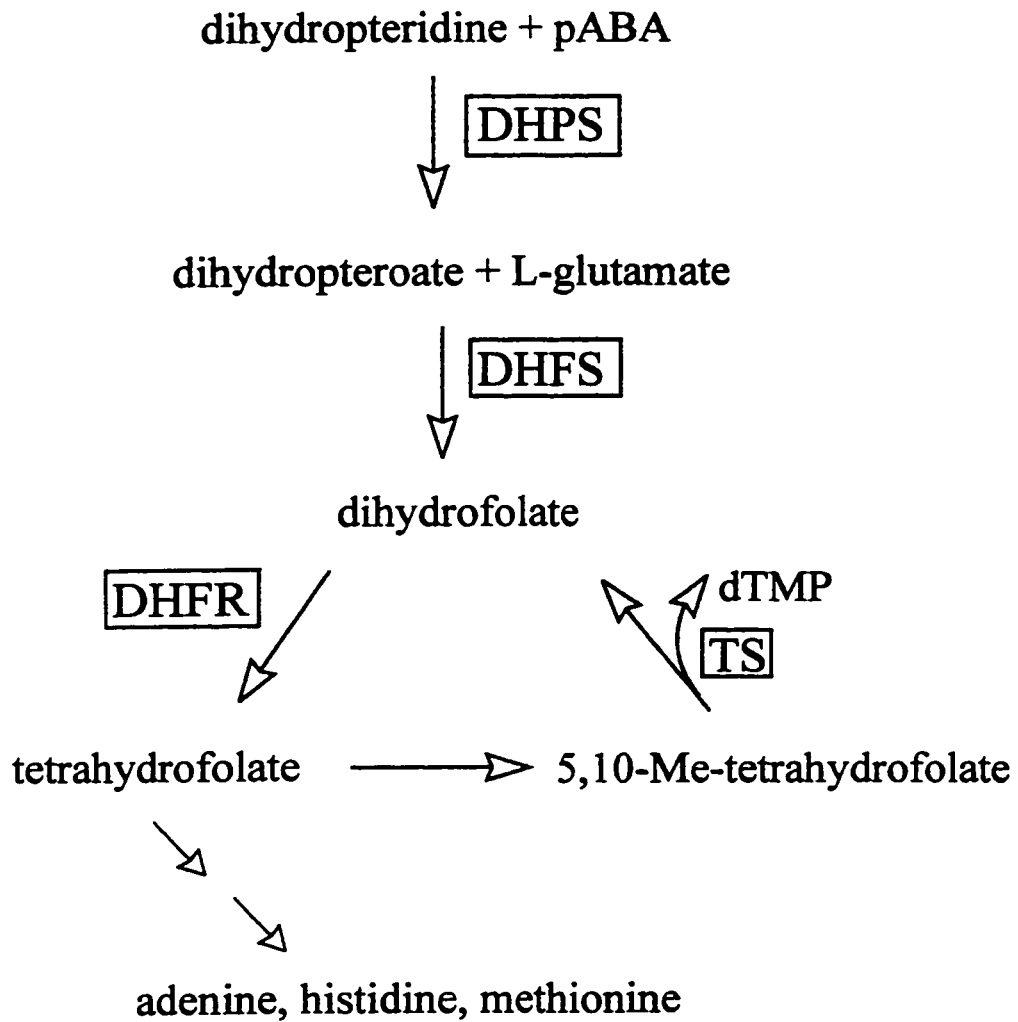


Figure 3: Key enzymes and intermediates of the folate pathway. DHPS, dihydropteridine synthase; DHFS, dihydrofolate synthase; DHFR, dihydrofolate reductase; TS, thymidylate synthase; dTMP, deoxythymidine.

addition of methyl group derivatives and used for making crucial metabolites. In yeast, these metabolites are adenine, methionine, histidine, and deoxythymidine (dTMP) (Little and Haynes, 1979). Other organisms require THF for generating serine or glycine as well. DHFR function is required in every organism, from bacteria to humans, and the enzyme catalyzes the same reaction in each species. Blocking DHFR function compromises the ability to synthesize these four nutrients, resulting in growth inhibition and death (Sirotnak, 1984). Although the DHFR coding sequence varies greatly from species to species, crystal structures of divergent DHFRs have revealed that the three-dimensional structure is highly conserved (Blakley, 1995). However, slight differences of spacing in the active site have been detected, explaining the existence of drugs that inhibit the DHFR of one species (the pathogen) but not another species (the patient). Because of slight steric differences, a compound may bind strongly in the active site of some DHFR enzymes while binding poorly or not at all in other active sites. This fact has been exploited for decades as chemotherapy against bacteria (trimethoprim, for example) and protozoal infections (pyrimethamine for malaria).

Inhibitors of the folate pathway have been known since the mid 1930's, when the pathway was first being elucidated (Stokstad and Jukes, 1987; Welch, 1983). Sulfanilamide, an inhibitor of DHPS, was the first to be discovered and it was the study of this compound that led to identification of pABA. It was quickly realized that while bacteria are sensitive to sulfanilamide and its relatives, animals are not (they lack the DHPS enzyme). This attribute makes the sulfa class of inhibitors excellent candidates for treating human infections. By 1947, inhibitors of DHFR had been synthesized. The first of these, x-methyl folic acid, was not very effective, but it led to aminopterin, which was tested on childhood leukemia with some success. This led to methotrexate, a better and less toxic inhibitor that has been used for cancer chemotherapy. Substitutions on the aminopterin/methotrexate backbone led to the

identification of pyrimethamine (an anti-malarial) and trimethoprim (an anti-bacterial) in the late 1940's and early 1950's. It was also discovered during this era that DHFR and DHPS inhibitors act synergistically when used concurrently. Since these early years, thousands of DHFR and DHPS inhibitors have been synthesized and wait to be tested on enzymes from various species.

In protozoa and plants, the DHFR enzyme activity is catalyzed by the amino terminal domain of a bifunctional protein with thymidylate synthase (TS, E.C. 2.1.1.45) catalyzed by the carboxyl terminal domain. The two domains are separated by a flexible junction domain. In other organisms, the DHFR and TS genes and proteins are separate entities. The TS enzyme uses 5,10-methyl tetrahydrofolate to generate dTMP and DHF. Since DHF is the substrate for DHFR, it is believed that the DHF generated by TS is channeled across the bifunctional enzyme to the DHFR domain. There is little evidence that this channeling actually occurs (Knighton *et al.*, 1994), but the presumed advantage that results is often cited as the explanation for the bifunctional arrangement.

A few DHFR inhibitors have been tested on *Cryptosporidium parvum* parasites in culture, but either the efficacy was poor or toxicity to host cells was high (McDonald et al., 1990; Woods *et al.*, 1996). *In vitro* studies with purified DHFR have revealed that compounds such as pyrimethamine (pyr), potent inhibitors of other apicomplexan protozoans (e.g. malaria and *Toxoplasma gondii*), do not inhibit the *C. parvum* enzyme at all (John Vasquez, personal communication). In *Plasmodium falciparum*, pyrimethamine resistance is generated by point mutations in the coding sequence that result in amino acid changes in the protein. Enzymes containing the amino acid changes show less inhibition by pyrimethamine. For instance, mutation of Ser 108 to Asn confers slight resistance. A second mutation at position 51 from Asn to Ile results in stronger resistance (Cowman *et al.*, 1988; Peterson *et al.*, 1988;

Sirawaraporn *et al.*, 1993; Zolg *et al.*, 1989). Vasquez and his colleagues (Vasquez *et al.*, 1996) have noted that the sequence of the *C. parvum* enzyme contains the amino acids expected of pyrimethamine resistant *P.f.* DHFR at the positions analogous to 51, 108 and possibly 164 in the *P.f.* enzyme (Table 1). Position 164 in *P.f.* DHFR is very sensitive to a change in amino acid and the Cys present in *C. parvum* may confer resistance to pyrimethamine. The authors have postulated that *C. parvum* is not sensitive to Pyr because it naturally has the amino acids selected by drug pressure in the *P.falciparum* population. If this is, in fact, the case, then DHFR inhibitors already characterized for other protozoal infections would likely not work on *C. parvum*. Therefore, a larger screening effort is required so that more novel compounds can be tested. Although this is difficult, slow and laborious in *C. parvum* cell culture or with purified enzyme, the yeast system provides an easy and quick system for screening of far more compounds than the alternative systems.

Table 1: Comparison of amino acid changes that confer pyrimethamine resistance in the *P. falciparum* DHFR to the analogous amino acids in the *C. parvum* DHFR

<i>P.f.</i> Codon	<i>P.f.</i> Wild Type Seq.	<i>P.f.</i> Resistant Seq.	<i>C. parvum</i> Amino Acid	<i>C. parvum</i> Codon
16	Ala	Val	-	-
51	Asn	Ile	Ile	30
59	Cys	Arg	Ser	38
108	Ser	Thr/Asn	Thr	59
164	Ile	Leu	Cys	113

Cryptosporidium is a ubiquitous organism and can be found in soil and water. Since *C. parvum* has the ability to infect many and varied species of animals and the infectious stage is very durable, the protozoan is difficult and expensive to

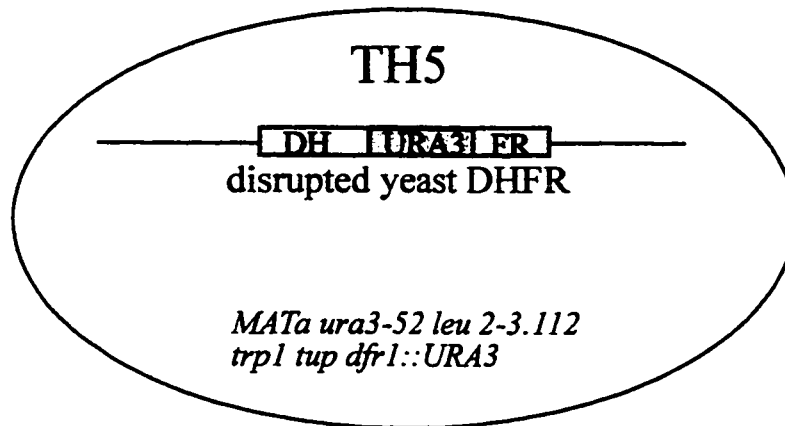
exclude from the public water supply. Cryptosporidiosis is a hazard to the immune-competent population and a life-threatening disease for immune-compromised people. A treatment must be found to lessen or eliminate the suffering caused by this disease. Expression of the *Cryptosporidium parvum* DHFR in the yeast system allows us to conduct experiments related to drug development that are not feasible to carry out with the organism itself. We can study the activity of the enzyme, rapidly screen inhibitors of the enzyme without the difficulties of cell culture, and generate more quantitative data than is possible with current culture methods. Potential drugs that are identified through use of this system could then be subjected to testing on actual parasites.

CHAPTER 1: SCREENING DHFR INHIBITORS FOR *CRYPTOSPORIDIUM* *PARVUM* SPECIFICITY USING *SACCHAROMYCES CEREVISIAE*

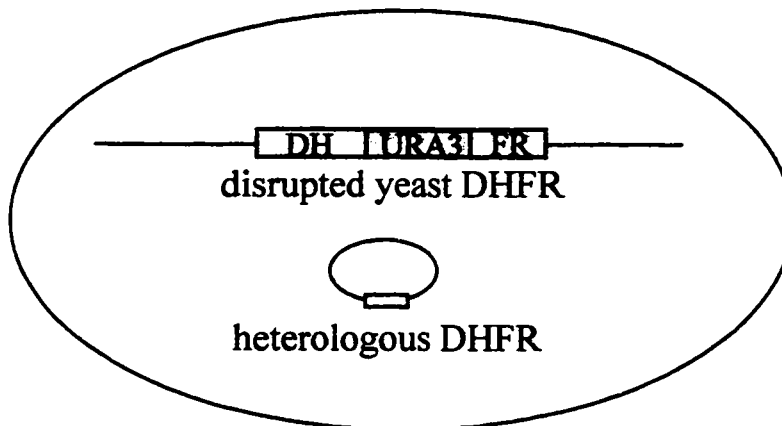
CHAPTER SECTION: INTRODUCTION

The parent *S. cerevisiae* strain used in these studies is designated TH5 and was a gift from Tun Huang (Huang *et al.*, 1992). TH5 (MAT a *trp1 ura3.112 leu2 tup1 dfr1::Ura3*) has its endogenous DHFR gene, *dfr1*, disrupted by *Ura3*. As a result, these cells are auxotrophic for the C1 metabolites adenine, methionine, histidine, and thymidylate (dTMP). Maintenance of the TH5 strain requires supplementation with these four nutrients but yeast are normally not permeable to dTMP. To overcome this, Huang and colleagues selected a mutant, *tup1*, that transported sufficient dTMP to allow growth of the DHFR deficient strain. The lesion is a point mutation in a gene that encodes a transcription factor involved in glucose regulation (Trumbly, 1992). The mechanism by which a mutation in this transcription factor allows dTMP uptake is not understood. The mutation is extremely pleiotropic; other consequences are poor mating, a somewhat elongated cell morphology, and slight flocculation in liquid cultures.

Expression of a heterologous DHFR in this yeast strain obviates the need for supplementation of the C1 metabolites since they are no longer auxotrophic for adenine, methionine, histidine and dTMP. Additionally, the yeast should now display the anti-folate drug sensitivity expected of the foreign DHFR (Figure 4). For instance, Jason Wooden showed that yeast expressing the endogenous DHFR are unaffected by high concentrations of pyrimethamine, but yeast dependent on low level expression of the *Plasmodium falciparum* DHFR are very sensitive to this antimalarial drug (Wooden *et al.*, 1997). We hypothesized that this situation would obtain for the



**No DHFR activity
Requires supplementation**



**Heterologous DHFR activity
Grows without supplementation
Sensitive to antifolates that
inhibit the heterologous DHFR**

Figure 4. *Saccharomyces cerevisiae* strains. TH5 is the parent strain used in these studies. Expression of a heterologous DHFR in TH5 relieves the DHFR deficiency and confers species-specific sensitivity to DHFR inhibitors.

Cryptosporidium parvum DHFR and that the yeast expressing this DHFR could be used to screen for potential inhibitors of this parasite. A yeast screen would allow for rapid testing of the thousands of anti-DHFR inhibitors that have been generated over the decades, a feat that is impractical to accomplish with the parasite itself.

Cryptosporidium is considered a zoonosis; human infection can result from contact with an infected animal's feces (Rose, 1997). At present, human infections are believed to primarily originate from two sources: bovines and humans. John Vasquez cloned the *C. parvum* DHFR-TS from two cDNA libraries (Vasquez et al., 1996). One library was generated from *Cryptosporidium* oocysts isolated from a human (Genbank accession U41366), the other from a calf (accession U41365). The sequence of the DHFR genes from these two isolates were not identical. Eleven nucleotides and nine amino acid differences were found in the two DHFR genes (Table 2). None of the polymorphisms occur in residues implicated in drug resistance in the analogous positions of the *P. falciparum* DHFR. We cannot rule out the possibility, however, that these differences may confer a variance in drug susceptibility. Accordingly, the yeast screen will include the DHFR from both the human and bovine isolates of *C. parvum*.

Table 2: Polymorphism in the *C. parvum* DHFR sequence. None are residues analogous to those implicated in drug resistance in *P. falciparum*.

	Human isolate	Bovine isolate
codon	amino acid	amino acid
3	E	K
17	S	R
41	N	S
43	K	N
71	I	K
89	V	I
99	E	K
106	S	T
174	I	V

CHAPTER SECTION: EXPRESSION OF HETEROLOGOUS DHFR SEQUENCES IN *SACCHAROMYCES CEREVISIAE*

The first step in this work was expressing the DHFR from the *C. parvum* human isolate in the TH5 yeast strain and determining whether that enzyme was able to complement the *S. cerevisiae* DHFR activity. I obtained the *C. parvum* DHFR-TS sequence as a cDNA cloned into the pET9d *E. coli* expression vector (a gift from John Vasquez). In order to express this sequence in yeast, the *C. parvum* gene was transferred to our yeast expression vector pEH2. The *C. parvum* gene was cloned into the vector in two forms; one includes the entire DHFR-TS to just after the stop codon and another that includes the DHFR and part of the junction sequence only, leaving the protein devoid of TS sequence and enzyme activity.

I also cloned the human DHFR sequence (Genbank accession U00140) into pEH2 in the same manner. The human DHFR sequence was a gift from John Vasquez and serves the purpose of determining the specificity of test compounds. For therapeutic use, a drug must inhibit the *C. parvum* DHFR but not the human DHFR. Thus, the expression of the human DHFR in the yeast allows us to identify those compounds that are specific for the parasitic DHFR. The human gene contains only the DHFR sequence and the entire coding region was used for the construct.

The plasmids were transformed into the *Saccharomyces cerevisiae* strain TH5 by a lithium acetate protocol (Ito *et al.*, 1983). Transformants were selected on yeast plates containing defined synthetic media supplemented with dTMP but lacking tryptophan (C-trp) so that DHFR function was not required but presence of the *Trp1* gene on the plasmid was required. Transformants were patched onto rich media containing dTMP. After growth at 30°C, the patch plates were double replica

plated (see methods) to rich media lacking dTMP. In order to grow on this media, the yeast must express sufficient levels of functional DHFR to provide dTMP. The yeast strains expressing the *C. parvum* DHFR and DHFR-TS coding sequences were able to grow in the absence of exogenous dTMP, indicating that the *dfr1* deficiency is complemented by the heterologous DHFR enzymes (data not shown). Both constructs complemented the deficiency equally well, indicating that the DHFR domain can function in the absence of the TS domain. The construct containing the human DHFR was transformed into TH5 and it also complemented the deficiency well.

The transformed yeast may be able to grow without supplementation for a trivial reason – the yeast may be a contaminant and possess an endogenous DHFR. I used several methods to determine if this was the case. First I checked the strain markers of the transformed yeast using replica plating. TH1 has the endogenous yeast DHFR gene expressed from the chromosome and does not require supplementation with any of the C1 metabolites. TH5 was able to grow in the absence of uracil despite the mutation in the chromosomal *ura3* because *dfr1* has been disrupted with a functional *URA3*. TH5 was not able to grow on leucine-minus plates, but once transformed with a tryptophan gene containing plasmid, it was able to grow on plates lacking tryptophan. I replica plated the yeast strains onto C - leu, C - ura, and C - trp media and observed the expected growth phenotypes, verifying that the strain that I transformed was TH5 (Table 3). To test the identity of the strain further, I streaked the *C. parvum* DHFR and DHFR-TS strains on rich media containing dTMP. This medium does not select for the plasmid and, in the absence of selection, a percentage of the yeast lose the plasmid with each round of replication. After two successive streaks, I streaked two colonies onto rich media lacking dTMP. The parent strain, TH5, is not able to grow on this media and likewise, the colonies were not able to grow. This experiment indicates that given the opportunity to lose the plasmid, the cells revert to a dTMP-requiring status and are therefore TH5. It also demonstrates

Table 3: Confirmation of the identity of the yeast strains and complementation of the *dhfr1* disruption. Each yeast strain was replica plated onto the specified media. Growth is indicated by +, no growth by -. The ability of the strains to grow on the various media matched expectations based on strain genotypes.

Origin of DHFR	Yeast Strain Marker Verification						Complementation Testing			
	C-Ura	C-Leu	C-Trp	C	D		C-Ade	C-Met	C-His	D-dTMP
<i>S.c.</i> on chromosome(TH1)	-	-	-	+	+		+	+	+	+
none (untransformed TH5)	+	-	-	+	+		-	-	-	-
Human	+	-	+	+	+		+	+	+	+
<i>C.p.</i> DHFR, human isolate	+	-	+	+	+		+	+	+	+
<i>C.p.</i> DHFR-TS, human isol.	+	-	+	+	+		+	+	+	+

all plates contain 100 µg/ml dTMP unless otherwise noted

that the ability to grow in the absence of supplemented dTMP is due to the presence of the plasmid.

In order to verify that the yeast are indeed expressing the proper plasmid, I recovered the plasmids from the cells. Yeast DNA (genomic and plasmid) was prepared by the Smash and Grab glass bead disruption method (Hoffman and Winston, 1987) and the DNA transformed into *E. coli*. Only the plasmid will confer ampicillin resistance, thus only bacteria transformed by the plasmid will grow on ampicillin-containing plates. Plasmid from the resulting colonies were analyzed by restriction analysis. I also verified the presence of the plasmids by PCR on the Smash and Grab DNA. The primers were specific for the DHFR and DHFR-TS regions and amplified sequences of the expected sizes; the results confirmed that the correct heterologous DHFR sequences were present in the yeast. Transformation of the plasmids into fresh TH5 also confirmed the complementation.

All of these tests to verify that the plasmid did indeed contain the *C. parvum* DHFR coding sequence and that the yeast were TH5 may seem excessive. However, as described below, we initially had difficulty obtaining the expected response from the yeast expressing the *C. parvum* and human DHFR enzymes. These various preliminary strain tests gave us confidence that the difficulty was operational and not due to contamination.

The product of DHFR is tetrahydrofolate, which is required for the production of C1 carbons used to generate dTMP, adenine, methionine, and histidine (Little and Haynes, 1979). If the heterologous DHFR was fully complementing the disruption, then the yeast should have been able to grow without supplementation of any of these four nutrients. By replica plating onto defined complete media lacking one nutrient (C - met, C - ade, C - his, and C - dTMP plates), I verified that my transformants were able to grow without these supplements. Therefore the *C. parvum*

and human DHFR proteins were fully complementing the disrupted DHFR activity (Table 3).

TH5 and TH5 expressing the *C. parvum* DHFR were streaked on several defined media plates (Figure 5). These plates showed that while untransformed TH5 were unable to grow without supplementation of the C1 metabolites, the strain expressing *C. parvum* DHFR was able to grow. Serine synthesis requires tetrahydrofolate (THF) in some organisms (e.g. humans), but yeast can make serine through another biosynthetic pathway. The C - ser plate verified that the TH5 yeast do not require serine (all plates are supplemented with dTMP). Additionally, arginine synthesis does not require THF; the C - arg plate demonstrated that the nutritional requirements are specific for the folate pathway.

No detectable differences had been observed between the *C. parvum* DHFR and DHFR-TS expressing strains (data not shown). Since the *C. parvum* DHFR-TS complemented just as well as the DHFR domain alone, we chose to continue the work with the bifunctional protein because it is the natural form of the enzyme. Further work with the *C. parvum* DHFR domain alone is described in the chapter on synergy.

As mentioned in the introduction, *C. parvum* from calves are a source of human infection. Since the DHFR domains differ by several amino acids (Table 2), both isolates must be tested with potential drugs. Therefore, I also cloned DHFR-TS from the bovine isolate *C. parvum* into the yeast vector for use in the drug screening assays.

The goal of this work was to develop a screen to identify inhibitors of the *C. parvum* DHFR. For the screen to be successful, we needed to be able to differentiate among effects that were non-specific for DHFR, non-specific for *C. parvum*, and compounds that could not enter the cells. To that end, several control

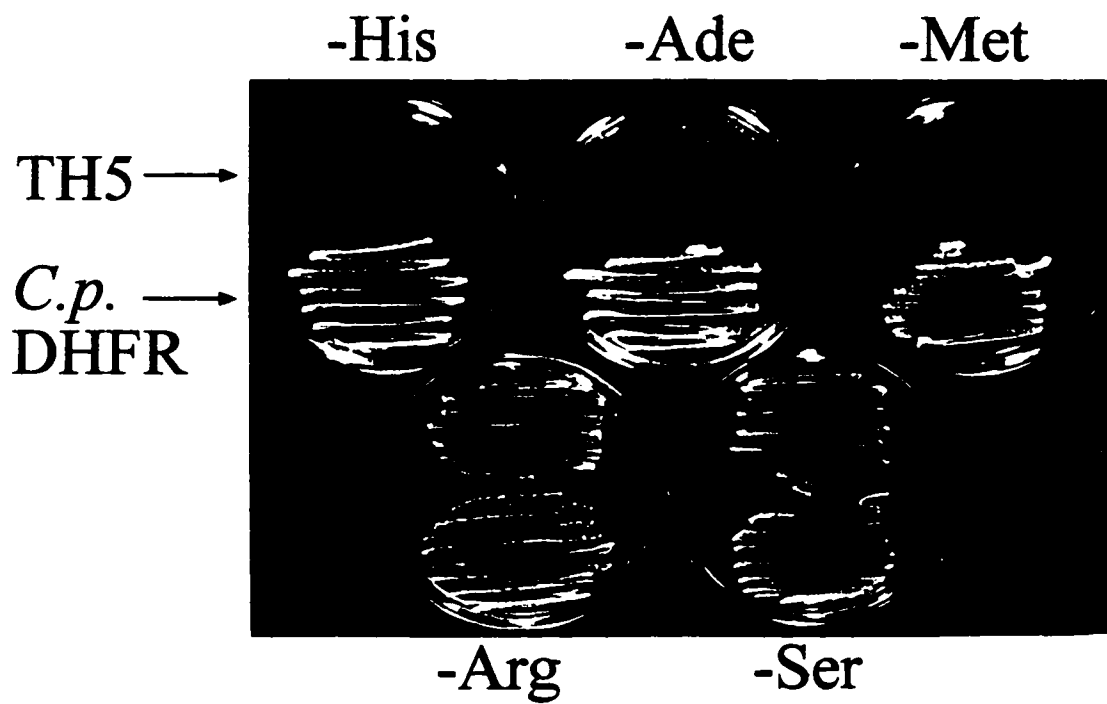


Figure 5: Complementation of the *dhf1* disruption by the *C. parvum* DHFR. Each plate was streaked with two strains; the top strain is the parent, untransformed TH5, the bottom strain is TH5 transformed with the yeast expression plasmid containing the *C. parvum* DHFR domain. All of the plates are supplemented with dTMP. The medium is synthetic complete (C) missing one amino acid. Histidine, adenine, and methionine require tetrahydrofolate to be synthesized. Arginine and serine are controls to show that the requirements are folate pathway specific.

DHFR genes were expressed in the yeast. Expression of the human DHFR (see above) tested whether the host enzyme would be inhibited by treatment with a particular compound. The strain with the yeast DHFR (Wooden et al., 1997) on the expression plasmid was expected to be insensitive to nearly every DHFR inhibitor (see discussion). Therefore if a compound inhibited this strain, we had reason to believe it may be non-specifically toxic to the yeast. The yeast expressing *P. falciparum* DHFR are extremely sensitive to DHFR inhibitors in this system. PyrS refers to the wild type form of the *Plasmodium falciparum* DHFR which is sensitive to the antimalarial pyrimethamine. PyrR refers to a form of the *P. falciparum* DHFR with two point mutations (at amino acids 51 and 108 in Table 1) that confer resistance to pyrimethamine. Thus, if no strain including the *P. falciparum* DHFR yeast show any inhibition to a particular compound, then the yeast may be impermeable to that drug and an *in vitro* assay with purified *C. parvum* DHFR enzyme will need to be performed to determine the efficacy of the compound.

The DHFR coding sequences from the opportunistic fungus *Pneumocystis carinii* and the opportunistic protozoan *Toxoplasma gondii* were also expressed from the yeast vector. A number of available compounds have been tested *in vitro* as inhibitors of *T. gondii* or *P. carinii* DHFR enzymes and their sensitivities are known. These enzymes, therefore, provided additional confirmation that the assay was functioning as expected. The single domain *P. carinii* DHFR was provided by NIH through the AIDS Research and Reference Reagent Program and Larry Gallagher cloned it into our yeast expression vector. Although *T. gondii* normally has a bifunctional DFHR-TS, the DHFR domain alone was cloned into the yeast vector by Mary Reynolds in David Roos' laboratory. These DHFR enzymes also fully complemented the *dfp1* deficiency and the strain markers agreed with expectations (Table 4). We expected the various controls to allow us to identify compounds that

Table 4: Complementation of the yeast *dhfr1* disruption by the control DHFR enzymes. Each yeast strain was replica plated onto the specified media. Growth is indicated by +, no growth by -. The ability of the strains to grow on the various media matched expectations based on strain genotypes.

Origin of DHFR	Yeast Strain Marker Verification						Complementation Testing			
	C-Ura	C-Leu	C-Trp	C	D	C-Ade	C-Met	C-His	D-dTMP	
<i>S.c. DHFR</i> on plasmid	+	-	+	+	+	+	+	+	+	+
<i>P.f. PyrS DHFR</i>	+	-	+	+	+	+	+	+	+	+
<i>P.f. PyrR DHFR</i>	+	-	+	+	+	+	+	+	+	+
<i>T.g. DHFR</i>	+	-	+	+	+	+	+	+	+	+
<i>P.c. DHFR</i>	+	-	+	+	+	+	+	+	+	+
<i>C.p. DHFR-TS</i> , bovine isol.	+	-	+	+	+	+	+	+	+	+

all plates contain 100 µg/ml dTMP unless otherwise noted

Table 5: Yeast strains used in this work.

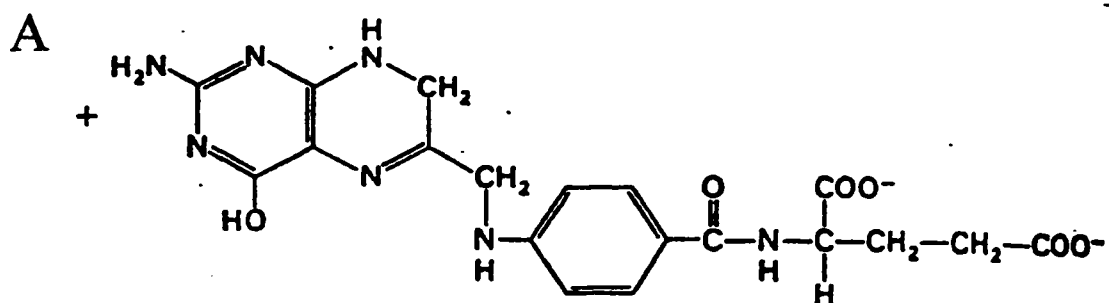
Origin of DHFR	Use in Assay
<i>S. c.</i> DHFR on plasmid	very insensitive, informs of non-DHFR toxicity
<i>P.f.</i> PyrS	very sensitive, informs about permeability of yeast to compound
<i>P.f.</i> PyrR	very sensitive, but less than PyrS, informs about permeability of yeast to compound
Human	informs whether compound inhibits the host's DHFR
<i>C.p.</i> bovine isol. DHFR-TS	enzyme of interest
<i>C.p.</i> human isol. DHFR-TS	enzyme of interest
<i>T.g.</i>	permeability information and known sensitivity to some DHFR inhibitors
<i>P.c.</i>	permeability information and known sensitivity to some DHFR inhibitors

are selective for the parasitic DHFR, generally toxic to yeast, or to which yeast are poorly permeable (Table 5).

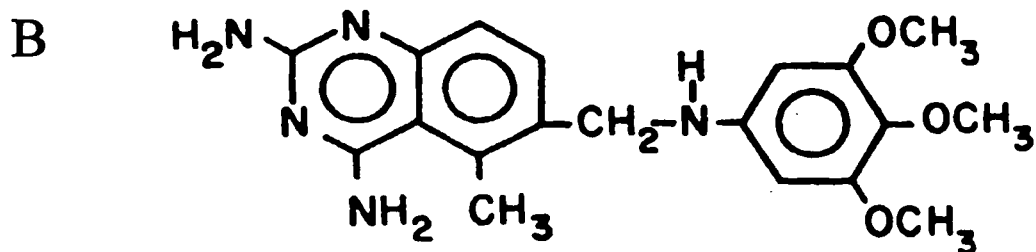
CHAPTER SECTION: OPTIMIZATION OF DRUG SENSITIVITY ASSAY

The various DHFR enzymes effectively complemented the yeast *dhfr1* deficiency. The next step was to test the drug sensitivity of the engineered strains. Trimetrexate (TMX) is an antifolate drug that is effective against *C. parvum* DHFR (John Vasquez, personal communication). Trimetrexate, an analog of the natural substrate DHF, binds and inhibits all DHFR enzymes (Figure 6). The human enzyme is therefore equally susceptible to inhibition by this drug, making it a poor choice for pathogen control, but a good choice for my initial studies. As a first measure to determine whether the engineered strains were sensitive to this drug as expected, I used the spoke assay, described in materials and methods. Each spoke on the plate is streaked with a different strain of yeast expressing a different DHFR. A master plate is replica plated and concentrated drug is placed in the center of each plate. The drug diffuses through the media, setting up a gradient of drug concentration with the highest at the center of the plate. The sensitivity of a given strain is reflected by the distance from the center of the plate to where growth begins. The more sensitive to the drug that a particular strain is, the greater the distance with no growth. A non-sensitive strain will grow throughout the length of its spoke.

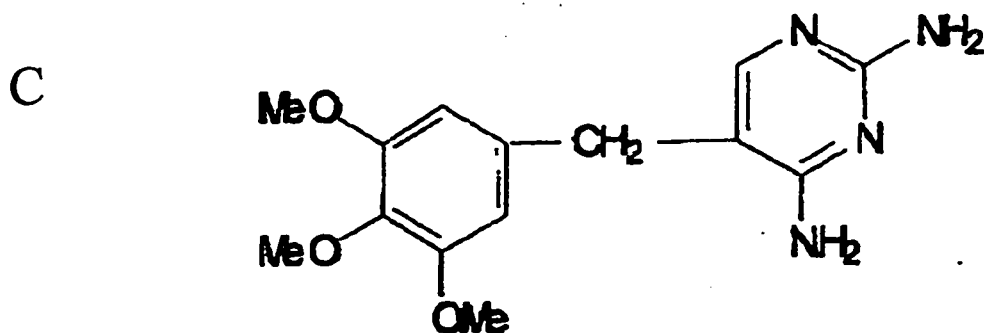
A D plate was streaked with the *C. parvum* DHFR, DHFR-TS (human isolate), and human DHFR yeast strains. As controls, I had streaked the *Plasmodium falciparum* DHFR constructs PyrS, *P.f.* Honduras (point mutation at residue 108; slightly resistant to pyrimethamine), and the yeast DHFR on the plasmid. Ten microliters of trimetrexate, 1.36×10^{-2} M (0.136 μ mole), was placed in the center of the plate. Contrary to expectations, none of my three strains showed any sensitivity to



Dihydrofolate



Trimetrexate



Trimethoprim

Figure 6: Chemical Structures. A) Dihydrofolate, the natural substrate for DHFR. B) Trimetrexate, an inhibitor of all DHFR enzymes. C) Trimethoprim, an inhibitor effective against many pathogens but not an inhibitor of the human enzyme.

trimetrexate (data not shown). Since PyrS and Honduras did show sensitivity to the drug, TMX was clearly able to permeate the yeast cells. I verified this result by doing a liquid IC_{50} , a more sensitive measure of drug susceptibility. In IC_{50} assays, the yeast are grown in liquid rich media (without exogenous dTMP) in the presence of varying concentrations of drug. The cell growth in wells with drug was compared to the growth in solvent alone to determine the degree of growth inhibition caused by the drug. I used the yeast expressing the human DHFR since that enzyme has been much better characterized than the *C. parvum* enzyme. I tested concentrations of the drug up to 1×10^{-4} M and obtained an estimated IC_{50} for the human enzyme of 1.5×10^{-4} (Figure 7). Human cells in culture have an IC_{50} of about 1×10^{-8} M. The IC_{50} for the PyrS DHFR from *P. falciparum* was 5.1×10^{-8} , a result within the expected range. The drug was able to enter the cells and reach the DHFR, but the strain expressing the human DHFR did not show the expected sensitivity. After much discussion, we concluded that the probable cause of the resistance was overexpression of the DHFR enzyme. Antifolate drugs, such as trimetrexate, are competitive inhibitors of DHFR. Thus, the higher the level of enzyme, the higher level of drug required for inhibition. Trimetrexate binds with such high affinity to all DHFR enzymes (Lin and Bertino, 1987; Myers *et al.*, 1975) that the binding is essentially stoichiometric. Therefore the amount of drug needed to inhibit the enzyme provides an estimate of the level of enzyme. Thus, the yeast expressing the human DHFR apparently have a much higher expression level than the yeast expressing the *P. falciparum* DHFR.

In order to test the hypothesis that differing sensitivity to TMX was the result of variation in expression level, I attempted to determine the level of DHFR protein in different *P. falciparum* DHFR expressing yeast strains by Western blot. We obtained a small amount of unpurified polyclonal antibody against the *P. falciparum* DHFR (Pradip Rathod, personal communication). I produced a Western blot that included TH5 and the yeast DHFR on the plasmid (negative controls) and various *P.*

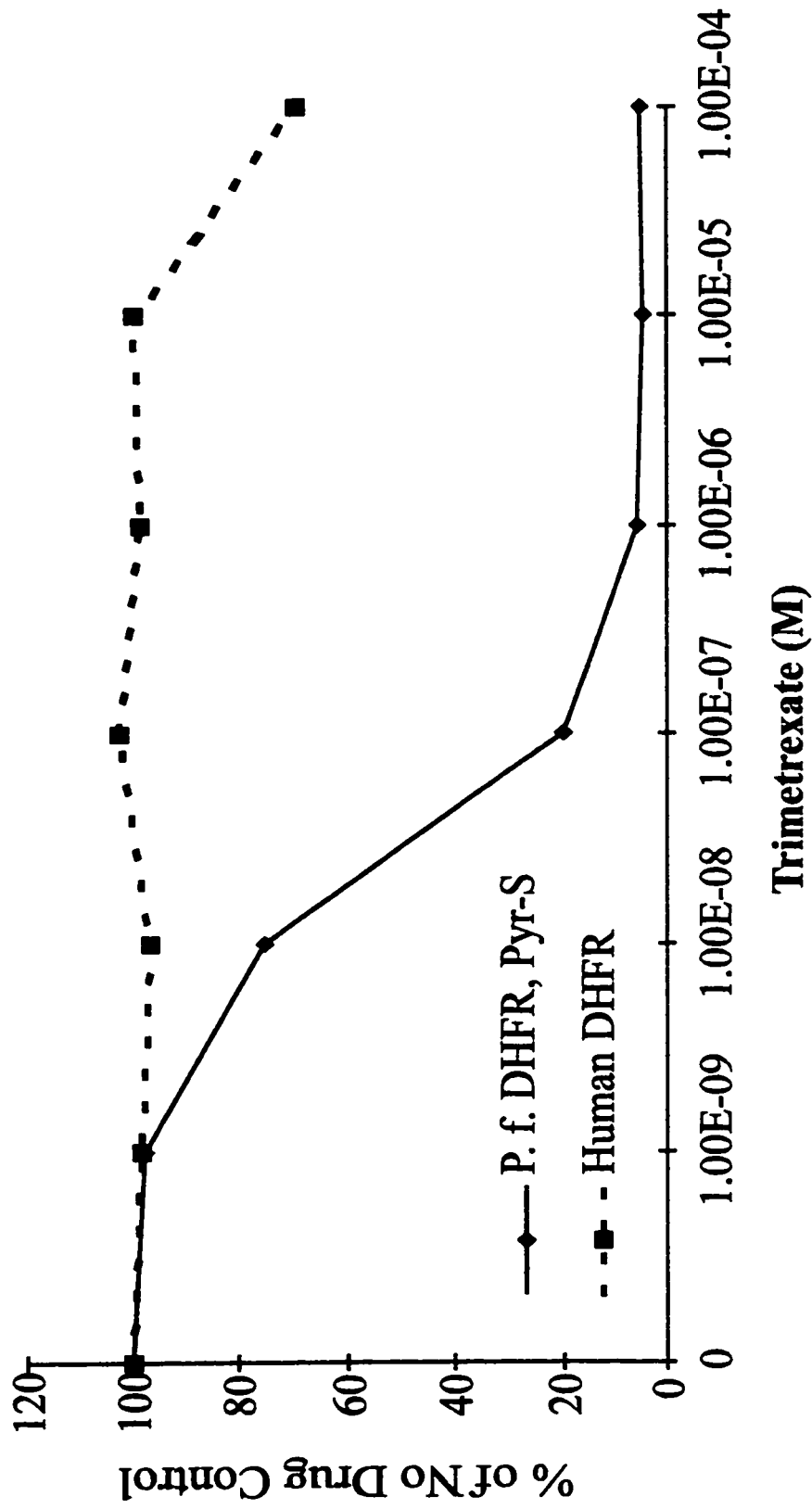


Figure 7. IC-50 assay with trimetrexate. The amount of cell growth after approximately 24 hours was determined spectrophotometrically at 650 nm. Cells incubated with solvent alone were taken as 100% growth. The relative growth for each drug concentration was determined by dividing the growth in drug by the solvent control.

falciparum DHFR variants, as well as purified protein (a gift from Jason Wooden) and probed the blot with the anti-DHFR antibody. I probed the blot with various dilutions of primary and secondary antibodies but was never able to see a specific signal from the yeast extracts. Purified protein was detected, but only when large amounts were present (200 ng) (Figure 8). The antibody needs to be purified and concentrated, but not enough is available for us to do this. Therefore, the Western analysis was unsuccessful.

Based on the assumption that overexpression was the source of the insensitivity to drugs that I observed with the human and *C. parvum* DHFR expressing yeast, I attempted to find a promoter that resulted in lower expression of the heterologous DHFR proteins. My initial strategy was to use the yeast Cyc1 promoter. This promoter, as determined by Lac Z expression, results in very poor expression (Mumberg *et al.*, 1995). The Cyc1 plasmid is derived from pRS314 (Sikorski and Hieter, 1989), as is our parent plasmid, so other than the promoter and terminator, the plasmid sequences are the same as pEH2. The Cyc1 plasmid was digested with Bam HI and Eag I, the human and *C. parvum* DHFR sequences ligated into the vector, and the ligations transformed directly into yeast. In order for the yeast to grow in the absence of dTMP, the plasmid must have successfully ligated a DHFR domain 3' of the promoter since the unaltered vector will not complement the *dfr1* disruption. Two colonies expressing the human DHFR provided complementation and were somewhat sensitive to TMX on plates but the IC_{50} s were still high: 7.3×10^{-6} and $> 10^{-5}$ M (Figure 9). None of the *C. parvum* DHFR expressing colonies were sensitive to TMX. The Cyc1 promoter provided somewhat better sensitivity for the human DHFR but was still less than optimal.

The next strategy used to decrease the promoter activity was to mutagenize the yeast DHFR promoter by error-prone PCR. The fidelity of PCR can be manipulated by altering the concentrations of various reaction components

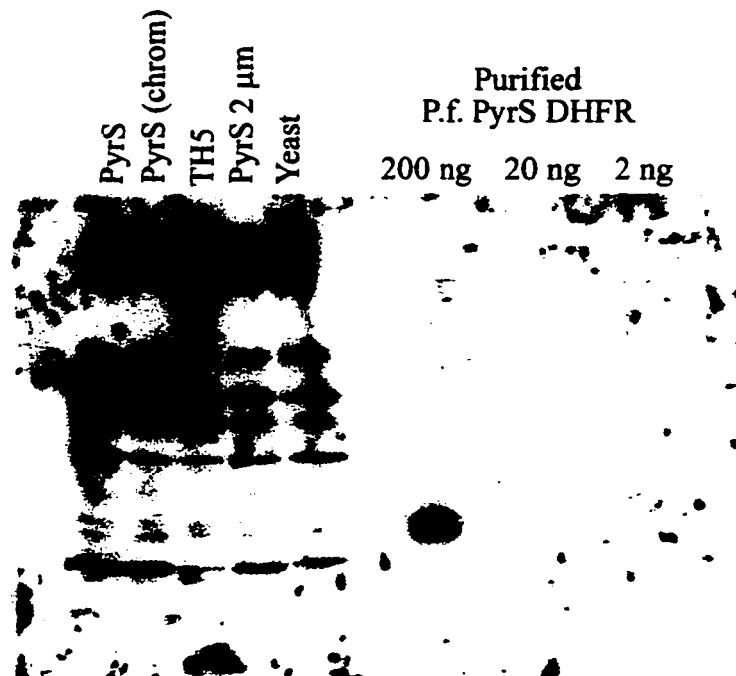


Figure 8: Western blot probed with an antibody directed against the P.f. DHFR. Extracts of various yeast strains expressing: PyrS: *P. falciparum* PyrS DHFR expressed from the plasmid, PyrS (chrom): P.f. PyrS DHFR expressed from the chromosomal location, TH5: no DHFR, PyrS 2 μ m: P.f. PyrS DHFR expressed from a plasmid with a 2 μ m origin for high copy number, Yeast: yeast DHFR expressed from the plasmid. Purified DHFR protein was used as a positive control. DHFR was detected in this assay only when large quantities of protein were present. No bands over background (TH5) were detected in the yeast extracts.

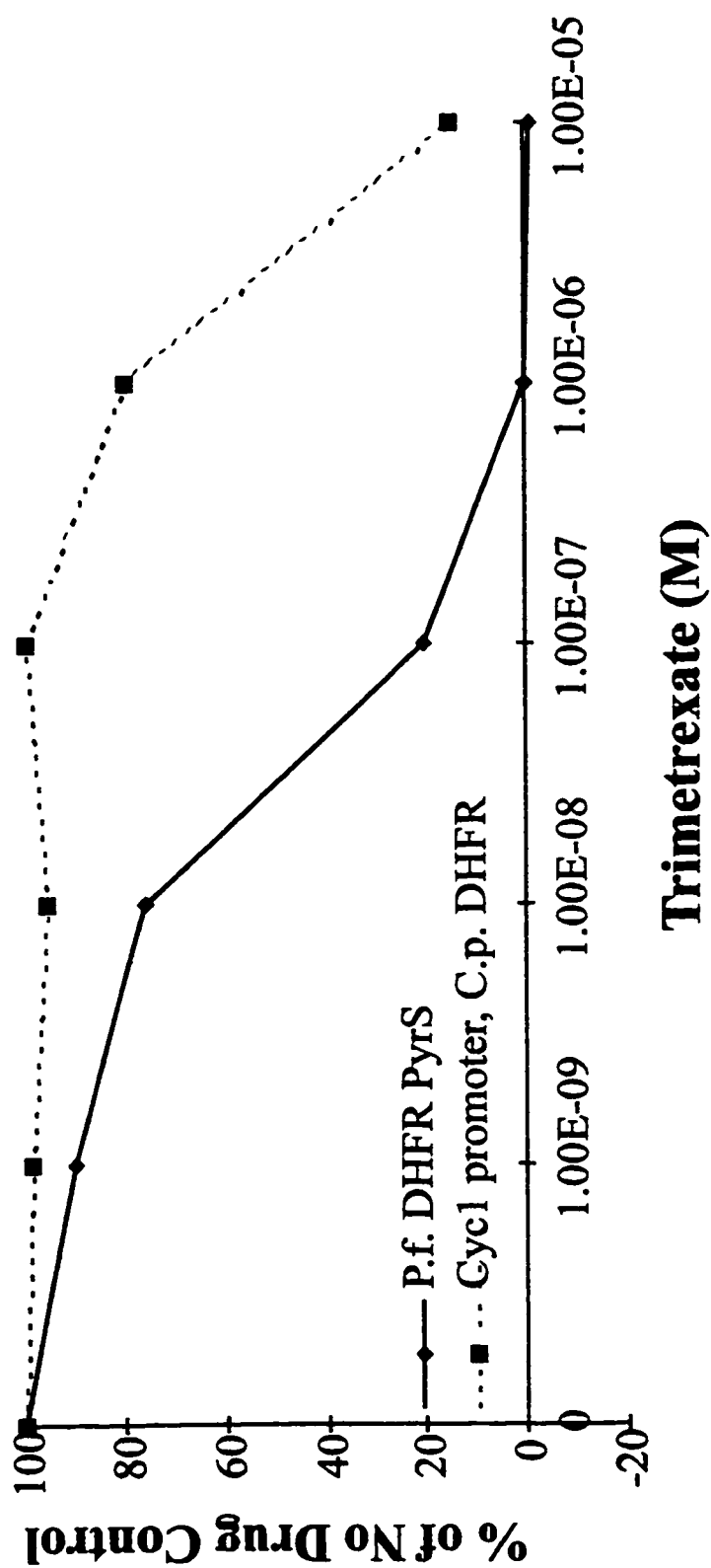


Figure 9. IC-50 Assay with trimetrexate (TMX). The *C. parvum* (C.p.) DHFR driven by the Cyc1 promoter was tested with varying concentrations of TMX. The *P.f.* DHFR PyrS was tested at the same time as a control.

(Zhou *et al.*, 1991). The population of error-containing promoter sequences was cloned back into the human DHFR containing vector, transformed into yeast, and plated on C minus tryptophan + dTMP plates. Colonies were screened for DHFR complementation and increased sensitivity to TMX. The yeast patches were first screened by replica plating onto plates containing various amounts of TMX. Promising patches that were able to grow in the absence of dTMP but not in the presence of 10^{-5} M TMX were tested by the spoke assay. Two promoters were identified that resulted in an IC_{50} for the human DHFR expressing yeast of approximately 3×10^{-6} M (Figure 10). I sequenced one of these promoters and discovered that the mutation was a truncation: a deletion of 142 bp of the 3' end of the promoter (Figure 11). The effect of this truncation is to disrupt the spacing of the promoter elements relative to the start of the coding sequence, apparently reducing the efficiency of the promoter.

The IC_{50} was still higher than desired so I repeated the PCR mutagenesis on both the truncated promoter and on the original promoter and screened for TMX sensitive candidates. Several more were identified, but the IC_{50} s were the same as the original truncation (Figure 12). Three of the eight new promoters were sequenced. All three were truncated even though the starting template was the original full length promoter. They also had a single base change just before the truncation but since the IC_{50} s are identical to the original truncation, this change apparently does not affect the promoter efficiency. The original truncation was chosen for further work.

The observation that mutagenesis of the promoter increased sensitivity of the DHFRs to TMX supported the reasoning that the expression level was the cause of the insensitivity. However, this new promoter still failed to reduce the expression level enough so that a practical level of sensitivity resulted. Although we could obtain a high enough concentration in the assay, it required a large amount of drug. Most

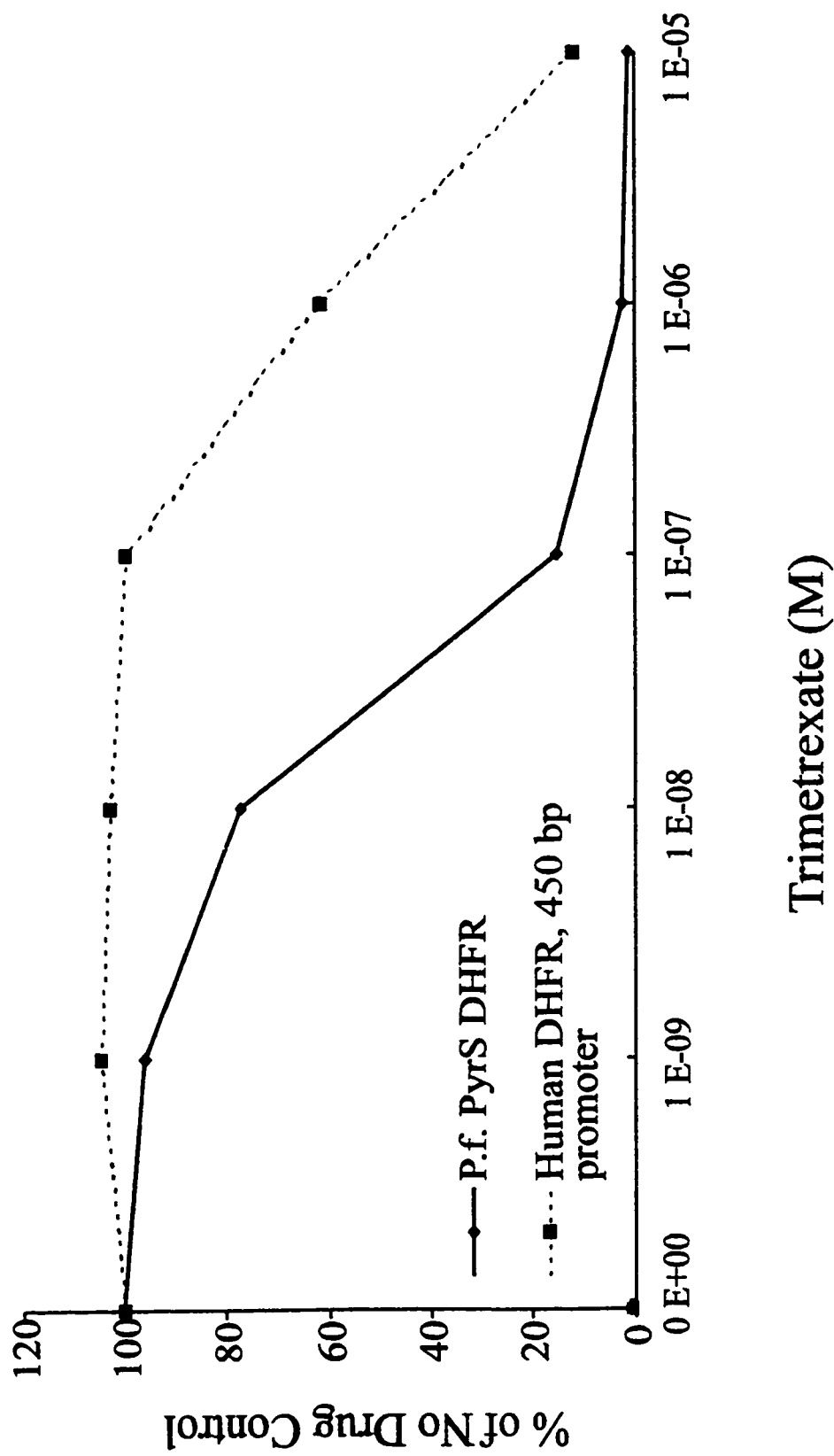


Figure 10: IC-50 of yeast expressing the human DHFR with the truncated promoter. The *P. falciparum* (*P.f.*) DHFR is included as a control.

CTATAGGAATCGTCACTCTTTGACTCTTCAAAAGAGCCACTGAATCCAACCTTGGTTGAT
 242
 GAGTCCCATAACTTTGTACCCAGAGTGAGAAACGAAATTGAATCTAAATTAGCTTGGTCCGCAATCCTTAGCGGTTG
 322
 GGCCATCTATAATTTTGAATAAAAAATTTGCTTTGCCTTGCATTGTAGTTTTTTCCTTTGGAAGTAATTACAATATTT
 402
 TATGGCCGATGATCTTGACCCATCCTATGTACTTCTTTTTGAAGGGATAGGGCTCTATGGGTGGGTACAAATGGCAAT
 482
 CTGACAAAGTTAACCACCTTTTTCTTTCTAAATTGTTTAAACCAAAGGTTTGGTTTTCACTTAAGAAATTGGATTAGT
 562
 TGGTGTGTAAATATAATTAATGTAGTCTTGGTTAGCTTAATGTATAGGTTCTTGATAGTATGACTCCACCTAAAAATCG
 642
 TCAAGAGCGACCGATGCGAAAACAAAAAATCGCTTTGCATCCTTACGTGCGTGAGATGGCATCGCTGGCCAAAGGGAAA
 722
 CGTTTCATTATTTTCTGTAGTTAACATTATGCTTTGCATGATAATAAGAGAAATTGAAGAGCGCAACGAACCTACGAGC

Figure 11: Promoter sequence. DNA sequence of the promoter region used in the yeast expression vector. The sequence within the box is deleted from the truncated promoter. Underlined sequences are putative TATA boxes and sequences over wavy lines are putative GCN4 binding sites.

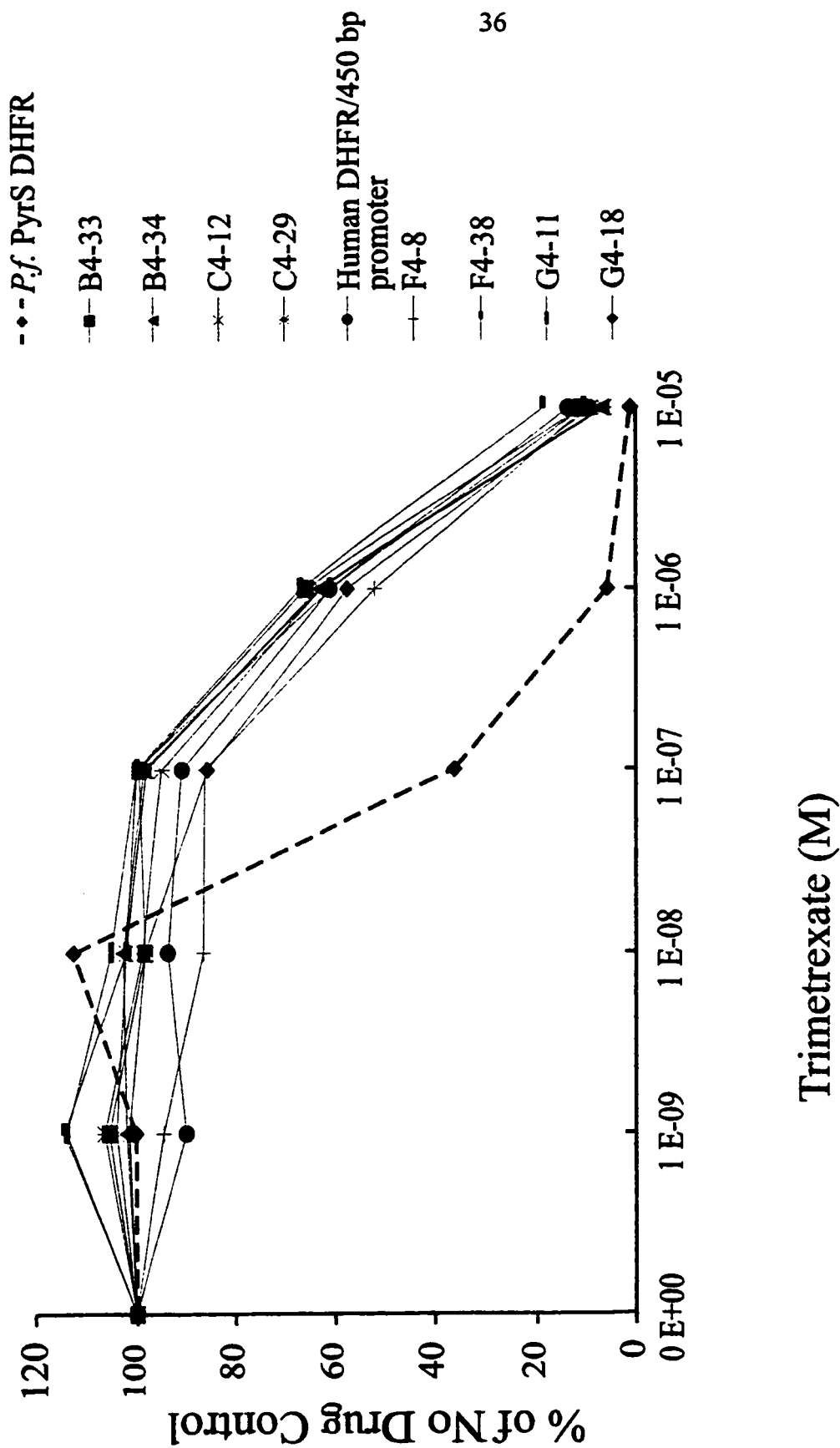


Figure 12: IC-50 assay of strains with various mutagenized promoters. Each clone represents an individual mutagenized promoter driving the human DHFR. The *P.f.* PyrS DHFR and the original truncated promoter are included as controls.

novel compounds are available in very small quantities and may not be very soluble. We tested a strategy to increase the sensitivity of the assay by using defined media plates. The spoke and IC₅₀ assays are normally conducted on rich media plates that contain the C1 metabolites except for dTMP. Inhibition of DHFR creates a shortage of these metabolites. Since met, his, and ade are abundant in the media, cells in the presence of a DHFR inhibitor are only limited for dTMP. We realized that we might be able to increase the sensitivity to antifolate compounds by using defined media lacking one of the C1 metabolites. The rationale was that the cells would be starved for more than one metabolite and would require less drug to achieve the same level of inhibition. To test this hypothesis, spoke assays were carried out on C - ade, C - met, and C - his plates. Some of the yeast strains were more sensitive to TMX on the defined media plates, but some were not (Figure 13). The best results were on the C - ade plates. On these plates, TMX completely inhibited the *P. falciparum* PyrS DHFR and inhibited *P. falciparum* PyrR very well. The human and *T. gondii* strains were inhibited fairly well, but the *P. carinii* not at all. The *C. parvum* DHFR-TS strains were expected to be inhibited to the same degree as the other strains, but this was clearly not the case. This strategy was only partially successful at increasing the sensitivity of the assay.

The next strategy was to increase the sensitivity of the assay by including a second drug directed against a different target. Clinically, antifolate drugs are combined with an inhibitor of the folate pathway enzyme dihydropteroate synthase (DHPS). This enzyme is two steps upstream in the folate pathway from DHFR (Figure 3). It condenses para-aminobenzoic acid (pABA) and dihydropteridine to form dihydropteroate. Drug combinations that inhibit both DHFR and DHPS produce a synergistic effect on susceptible parasites (Berenbaum, 1978; Hewlett, 1969): a greater degree of inhibition is obtained with the two drugs together than would have been predicted based on the efficacies of the drugs singly. We reasoned that if we

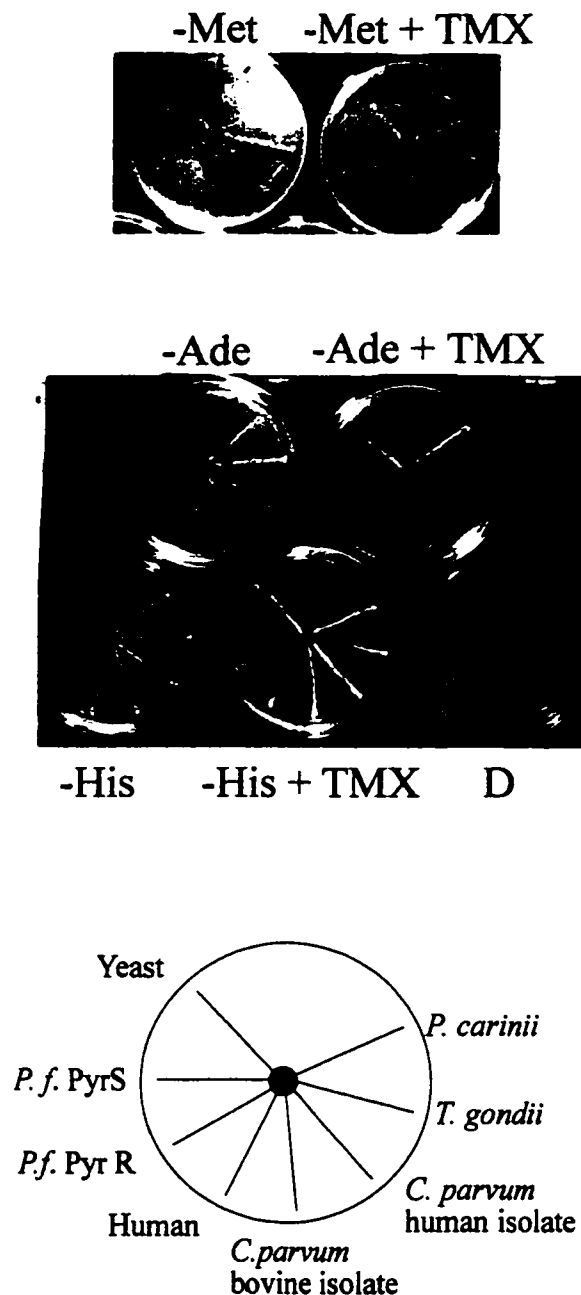


Figure 13. Spoke assays on defined media lacking one C1 metabolite. The identity of each spoke is shown in the plate legend. For each type of plate, there is a no drug control to verify that the strain can grow in the absence of that metabolite. Another plate had TMX placed in the center. In this experiment, the human DHFR strain did not grow on C-Met plates but did grow on these plates in previous experiments.

inhibited the yeast DHPS with a sulfonamide drug, then we should observe greater sensitivity of the DHFR to the antifolate compounds.

We tested this idea using the DHPS inhibitor sulfanilamide. This drug has often been used experimentally to inhibit the yeast DHPS (Colonna *et al.*, 1977; Miyajima *et al.*, 1984). Yeast rich media plates were spread with sulfanilamide to generate a final concentration of 1 mM. These plates were then used for spoke assays. A typical experiment is shown in Figure 14. These plates contain *P. falciparum* (PyrS), human (original and truncated promoter), and eight colonies expressing *C. parvum* DHFR-TS, human isolate. Plates containing TMX alone showed inhibition of the *P. falciparum* DHFR strain and a small degree of inhibition of the human DHFR with the truncated promoter (Figure 14A). Plates containing sulfanilamide alone showed inhibition of only the *P. falciparum* strain (Figure 14B). In the vast majority of experiments, the *P. falciparum* strain does grow on 1 mM sulfanilamide, albeit less well. Plates containing both sulfanilamide and TMX showed good inhibition of all of the strains except for that expressing the yeast DHFR (Figure 14C). Even the human DHFR expressing strain with the original 600 bp promoter is inhibited by the TMX/sulfanilamide combination, although the truncated promoter results in even better sensitivity. All eight of the *C. parvum* DHFR-TS colonies showed essentially the same degree of sensitivity to the drug combination. Adding sulfanilamide to the plates dramatically improved the sensitivity of the various strains to TMX. The susceptibility is specific to the folate pathway because inclusion of dTMP in the plates prevents inhibition of the various strains by the drug combination (Figure 14E).

The human DHFR and *C. parvum* DHFR-TS expressing yeast strains (human and bovine isolates) were tested in an IC_{50} assay with the TMX/sulfanilamide combination (Figure 15). This assay confirmed the plate results that sulfanilamide clearly enhances the yeast sensitivity to TMX. The IC_{50} s were much lower in the presence of 1 mM sulfanilamide and were now in a practical range. Sulfanilamide is

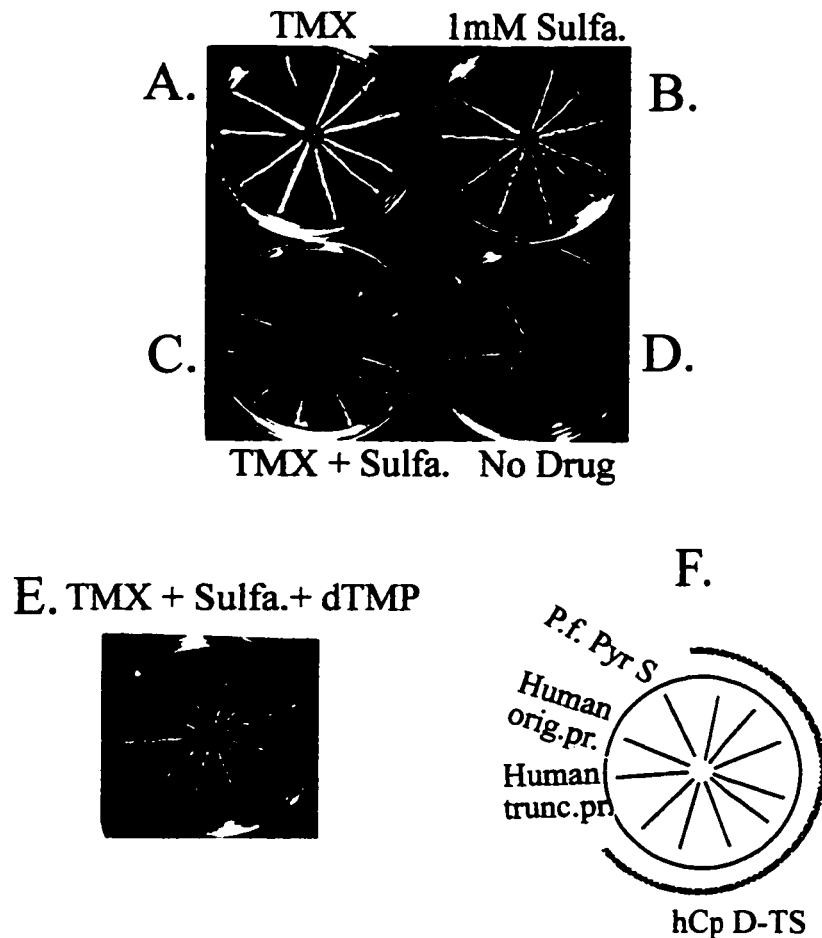
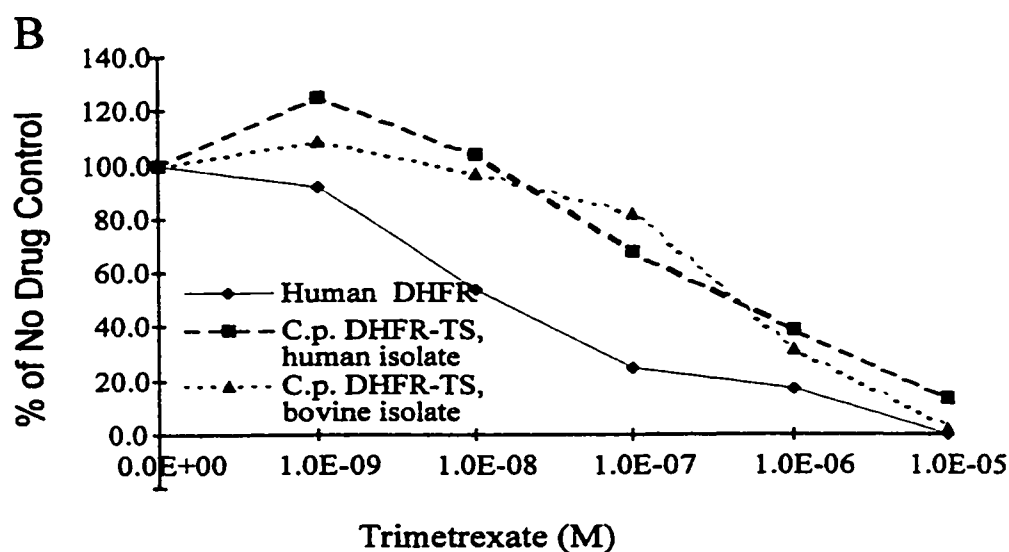
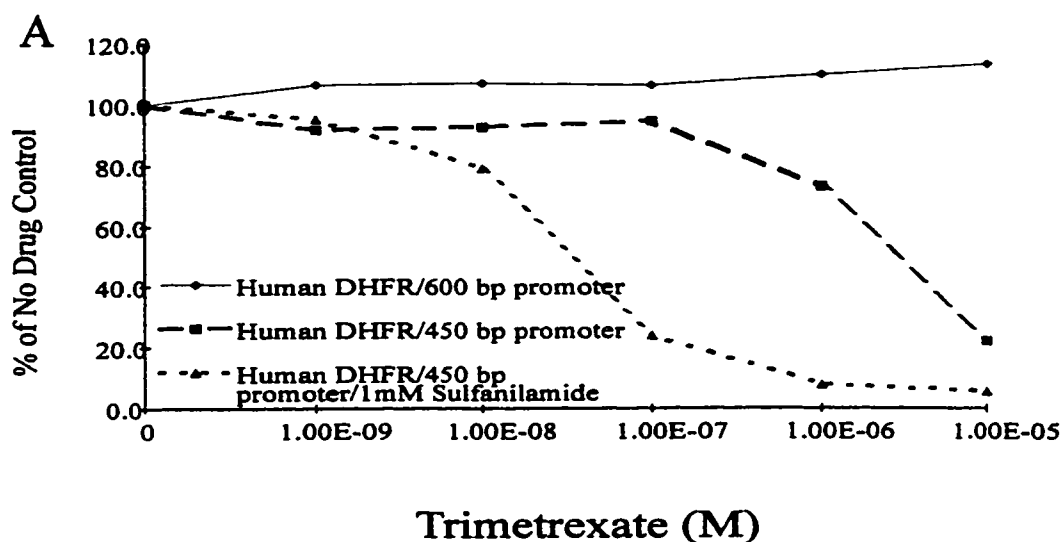


Figure 14. Synergism between TMX and Sulfanilamide. A) 10 μ l of a 5 mg/ml solution of TMX was placed in the center of the plate and the plates allowed to grow for two days. B) sulfanilamide was spread evenly on the plate to generate a final concentration of 1 mM. C) Both TMX and sulfanilamide were used on the plate as described above. D) No drug E) Both TMX and sulfanilamide. In addition, dTMP was spread evenly on the plate. F) Strain Legend. The spoke arrangement on each plate is identical and is shown in this diagram. orig. pr = original, 600 bp promoter trunc. pr. = truncated promoter, 450 bp. hCp DHFR-TS refers to several clones expressing the human isolate of *C. parvum* DHFR-TS.



	IC-50 (M)
Human DHFR	2.2×10^{-8}
<i>C. parvum</i> DHFR-TS, human isolate	6.4×10^{-7}
<i>C. parvum</i> DHFR-TS, bovine isolate	6.7×10^{-7}

Figure 15: IC-50 assay using sulfanilamide in the media. A) comparing sensitivity of yeast expressing human DHFR driven by two different promoters and in the presence of 1 mM sulfanilamide. The 600 bp promoter is the wild type portion taken from the endogenous yeast DHFR upstream region. The 450 bp promoter is the truncated version identified through PCR mutagenesis. B) Comparison of yeast expressing the two version of the *C. parvum* DHFR-TS and the human DHFR in the presence of 2.5 mM sulfanilamide.

not a limiting reagent, whereas the novel DHFR inhibitors are. This strategy allowed us to screen compounds at practical concentrations.

CHAPTER SECTION: SCREENING OF POTENTIAL INHIBITORS OF *C. PARVUM* DHFR-TS

With the addition of sulfanilamide, all of the strains showed good sensitivity to TMX (except yeast, the negative control). In order to determine if the assay worked for other compounds, we obtained fourteen compounds from the National Cancer Institute (NCI) and tested them for efficacy against the *Cryptosporidium* DHFR-TS in the yeast system. The structures of many of the compounds tested are included in Appendix 1. These compounds had been tested *in vitro* with purified *C. parvum* DHFR-TS and human DHFR enzyme by John Vasquez. Thus, we could confirm the validity of our results by comparison with the *in vitro* data. The results are summarized in Table 6.

We observed one compound that caused general toxicity in the yeast, 107288. Every strain, including the yeast DHFR which is very resistant to inhibition, was inhibited by the compound. The inhibition of the yeast DHFR served as a warning and the compound was tested in the presence of dTMP and rich media. In these conditions, the folate pathway is not required since the products are provided in the media. Compound 107288 still inhibited the growth in the presence of dTMP; thus this compound inhibits the yeast by an unknown mechanism.

Most of the compounds did not inhibit the DHFR-TS from either *C. parvum* isolate. With the exception of 77028 and 47532, all of those that did not inhibit *C. parvum* did affect at least one other strain, indicating that the drug can enter the cells and reach the DHFR. These two compounds did not inhibit any of the strains and may not be able to permeate the yeast.

Table 6: Drug sensitivity to the National Cancer Institute (NCI) compounds. The left side of the table presents John Vasquez' *in vitro* data using purified enzyme. The right side presents data obtained using the spoke assay and yeast expressing heterologous DHFR enzymes. The numbers represent the distance in centimeters from the center of the plate to the beginning of yeast growth ("kill zone"). The symbol - represents no inhibition detected.

Compounds	ENZYME IN VITRO				YEAST INHIBITION							
	IC-50 (μ M)				(cm in spoke assay)							
	<i>C.p.</i> DHFR-TS human isolate	<i>C.p.</i> DHFR-TS bovine isolate	Human DHFR		<i>C.p.</i> DHFR-TS human isolate	<i>C.p.</i> DHFR-TS bovine isolate	Human DHFR	<i>P.f.</i> DHFR PyrS	<i>P.f.</i> DHFR PyrR	<i>T.g.</i> DHFR	<i>P.c.</i> DHFR	Yeast DHFR
Trimetrexate	0.004	0.001	0.001		2.3	2.5	2.9	>3.5	3	2.7	1.8	-
61670	>1000	nd	700		-	-	-	>2	-	-	-	-
104126	>100	>100	>100		-	-	-	0.9	-	-	-	-
106568	5	2	600		1.5	2	-	>2.5	1.6	-	-	-
107242	>100	>100	300		-	-	-	>1.7	-	-	-	-
112421	0.07	0.1	0.2		1.2	1.6	1.4	>2.2	-	-	-	-
117288	>1000	nd	>1000		0.6	0.6	0.7	1.8	0.9	0.9	0.6	0.7
121146	0.006	0.01	0.1		1.1	1.2	1.5	>2.2	-	-	-	-
3081	200	60	5		-	-	1.8	>2.3	2.8	2	-	-
47532	200	10	>100		-	-	-	-	-	-	-	-
77028	100	100	50		-	-	-	-	-	-	-	-
104133	80	30	2		-	-	0.9	>2.5	2.4	1.2	-	-
114923	30	20	2		-	-	-	0.9	-	-	-	-
127916	100	100	20		-	-	-	>2.1	-	-	-	-
Chlorasquin					1.9	2.2	2.1	>3	2.3	1.7	2	-

In addition to trimetrexate, four compounds were reasonable inhibitors of the *C. parvum* DHFR-TS strains. One was chlorasquin, a drug similar to TMX in that it inhibits all DHFR enzymes fairly equivalently. Two compounds, 121146 and 112421, showed borderline selectivity in the spoke assay. These were tested in the liquid assay to obtain more quantitative data. The IC₅₀ results do not indicate that either of these two compounds shows significant selectivity for the *C. parvum* DHFR over the human DHFR (Figure 16).

One compound, 106568, was selective for the *C. parvum* DHFR-TS over the human DHFR. The spoke assay showed a clear difference in sensitivity between the yeast expressing a *C. parvum* DHFR and the human DHFR. The IC₅₀s were 6.8×10^{-6} for the human isolate and 3.3×10^{-6} for the bovine isolate but $>10^{-5}$ for the human DHFR (Figure 17). When the numerical coding was broken, compound 106568 turned out to be trimethoprim, an old and well-used antibacterial DHFR inhibitor. Although the *C. parvum* enzyme is not sensitive enough to this compound to make it useful clinically, analogs of trimethoprim may be more effective and still maintain selectivity.

The 14 NCI compounds were tested *in vitro* by John Vasquez in Richard Nelson's laboratory at UCSF (Table 6). He used purified *C. parvum* and human enzymes and a biochemical assay for DHFR activity. Those compounds that did not *inhibit C. parvum* DHFR-TS in the yeast system also did not inhibit the enzyme *in vitro* or had high IC₅₀s. Two compounds were very slightly selective *in vitro* and in the yeast system the difference was very slight (112421 and 121146). Compounds 77028 and 47532 inhibited none of the yeast strains and the *in vitro* data supported that result with high IC₅₀ values.

One compound was clearly selective *in vitro*: 106568. This compound, trimethoprim, is the one identified as selective in the yeast system.

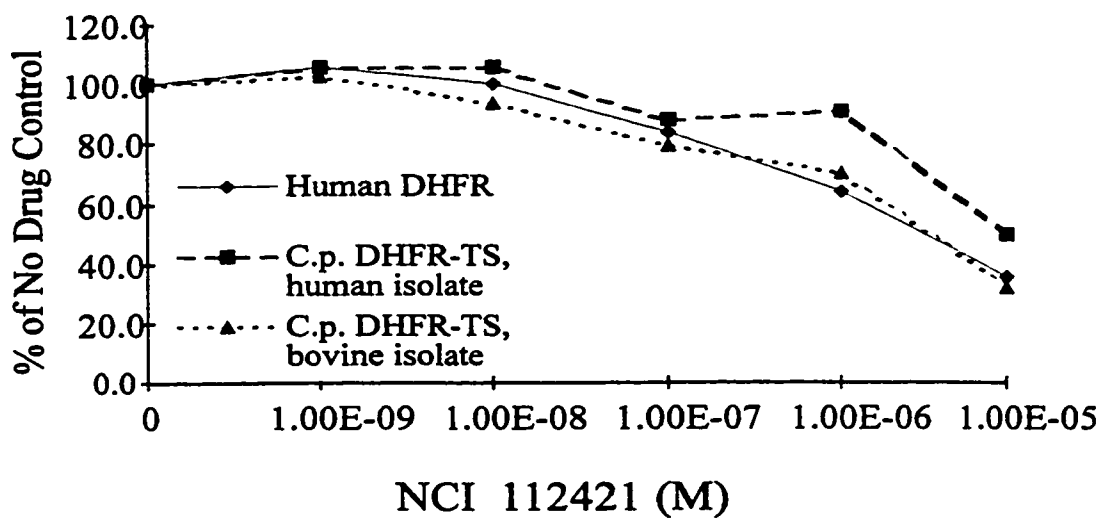
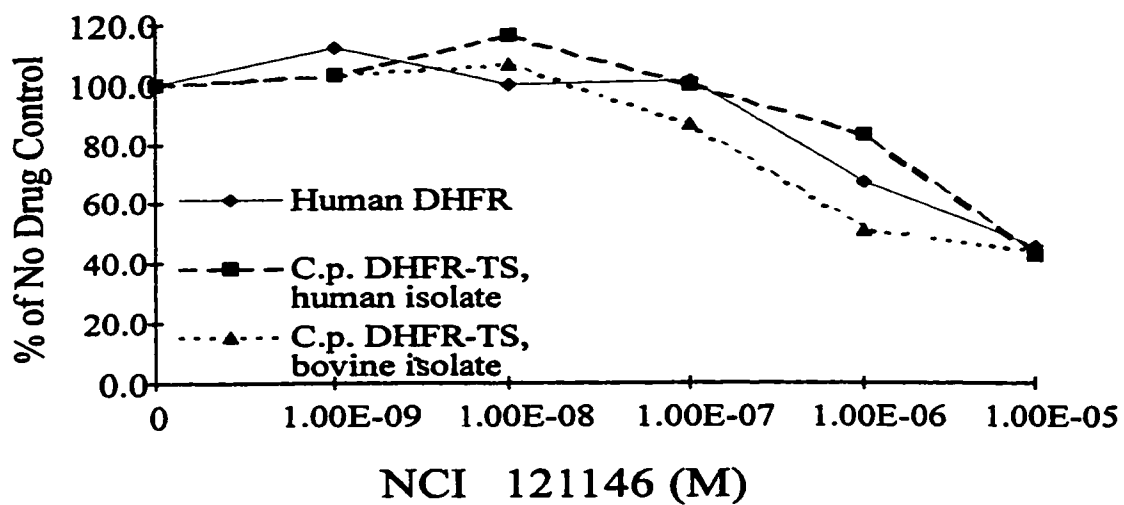


Figure 16: IC-50 Assays with NCI compounds 121146 and 112421. These data suggest that these compounds are not significantly selective for the human DHFR over the *C. parvum* DHFR-TS.

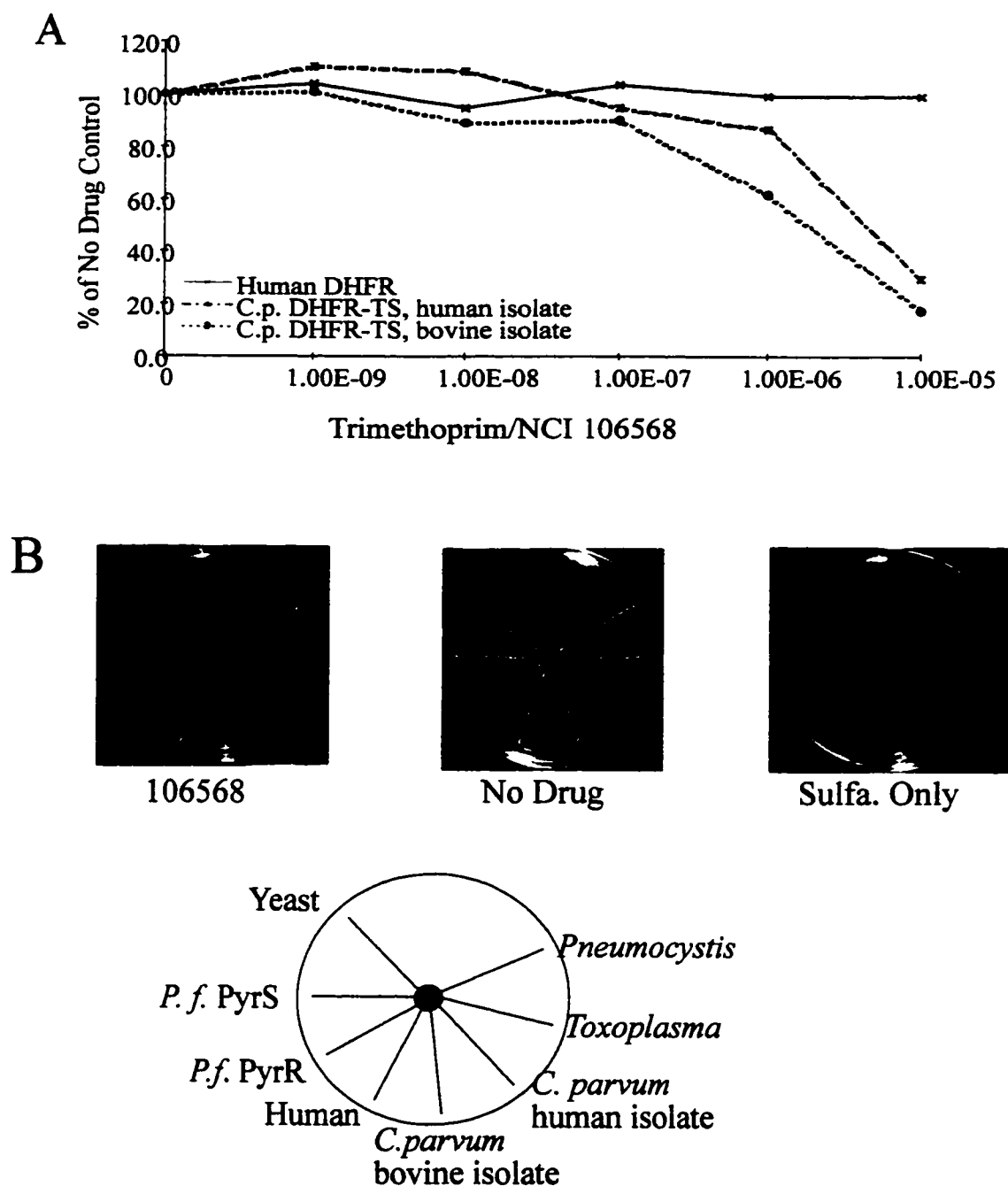


Figure 17: Sensitivity to NCI 106568/Trimethoprim. A) IC-50 assay with yeast expressing human or *C. parvum* DHFR. B) Spoke assay showing selective inhibition of *C. parvum* DHFR-TS but not human DHFR expressing yeast. Plates with no drug or sulfanilamide alone are shown as controls. The plate diagram shows the location of each strain of yeast on each plate.

Trimethoprim is 120 fold more effective against the human isolate *C. parvum* DHFR-TS and 300 fold more effective against the bovine isolate than against the human DHFR. Comparison of the *in vitro* data with the yeast *in vivo* data indicates that the yeast system is a valid way to initially screen novel compounds.

We also obtained and tested 22 novel compounds we received from Andre Rosowsky, a medicinal chemist at Dana-Farber Cancer Institute. These compounds were designed to be lipophilic, so they ought to pass through the plasma membrane easily (Camenisch *et al.*, 1996). Many of these compounds were very effective at inhibiting the *C. parvum* DHFR (Table 7). However, they inhibited the human DHFR as well or better than the parasite DHFR. A few were tested in the liquid IC₅₀ assay and showed low IC₅₀s. For instance, PY 490 gave IC₅₀s of 6.0×10^{-9} M for the human DHFR, 5.9×10^{-9} M for the human isolate of *C. parvum*, and 9.4×10^{-9} M for the bovine isolate (Figure 18). Two, PY 821 and PY 833, inhibited none of the yeast and may not pass through the membrane despite being designed to be lipophilic. These would need to be tested *in vitro* in order to determine their efficacy. Several compounds inhibited well the yeast expressing either the *P. falciparum* sensitive or resistant DHFR but did not inhibit the human DHFR and are possible leads for treatment of malaria (PY 359, PY 460, PY 841, PY 888). Three compounds inhibited the yeast DHFR (PY 489, PY 497, and PY 896) but were not pursued further to determine whether the inhibition was specific. In summary, although none of the compounds were selective for the *C. parvum* DHFR-TS, several were very effective and may be good lead compounds.

In light of the observation that trimethoprim (TMP) was selective for *C. parvum*, we obtained six TMP analogs from the Walter Reed Army Institute for Research (WRAIR). The six compounds were chosen randomly from an inventory search comparing all derivatives of trimethoprim and were intended to represent functional group variations from TMP (for proprietary reasons, the structures are not

Table 7: Drug Sensitivity to the Dana-Farber compounds. The data were obtained from spoke assays using yeast expressing heterologous DHFR enzymes. The numbers represent the distance in centimeters from the center of the plate to the beginning of yeast growth ("kill zone"). The symbol - represents no inhibition detected. Shading indicates compounds that were particularly effective on the *C. parvum* DHFR-TS.

Compounds	YEAST INHIBITION (cm in spoke assay)							
	C.p. DHFR-TS human isolate	C.p. DHFR-TS bovine isolate	Human DHFR	P.f. DHFR Pyr. sensitive	P.f. DHFR Pyr. resistant	T.g. DHFR	P.c. DHFR	Yeast DHFR
Trimetrexate	2.6	2.7	3	>3.5	3	2.5	2.1	-
PY 359	-	-	-	3.6	0.8	-	-	-
PY 361	2.5	2.9	3.4	>3.5	2.8	1.9	1.9	-
PY 365	2.4	2.7	2.8	3.4	1.3	1.9	1	-
PY 460	-	-	-	>3.5	1.4	-	-	-
PY 461	1.4	1.7	2.8	>3.5	2.9	1.7	1.5	-
PY 468	-	-	0.9	3.4	2	-	-	-
PY 488	1.5	1.7	2.6	>3.5	2.8	1.7	1.8	-
PY 489	1.8	1.8	2.5	>3.5	3	1.7	1.9	0.9
PY 490	2.7	2.9	3.1	>3.5	2.7	2.2	1.2	-
PY 497	1.8	2.8	3.1	>3.5	3.1	2.1	1.3	0.7
PY 821	-	-	-	-	-	-	-	-
PY 823	0.8	0.8	0.8	1.7	1.4	0.8	-	-
PY 826	0.8	0.8	0.8	0.8	0.8	-	-	-
PY 833	-	-	-	-	-	-	-	-
PY 841	-	-	-	2.1	1.9	-	-	-
PY 842	-	-	-	2.2	-	-	-	-
PY 875	1.1	1.7	2	>3.5	2.9	1.9	1.6	-
PY 888	-	-	-	>3.5	2.5	-	1	-
PY 890	-	-	-	>3.5	-	-	-	-
PY 896	2.7	3.2	3.5	>3.5	>3.5	3.6	3.5	2.4
PY 898	2.3	2.7	3.1	>3.5	>3.5	3	2.5	-
PY 899	2.7	2.8	3.1	>3.5	3.2	2.7	2.6	-

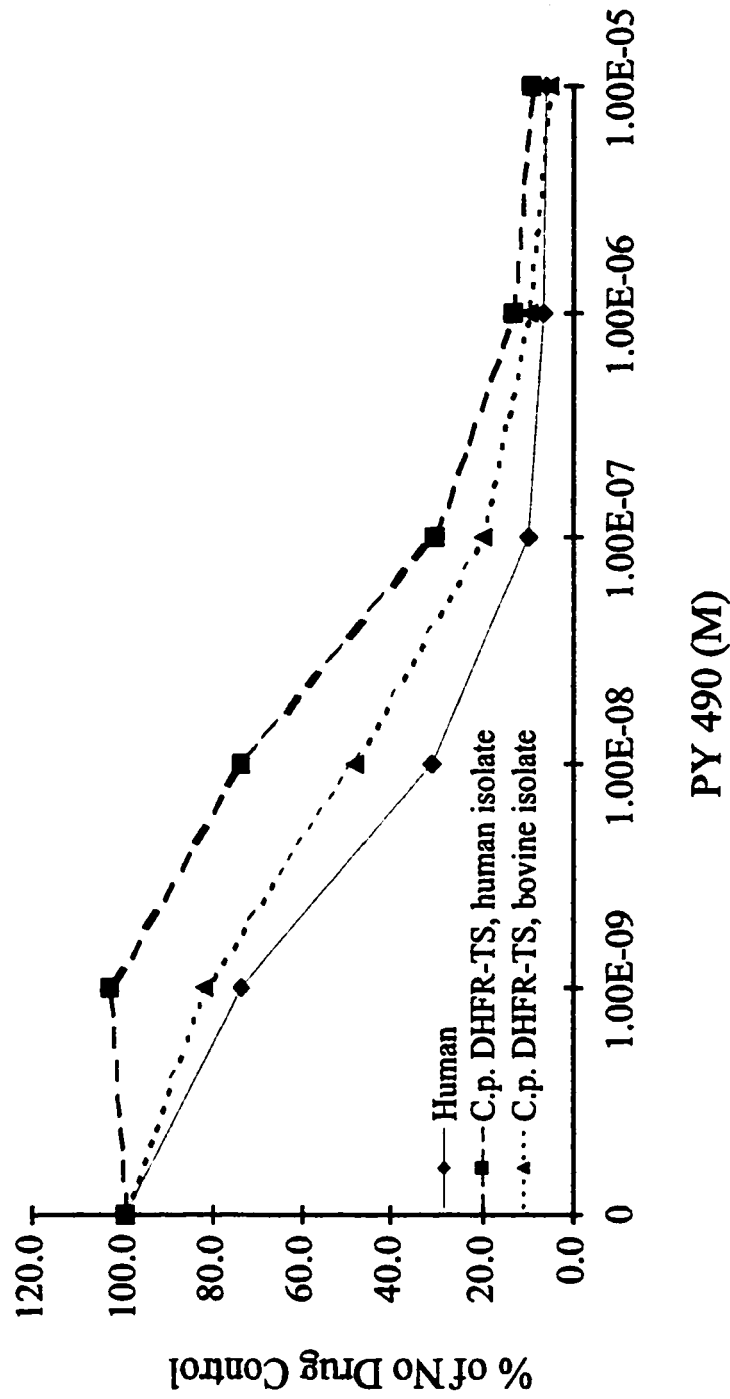


Figure 18: IC-50 assays with PY 490. Liquid assays with yeast expressing the DHFR from human, human isolate of *C. parvum*, or bovine isolate of *C. parvum* were conducted with varying concentrations of PY 490.

shown). When tested in the spoke assay, three showed promise as being selective against *C. parvum* (Table 8). When tested in liquid IC₅₀ assays, two showed good selectivity that resembled that shown by TMP (Figure 19). While none of these compounds was better than TMP, the fact that two out of six were selective is promising. WRAIR has hundreds of analogs of TMP that could be tested in this yeast assay, a task that is not possible in the parasite itself and would be very time-consuming in the *in vitro* assay.

CHAPTER SECTION: DISCUSSION

Cryptosporidium parvum infection causes life-threatening illness in immunocompromised individuals and no treatment has yet been found. Culture of *C. parvum* in the lab is difficult and laborious and *in vitro* biochemical assays on purified protein are time-consuming. These obstacles have slowed the progress of identification of a therapy. Therefore, we developed a rapid and technically easy way to screen potential inhibitors of *C. parvum* DHFR-TS using the model system *Saccharomyces cerevisiae*. We expressed the DHFR enzymes from five species in yeast and observed complementation of the *dfr1* deficiency by all of them. Although the nucleotide and amino acid sequences show wide divergence, the DHFR enzymes are functionally very conserved. This enzyme is essential and catalyzes the same reaction in all organisms. Inhibitors function by binding in the active site of the enzyme and preventing the substrate from binding. The sequence divergence leads to sufficient differences in active sites to allow particular drugs to inhibit the enzymes of some species and not others. This phenomenon has been exploited for decades as chemotherapy for bacterial and protozoal infections and we hope to use it to identify an inhibitor of *C. parvum*.

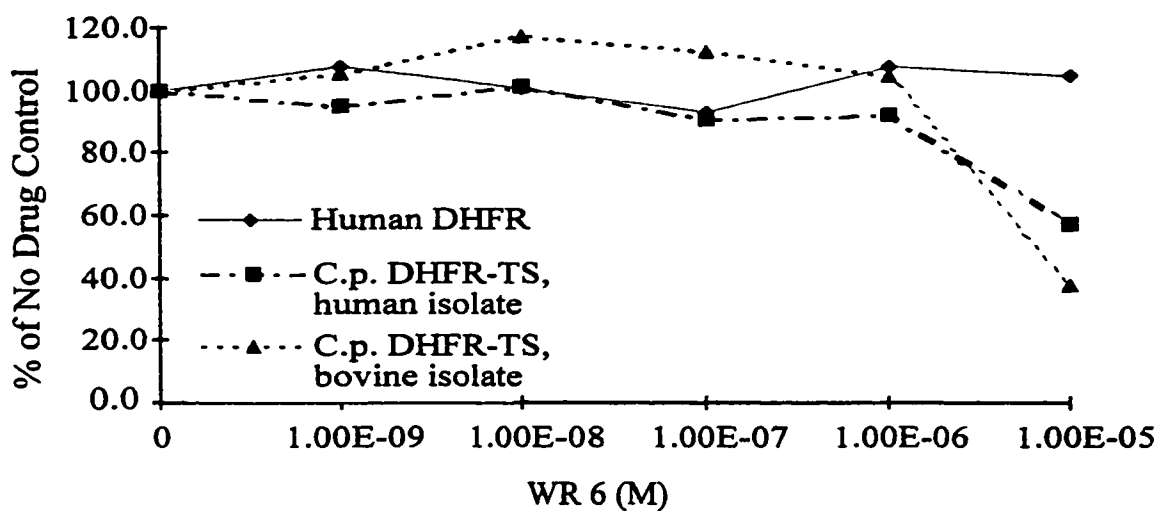
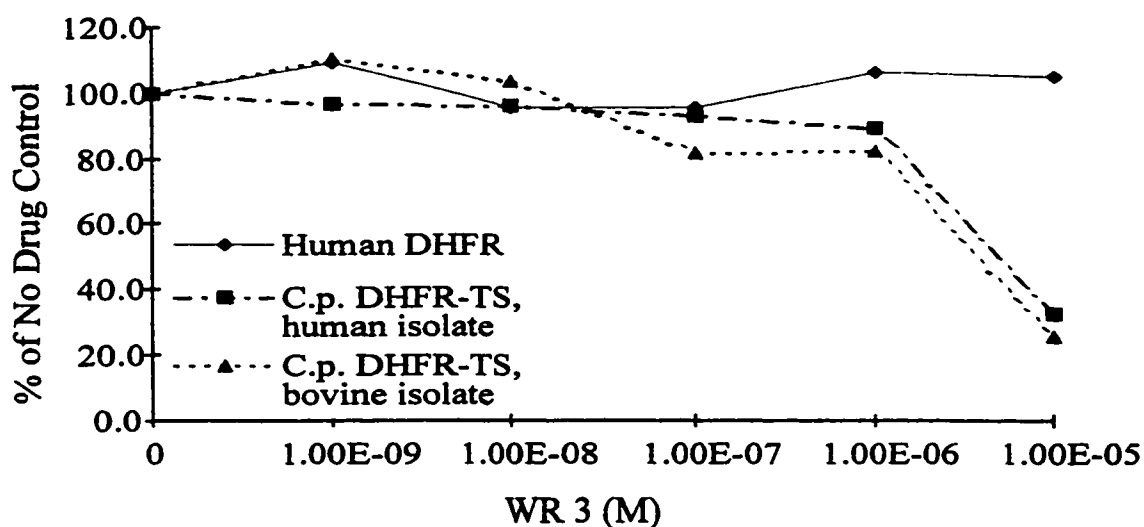
In developing this screening system, we encountered a problem with enzyme sensitivity. The first heterologous DHFR that our lab expressed in yeast was

Table 8: Drug Sensitivity to trimethoprim analogs from WRAIR. The data were obtained from spoke assays using yeast expressing heterologous DHFR enzymes. The numbers represent the distance in centimeters from the center of the plate to the beginning of yeast growth ("kill zone"). The symbol - represents no inhibition detected.

Compounds	YEAST INHIBITION (cm in spoke assay)								
	<i>C.p.</i> DHFR-TS human isolate	<i>C.p.</i> DHFR-TS bovine isolate	Human DHFR	<i>P.f.</i> DHFR Pyr. sensitive	<i>P.f.</i> DHFR Pyr. resistant	<i>T.g.</i> DHFR	<i>P.c.</i> DHFR	Yeast DHFR	
	2.5	2.5	3.4	>3.5	3.4	3.3	2.2	-	
Trimetrexate	-	-	-	>3.5	-	-	-	-	
WR 1	-	-	-	>3.5	-	-	-	-	
WR 2	-	-	-	>3.5	-	-	-	-	
WR 3	1.1	1.0	-	>3.5	-	-	0.7	-	
WR 4	-	-	-	>3.5	1.3	-	-	-	
WR 5	-	-	-	2.0	-	-	-	-	
WR 6	-	1.0	-	>3.5	2.8	-	-	-	

IC-50 Assay

Drug	DHFR		
	Human	hCp	bCp
Trimethoprim	>10 ⁻⁵	6.8 x 10 ⁻⁶	3.3 x 10 ⁻⁶
WR 3	>10 ⁻⁵	7.3 x 10 ⁻⁶	6.1 x 10 ⁻⁶
WR 6	>10 ⁻⁵	1.2 x 10 ⁻⁵	8.4 x 10 ⁻⁶



Drug	DHFR		
	Human	C.p. human isolate	C.p. bovine isolate
Trimethoprim	$> 10^{-5}$	6.8×10^{-6}	3.3×10^{-6}
WR 3	$> 10^{-5}$	7.3×10^{-6}	6.1×10^{-6}
WR 6	$> 10^{-5}$	1.2×10^{-6}	8.4×10^{-6}

Figure 19: IC-50 assays with trimethoprim analogs WR 3 and 6. Both compounds show similar selectivity as trimethoprim for *C. parvum* DHFR-TS. The calculated IC-50s for these two drugs and trimethoprim are listed.

the malaria (*P. falciparum*) DHFR (Wooden et al., 1997). This enzyme nicely complemented the yeast deficiency and was sensitive to *P. falciparum* DHFR-specific drugs at concentrations that are close to those used to inhibit the parasite itself in culture. We expected this to be true for other heterologous DHFR enzymes, but discovered that the other enzymes were much less sensitive in this system. TMX, the drug used to optimize the assay, is a close analog of DHF, the natural substrate, and binding of TMX to DHFR enzymes is close to stoichiometric. Thus, the amount of drug needed to inhibit a particular yeast strain reflects the amount of enzyme present. Since more than three orders of magnitude more TMX was needed to inhibit the new strains, we concluded that these strains must express far more enzyme. The observation that a mutated promoter resulted in increased sensitivity supports this hypothesis. The truncated version of the promoter reduced the expression level sufficiently that the new strains could be inhibited concentrations of TMX in a practical range.

For codons that are redundant, each organism preferentially employs particular codons over others and apparently adjusts its tRNA expression and charging level accordingly (Kurland, 1991; Kurland, 1993). The heterologous DHFR enzymes we expressed in yeast have codon preferences that differ from yeast, sometimes markedly. For example, the *P. falciparum* genome is almost 80% A:T and the yeast expressing the *P. falciparum* DHFR are more sensitive to antifolates apparently because the coding sequence contains many rare codons and the enzyme is thus expressed at a much lower level. A prevalence of rare codons has been correlated with poor translation efficiency because the yeast do not express the higher levels of tRNA's needed by the *P. falciparum* sequence. In particular, it is believed that the occurrence of several rare codons in a row pauses translation. Less translation means a lower level of protein and presumably greater sensitivity to DHFR inhibitors. Evidence that supports this explanation comes from a sequence we obtained from

Worachart Sirawaraporn (Sirawaraporn et al., 1993). This sequence encodes the same protein as the D6 *P. falciparum* DHFR coding sequence (PyrS), but the codons have been altered to match the *E. coli* codon bias. This alteration results in higher expression in *E. coli* and apparently in yeast as well. When Kelly Hamilton in our laboratory transferred this sequence to our expression vector and expressed it in yeast, he observed a high degree of resistance to pyrimethamine (personal communication). The protein sequences are the same, but the codon composition is very different, suggesting that codon frequency may indeed be affecting the level of expression and therefore antifolate sensitivity. We suggest that the human and *C. parvum* enzymes do not suffer from severe expression limitations and thus expression from the 600 bp promoter provides far too much enzyme for the screen to be successful.

An alternative hypothesis to explain the difference between the native and engineered sequence is the prevalence of inappropriate transcription termination signals. Transcription termination signals in yeast are A/T rich sequences and are not normally present in the coding region. Protozoal genomes are A/T rich and may use different sequences or mechanisms to stop transcription. Thus the yeast transcription termination sequences may be fortuitously present in the protozoal coding region. This has been observed with the *P. falciparum* topoisomerase II gene (Sibley *et al.*, 1997). Removal of those sites from the coding sequence enhanced the expression level of that gene in the yeast. The *P. falciparum* DHFR coding sequence has many putative transcription termination signals as well. Thus altering the codon frequency for *E. coli* preferences (~ 52% G/C) may remove many of the inappropriate transcription termination signals, thereby improving expression level. Most likely, both codon preference and transcription termination signals play a role in reducing the expression level of *P. falciparum* DHFR. The human and *C. parvum* DHFR genes apparently do not suffer as much from these difficulties, resulting in a higher expression level. Human sequences tend to be slightly G/C rich (53%). The *C.*

parvum gene is A/T rich but has few potential transcription termination signals. Thus the expression of these DHFR enzymes in the yeast was in excess of that required to provide sensitivity to drugs targeting this enzyme.

The truncated promoter still gave an insufficient degree of sensitivity. To boost the sensitivity, we added 1 mM sulfanilamide to the assays. This improved the sensitivity markedly and allowed us to test these novel compounds at a low enough concentration to be practical. Clinically, a DHFR inhibitor is always used in conjunction with a sulfa drug (except to treat human cancer). Thus, addition of sulfanilamide to the assay does not detract from the validity of the approach and resulting data.

Comparison of the *in vitro* data with the yeast data reveals that the compounds differ in their ability to permeate the yeast. For instance, 112421 has an *in vitro* IC_{50} of 0.07 μ M for the human isolate of *C. parvum* but in yeast the IC_{50} is 14 μ M. Yet trimethoprim, with an *in vitro* IC_{50} of 5 μ M has a yeast IC_{50} of 6.8 μ M. Even though 112421 shows a greater efficacy *in vitro* than TMP, in the yeast the *C. parvum* enzymes are more sensitive to TMP. It is possible that the yeast may be more permeable to TMP or that they may pump 112421 back out of the cell. This may be valuable information since a particular compound such as 112421 that has difficulty entering the yeast may also have trouble permeating mammalian and *C. parvum* cells. The same rationale applies if a compound is easily transported out of the cell. Importantly, the permeability or transport characteristics for the yeast strains expressing various heterologous DHFR's will be the same, so relative sensitivity for different species of DHFR with the same drug still will be valid.

The permeability issue is one disadvantage of the yeast model, but many compounds, such as those designed and synthesized Andre Rosowsky at Dana-Farber, have been designed to be lipophilic. These compounds probably cross the

plasma membrane easily, without the need for a transport protein. Drugs in this class are preferable because resistance cannot occur by mutation of a transport system. Resistance to drugs that are poorly taken up such as the cancer drug methotrexate (MTX) often occurs by a mutation that affects the reduced folate transport system which is responsible for transporting the drug into the cell. Lipophilic drugs, on the other hand, pass directly through the lipid bilayer and can achieve higher concentrations within the cell (Lin and Bertino, 1987). Indeed, Dr. Rosowski's compounds did inhibit very well. Unfortunately, they were not selective. Combining the lessons from TMP (selective) and the lipophilic compounds (effective) may lead to a clinically useful agent against *Cryptosporidium parvum*.

The yeast expressing *P. falciparum* DHFR, when grown in 1 mM sulfanilamide, are extremely sensitive to DHFR inhibitors. We have found that this strain is inhibited by nearly all of the compounds we have tested. The inhibition of *P. falciparum* DHFR confirms that the novel compounds are able to enter the cells, although we can not distinguish between inhibition that is due to good sensitivity of the enzyme to that particular drug and inhibition due to permeability of the cells to that compound. If the *P. falciparum* DHFR yeast strain is not inhibited by a particular compound, the explanation could be poor permeability or true insensitivity of the enzyme. Compounds that inhibit none of the strains may suffer from poor permeability and must be tested for *in vitro* enzyme inhibition.

The yeast strain with its own DHFR on a plasmid serves as a control for generally toxic compounds that inhibit by means other than DHFR. This strain is very insensitive to various DHFR inhibitors. Thus, when this strain is inhibited, non-DHFR inhibition of the yeast is suggested. The specificity of that particular compound can be tested by repeating the experiment in the presence of dTMP. The assay uses D plates which contain adenine, methionine, and histidine, three of the four products of the folate pathway. Supplementation with dTMP removes all need for a functioning

folate pathway. If the compound still inhibits in these conditions, then it is acting on a non-folate pathway target. This non-specificity was observed with NCI compound 117288. However, the *P. falciparum* DHFR was inhibited somewhat more in the absence of dTMP, suggesting that 11728 inhibits both at DHFR and at a second site.

The strain expressing the yeast DHFR is probably less sensitive because of the high level of DHFR expression. We have observed that the lower the expression level of DHFR, the slower the yeast grow. The parent strain, with DHFR on the chromosome driven by the native promoter, grows much more rapidly than the strain in which the same DHFR is on the plasmid. The yeast DHFR on the plasmid is driven by the 600 bp promoter; a truncated version of the chromosomal yeast DHFR promoter, this shorter promoter provides enough expression to override sensitivity of the human and *C. parvum* DHFR enzymes to trimetrexate (Figure 15A). Additionally, the yeast DHFR coding region does not suffer from a different codon bias as the heterologous sequences do (see above). Thus, the yeast DHFR on the plasmid is probably expressed at such a high level that the strain is rarely specifically inhibited because the drug concentrations in the spoke and liquid IC₅₀ assays do not achieve a sufficient level.

The yeast DHFR exists as a single domain protein and the yeast thymidylate synthase (TS) is a separate coding sequence. The strain of yeast we use has the endogenous DHFR disrupted but not the TS. Hence the yeast expressing the *C. parvum* DHFR-TS protein have two copies of the TS gene. While the additional copy of TS may cause some interference, we have not observed any indications that two copies provide significant interference.

While we found no compounds that are potentially useful clinically, we did identify several interesting leads. Trimethoprim (NCI 106568) is selective for both *C. parvum* enzymes over the human enzyme, a requirement for clinical use.

Although the *C. parvum* sensitivity to this particular drug is not very high, hundreds of analogs have been synthesized and are available from Walter Reed Army Institute for Research (WRAIR). This collection may contain compounds with greater effectiveness against *C. parvum* that still maintain selectivity. I tested six of those compounds and two showed similar sensitivities as TMP. Further screening may identify better inhibitors. Additionally, NCI compounds 112421 and 121146 and several Dana-Farber compounds were very effective against the *C. parvum* enzymes. Using these data, chemists may be able to rationally design better inhibitors based on observed sensitivities of existing compounds.

The screen described here using yeast expressing heterologous DHFR enzymes provides a rapid method for identifying potential drugs for treatment of Cryptosporidiosis. One limitation of the assay is the differing permeability characteristics of the compounds. Misleading data may result from compounds that cannot enter the cells efficiently. The various DHFR enzymes employed as controls should minimize that risk by identifying a total lack of inhibition as a compound with potentially poor permeability. In addition, poor permeability in yeast may be predictive of the same problem in the parasite and the host. The several controls can provide other information as well. A *C. parvum* culture system can only classify compounds as effective against the parasite or toxic to the host cells. The strain expressing the yeast DHFR on the plasmid, however, can identify non-specific inhibition that may lead to description of new drug targets. In addition, compounds may be identified that specifically inhibit the control DHFR enzymes and could be pursued as therapeutic leads for the infections caused by those organisms. Furthermore, the data can be used for structure-function analysis to rationally design inhibitors for each species of DHFR in the assay.

CHAPTER 2: COMPARISON OF THE *CRYPTOSPORIDIUM PARVUM* BIFUNCTIONAL DHFR-TS TO THE ENGINEERED MONOFUNCTIONAL DHFR

CHAPTER SECTION: INTRODUCTION

A better understanding of the drug target improves the search for inhibitors. The DHFR enzymes of protozoa naturally exist as a bifunctional enzyme with the DHFR domain on the amino-terminus and the thymidylate synthase (TS) domain on the carboxyl terminus (Ivanetich and Santi, 1990). With the exception of some plants (Cella *et al.*, 1991; Lazar *et al.*, 1993), other organisms, including humans, maintain DHFR and TS as separate open reading frames and proteins. An understanding of the characteristics and importance of the bifunctionality in protozoa may lead to better design of inhibitors that are selective for the parasite enzyme while not affecting the host. The goal of this chapter is to compare the activity and functionality of the *C. parvum* native DHFR-TS to the engineered DHFR domain alone. The bifunctional arrangement of DHFR-TS presumably confers an advantage over separate proteins, but little work has addressed this question (Knighton *et al.*, 1994; Sirawaraporn *et al.*, 1993). This chapter describes the use of both the yeast model system developed for screening DHFR inhibitors (Chapter 1) and purified enzymes to investigate the functional differences between the *C. parvum* DHFR and DHFR-TS.

Inhibitors of the folate pathway enzymes DHPS and DHFR (Figure 3) are administered together in the clinical setting for treating bacterial and protozoal infections. When used concurrently, the synergy between them results in a greater degree of inhibition than would be predicted based on the efficacies of each drug

alone (Berenbaum, 1978; Hewlett, 1969). This phenomenon allows the clinician to administer less drug and still see excellent inhibition. The combination also decreases the likelihood of drug resistance being selected in the population of pathogenic organisms. One mM sulfanilamide, a DHPS inhibitor, was added to the yeast media in these assays to increase sensitivity to the DHFR inhibitors, which are frequently available in very limited quantities. The synergism between the two reagents was a key to the successful development of the assay.

In developing the screening assay, the *C. parvum* DHFR-TS was expressed in the yeast as both the DHFR domain alone and as the full-length bifunctional DHFR-TS. Initially, no significant differences between the yeast dependent upon the *C. parvum* DHFR and those dependent upon the bifunctional *C. parvum* DHFR-TS were observed. However, addition of sulfanilamide to the yeast assay revealed two large differences between the strains expressing the two versions of the enzyme. First, the yeast expressing the *C. parvum* DHFR domain alone were much more sensitive to sulfanilamide than the yeast expressing DHFR-TS. Second, the yeast reliant on the DHFR domain alone failed to show the expected synergism between TMX and sulfanilamide while the yeast expressing DHFR-TS did show synergism. Further investigation of this observation revealed additional interesting differences between the two forms of the enzyme.

These observations were investigated for several reasons. First, most of the work on the *P. falciparum* enzyme has been done on the DHFR domain alone because until recently it was not possible to express the recombinant bifunctional enzyme in *E. coli* (Prapunwattana *et al.*, 1996; Sirawaraporn *et al.*, 1993; Sirawaraporn *et al.*, 1990). The comparison of the two forms of the purified *P. falciparum* enzymes *in vitro* showed that there was little difference between them (Sirawaraporn *et al.*, 1993). One can reason that the separated domains of the bifunctional protein should function individually, since most organisms express DHFR

and TS as separate proteins. Thus, it has been thought that there is no meaningful difference between the natural DHFR-TS and the single domain DHFR forms of the enzyme. Preliminary data described below on the *C. parvum* enzyme, however, suggested that there are significant differences between the two forms of the enzyme. The question was investigated further to determine whether that inference was correct. If so, then this work will have important implications for the work on the isolated domain of *P. falciparum* DHFR.

A second reason for further study of this problem is that the mechanism of synergy is not understood and is, in fact, still debated (Sims *et al.*, 1998; Watkins *et al.*, 1997). Two schools of thought exist to explain synergy. One reasons that the sulfa drugs and DHFR inhibitors must bind to the same protein (Segel, 1975; Webb, 1963). The other, sequential blockade, argues that the two drugs inhibit different proteins that act sequentially in the same pathway (Black, 1963; Grindley, 1975). While the latter hypothesis is more generally accepted, some still adhere to the first explanation and indeed cases have been found where synergy does not result from sequentially acting drugs (Rubin, 1964). The data reported here indicated that the yeast expressing the DHFR-TS from *C. parvum* showed synergy between TMX and sulfanilamide but the yeast dependent on the DHFR alone did not show synergy (see below). This was a very surprising result and highlighted the fact that the mechanism for synergy is not understood. The investigation of the two forms of the *C. parvum* DHFR can provide evidence to differentiate between the two models of the synergy mechanism. Lastly, I wanted to elucidate the basis for the differences between the two forms of the enzyme because I found it a very interesting problem that may have ramifications for our yeast model system.

CHAPTER SECTION: DIFFERENCES BETWEEN *C. PARVUM* DHFR AND DHFR-TS EXPRESSED IN YEAST

The initial observation of differences between the DHFR and DHFR-TS forms of the *C. parvum* enzyme was made in the yeast expression system. The DHFR domain alone or the full-length DHFR-TS was expressed from the same yeast expression vector. The strain of yeast used was TH5, which has the endogenous yeast DHFR (*dfr1*) disrupted so that the transformed yeast rely on the function of the heterologous DHFR to survive (see chapter one for more details). These experiments were all conducted with the *C. parvum* enzyme that originated from a human isolate of the parasite.

The *C. parvum* DHFR and DHFR-TS were expressed in the yeast strain TH5 as described in chapter 1. The growth of these yeast was tested in liquid culture assays in the presence of varying concentrations of sulfanilamide. The amount of growth in each concentration of sulfanilamide relative to the solvent control (no drug) was determined and the IC_{50} calculated (concentration at which growth is inhibited by 50%). The strain of yeast relying on the *C. parvum* DHFR-TS showed an IC_{50} of 4.1×10^{-3} M while the IC_{50} of the *C. parvum* DHFR strain was 8.13×10^{-5} M (Figure 20). Sulfanilamide is supposed to target the endogenous yeast DHPS enzyme and these two strains of yeast are isogenic except for the DHFR. Therefore, this differential sensitivity to sulfanilamide was unexpected and intriguing.

During the course of optimizing the DHFR inhibitor screening assay, I noticed that sulfanilamide addition to the IC_{50} assays seemed to have a greater impact on the TMX sensitivity of the yeast expressing *C. parvum* DHFR-TS than on the DHFR domain alone. To investigate this observation further, I generated isobolograms for these two strains. An isobologram is a graphical method for

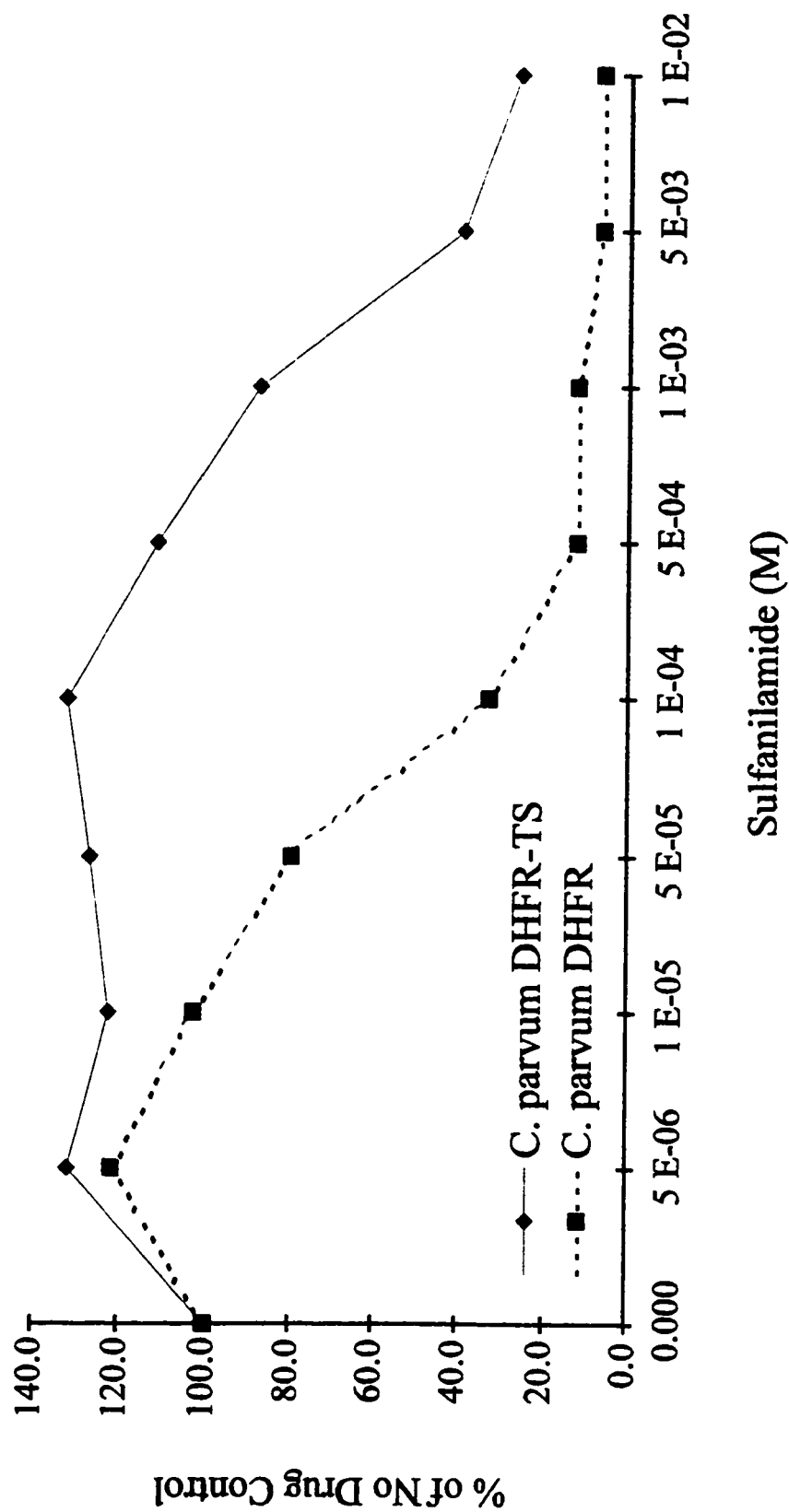


Figure 20: IC-50 Assay. Yeast expressing *C. parvum* DHFR or DHFR-TS growth was measured in the presence of varying concentrations of sulfanilamide.

determining the degree of synergy between two drugs (Figure 21). The data required for an isobologram are generated by a two-way titration of the drugs. IC_{50} assays are conducted with each drug alone and with a fixed amount of one drug while varying the other. The IC_{50} values for each drug alone are plotted on each axis and connected by a line. The IC_{50} values for the two drugs at varying concentrations are plotted on that graph. If the points fall along the line connecting the single point IC_{50} values, the two drugs interact additively – there is no advantage to using the combination. You could obtain the same results by using more of one of the drugs. If instead the points fall above the line, then the two drugs antagonize each other and less inhibition is observed with the combination than with the drugs separately. If the points fall below the line, then the two drugs synergize and more inhibition is observed with the combination than separately: the further below the line the points lie, the more synergistic the interaction.

The yeast strain expressing *C. parvum* DHFR-TS was analyzed with this technique using trimetrexate and sulfanilamide. Table 9 shows the raw data from that experiment to clarify the derivation of the isobologram. The IC_{50} for TMX in the presence of each concentration of sulfanilamide was plotted (Figure 22A), with TMX concentration on the Y axis and sulfanilamide concentration on the X axis. The IC_{50} points fall well below the additivity line, demonstrating the potent synergy expected for these two drugs.

The experiment was repeated using yeast expressing the *C. parvum* DHFR domain alone. The data were plotted as before, but this time the IC_{50} values fell along the additivity line (Figure 22B). Contrary to expectations, this DHFR did not show synergy; the two drugs act additively on this strain. This yeast strain was more sensitive to sulfanilamide, but the concentrations of that drug used were in an appropriate range for this strain. The lowest concentration of sulfanilamide used in

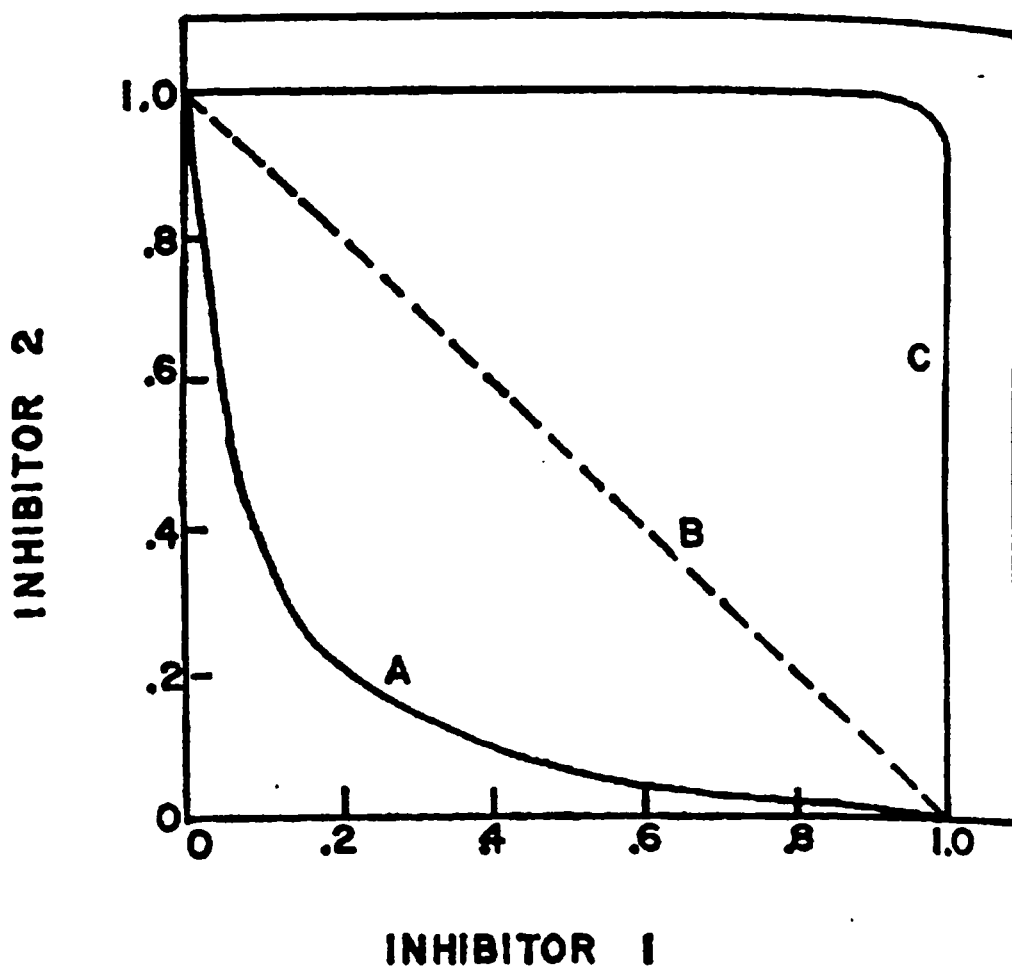


Figure 21: Isobologram diagram. Line A represents the curve expected when synergy is present. B represents the line expected when the two inhibitors act additively. C represents the curve expected when the inhibitors antagonize each other. Diagram from Rubin, R. J., Reynard, A., Handschumacher, R. E. (1964). An Analysis of the Lack of Drug Synergism during Sequential Blockade of *de Novo* Pyrimidine Biosynthesis. *Cancer Research* 24, 1002-1007.

Table 9: Sample data used for plotting isobologram. A) Calculation of IC-50 values B) Table compiling data used for plotting isobologram. Values are the IC-50's for each pair of drug concentrations. Except for sulfanilamide alone, the values are taken from the data in A.

A

		% of No Drug Control											
TMX (M)	Sulfanilamide (M)												
		0	5.00E-06	1.00E-05	5.00E-05	1.00E-04	5.00E-04	1.00E-03	5.00E-03	1.00E-02	5.00E-02	1.00E-01	1.00E-01
0	0	100	100	100	100	100	100	100	100	100	100	100	100
1.E-09	133.5	103.2	106.4	108.5	101.4	117.8	91.7	104.6	97.6	102.4	59.8	36.2	26.8
1.E-08	124.9	119.1	105.4	103.3	114.1	118.3	89.7	89.3	52.6	23.5	11.2	5.1	7.9
1.E-07	137.1	111.3	109.8	121.8	111.3	107.0	63.5	52.6	23.5	11.2	5.1	7.9	7.9
1.E-06	138.3	115.0	111.3	110.9	96.8	54.7	22.2	23.5	11.2	5.1	7.9	7.9	7.9
1.E-05	103.7	82.8	78.0	56.5	39.2	8.3	5.0	11.2	5.1	7.9	7.9	7.9	7.9
1.E-04	21.5	14.7	18.8	14.4	8.3	12.6	2.3	5.1	7.9	7.9	7.9	7.9	7.9

66

slope	-912779	-756430	-657966	-467928	-6404438	-5155875	-4.6E+07	-3.2E+07	-2.6E+07
intercept	112.7789	90.3177	84.55682	61.14616	103.2274	59.83213	68.11927	55.78231	62.46719
IC-50	6.88E-05	5.33E-05	5.25E-05	2.38E-05	8.31E-06	1.91E-06	3.95E-07	1.79E-07	4.75E-07

B

50% inhibition obtained at:

Sulfanilamide	0	5.00E-06	1.00E-05	5.00E-05	1.00E-04	5.00E-04	1.00E-03	5.00E-03	1.00E-02	4.10E-03
TMX	6.9E-05	5.3E-05	9.3E-05	2.0E-05	8.3E-06	1.9E-06	4.0E-07	1.8E-07	4.8E-07	0

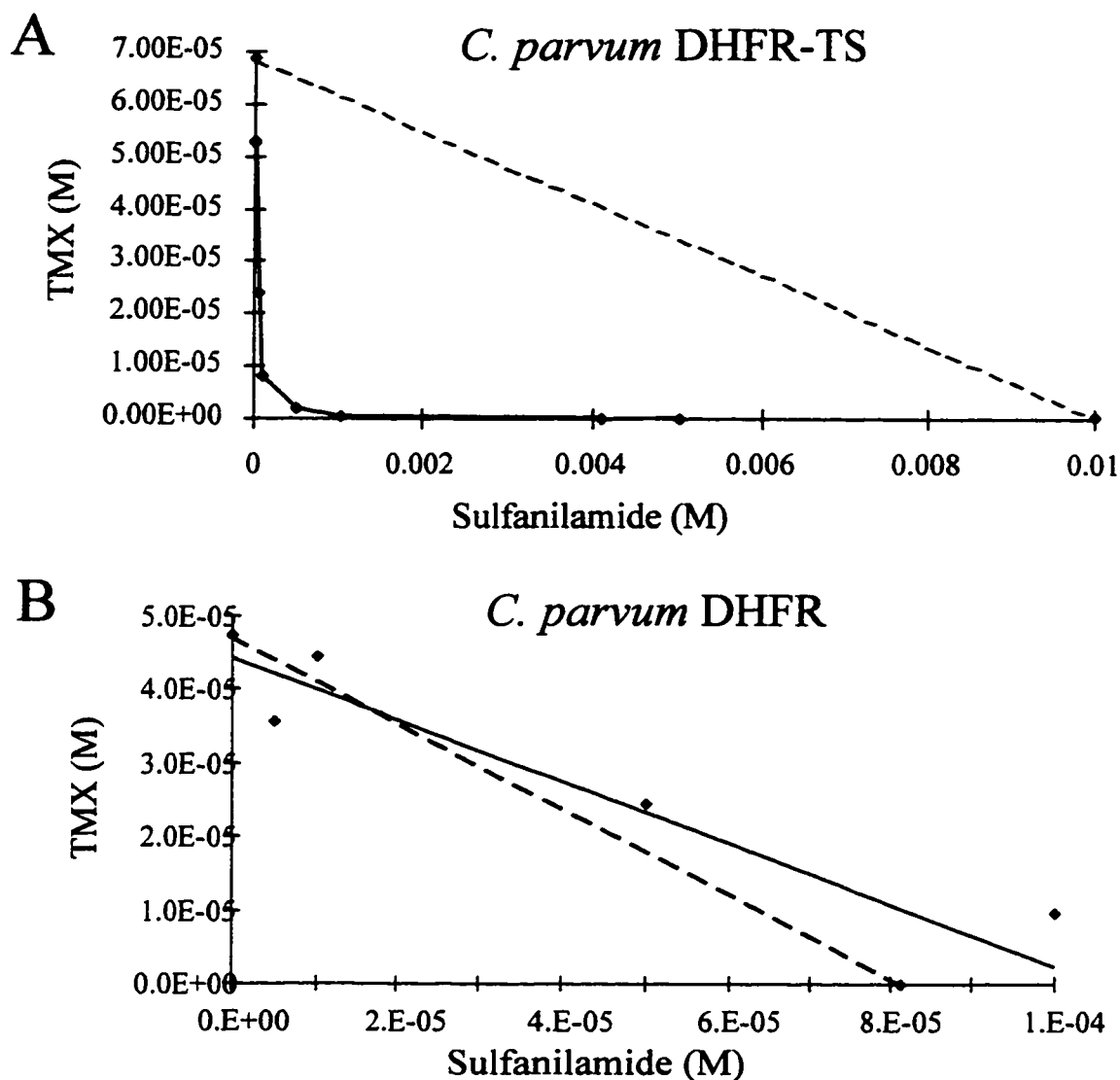


Figure 22: Isobolograms. The points are the TMX IC-50 values in the presence of that concentration of sulfanilamide. The dashed line connects the IC-50 values for each drug individually. A) yeast expressing *C. parvum* DHFR-TS. The red line connects the IC-50 values for the two drugs concurrently. B) yeast expressing *C. parvum* DHFR. The red line is the trend line for the IC-50 values for the two drugs concurrently.

concentration with TMX was below the concentration required to inhibit the yeast on its own.

One possible explanation was that DHFR enzymes that are single domains in general do not show synergy in the yeast system. To address that concern, I constructed an isobologram using yeast expressing the human DFHR which is naturally a single domain protein (Figure 23). Like the DHFR-TS, the isobologram showed good synergy between TMX and sulfanilamide. Thus, the synergy was not dependent on a bifunctional DHFR-TS.

An isobologram was also generated for the single domain DHFR from *P. falciparum* strain D6 (Figure 24). The yeast expressing the D6 DHFR showed modest synergy between TMX and sulfanilamide but not nearly as much as expected (e.g. the synergy shown by *C. parvum* DHFR-TS). At the time of these experiments, a *P. falciparum* DHFR-TS construct was not available to test in this method. Som Mookerjee, in our laboratory, has since generated yeast expressing the bifunctional protein and his preliminary data show that this version does indeed show potent synergy (data not shown). Therefore, synergy is observed in yeast reliant on either *C. parvum* and *P. falciparum* DHFR-TS proteins but not in yeast reliant on the DHFR domains alone.

CHAPTER SECTION: PURIFICATION OF *C. PARVUM* DHFR AND DHFR-TS

Work with purified DHFR enzymes has shown that sulfa drugs can inhibit the DHFR enzyme directly, at least at high concentrations. Sulfanilamide is an analog and competitive inhibitor of para-aminobenzoic acid (pABA), one of the two substrates of DHPS. The natural DHFR substrate, dihydrofolate (DHF), contains the

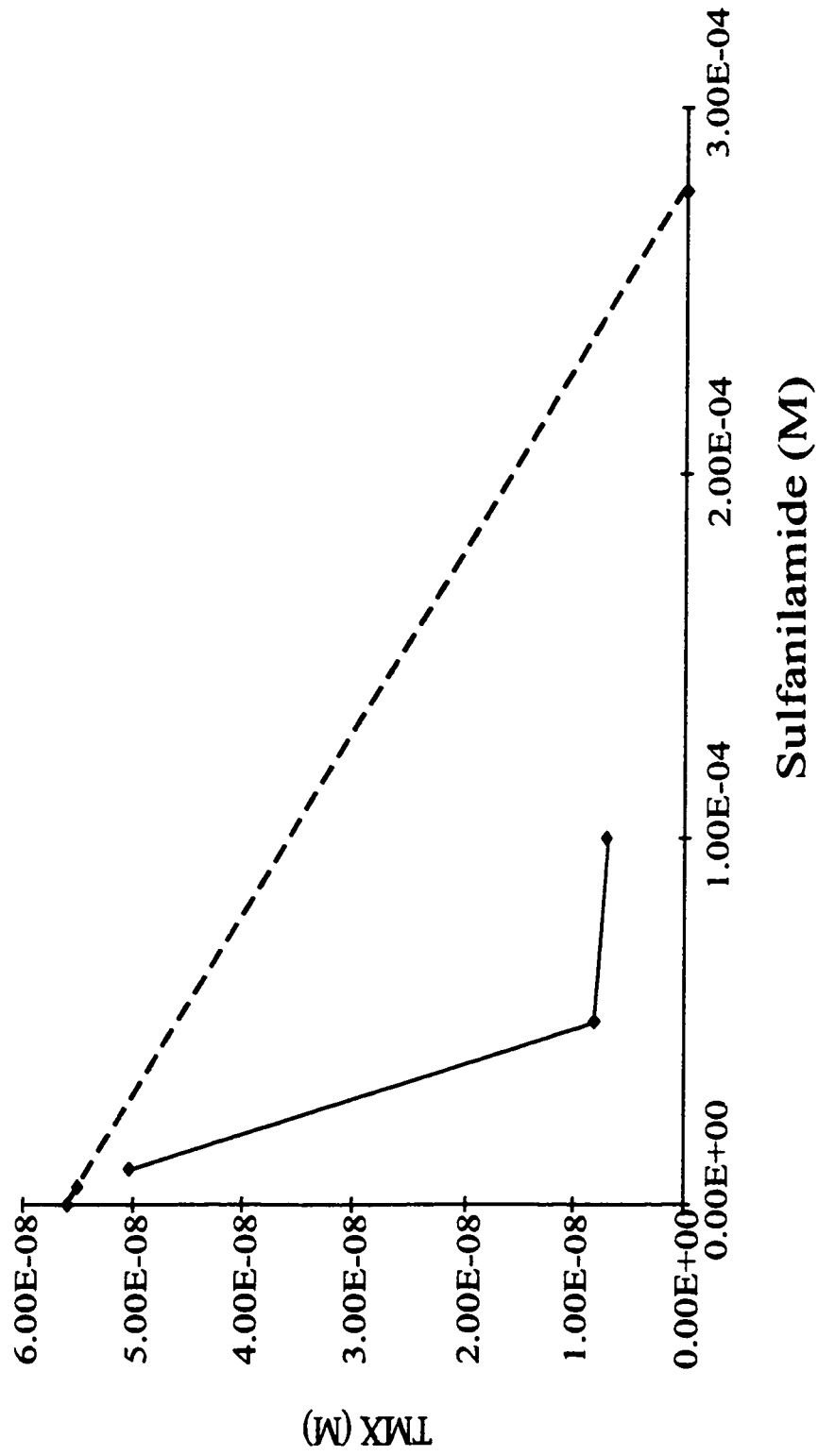
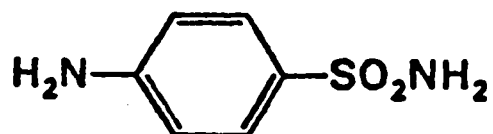


Figure 24: Isobologram for yeast expressing the *P. falciparum* DHFR.

A



B



C

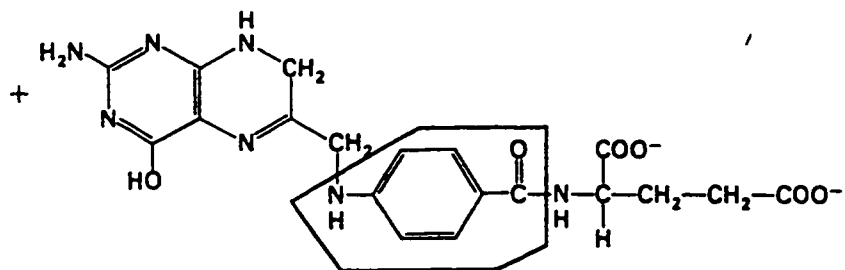


Figure 25: Chemical structures. A) pABA, the natural substrate of DHPS. B) Sulfanilamide, an inhibitor of DHPS. C) DHF, natural substrate of DHFR. The pABA moiety of DHF is enclosed by a box.

pABA moiety. Presumably, that moiety occupies a portion of the DHFR active site. It is possible that sulfa drugs are able to bind in that portion of the DHFR active site (Figure 25).

Sirawaraporn and Yuthavong (1986) showed that the *Plasmodium chabaudi* DHFR-TS purified enzyme showed synergy *in vitro* between sulfadoxine (a relative of sulfanilamide) and pyrimethamine (a specific inhibitor of the *Plasmodium* DHFR enzyme). An isobologram generated with the purified DHFR-TS gave a curve for synergy, although the degree of synergy observed was not as great as seen *in vivo*. These results suggest that the sulfa is binding and inhibiting the DHFR-TS directly and that the *in vivo* synergy may partially result from the two drugs acting on the same target. Additionally, sulfa drugs have been found to inhibit the *E. coli* DHFR *in vitro* (Poe, 1976). All of these experiments, however, demonstrated that the IC_{50} of sulfa drugs for the DHFR is very high (2.8×10^{-3} M for *P. chabaudi*) while the IC_{50} for the same drugs on the DHPS target is in the 10^{-5} M range. The concentration of sulfanilamide used in the yeast assays is 1 mM. We do not know how much of the sulfanilamide is actually able to enter the cell and thus the intracellular concentration is unknown. The drug may be present at a high enough concentration inside the yeast cells to be affecting the DHFR directly. To investigate whether the sulfanilamide is able to inhibit the *C. parvum* DHFR directly, I purified the DHFR and DHFR-TS proteins and tested their sensitivity *in vitro*.

The first step was to purify the *C. parvum* DHFR from the yeast. To evaluate the feasibility, I made yeast extracts and used the biochemical assay on the crude extracts. The yeast strains were the parental TH1 line with the yeast DHFR expressed at a relatively high level from the chromosomal location and the TH5 line with no DHFR activity. The *in vitro* assay for DHFR measures the decrease in absorbance of NADPH as it is used in the reaction: $DHF + 2NADPH \rightarrow THF + 2NADP$. Other reductases in the cell also use NADPH. Thus, TH5 is used as a

control for the non-DHFR background activity in the cell extract. DHFR activity was detectable in TH1 extracts over the TH5 background but at a low level. No activity over background was detectable in extracts from yeast expressing the *P. falciparum* DHFR from the usual Cen plasmid or from a higher copy number (higher expression level) 2 μ m plasmid. Thus it was clear that the *in vitro* assay was not sufficiently sensitive to measure enzyme activity in crude yeast extracts.

The next step was to purify the TH1 DHFR using a commercial methotrexate affinity resin (Sigma, St. Louis, MO). Despite starting with 500 ml of yeast cells, no activity was recovered from the column fractions. Since recovering DHFR from the yeast proved to be very difficult, we decided to try overexpressing the *C. parvum* DHFR and DHFR-TS in *E. coli*.

The *C. parvum* DHFR-TS, upon induction, was overexpressed from the pET-9d plasmid in the BL21 (λ DE3) strain of *E. coli*. Good enzyme activity was detected in the induced *E. coli* extract and the DHFR-TS extract was purified over the MTX affinity column. The yield of protein from the column was 0.99 mg of protein and 16 U of activity. The *C. parvum* DHFR domain alone was also purified by the MTX column, using the same conditions. Although activity could be detected in the crude extract, none was detected in the column fractions.

A possible explanation was that the DHFR protein is in inclusion bodies. Crude extract and the pellet from the extraction were analyzed on an SDS-PAGE gel and stained with Coomassie brilliant blue. Inclusion bodies would be expected to show up as a DHFR-sized band in the pellet. A band of the expected size did not appear in either lane (data not shown). If protein was in inclusion bodies, there was not enough of it to be detected by this method.

Since DHFR activity was detected in the crude extract but not in the column fractions, we concluded that the protein was not being recovered from the column. Activity disappeared from the extract after being passed over the column, so the protein was binding to the resin. The loss could have occurred in the wash step (too stringent) or in the elution step (protein is left on the column). Alternative washing and elution conditions were tested, but no *C. parvum* DHFR protein was ever recovered.

The codon usage in the *C. parvum* DHFR deviates significantly from the *E. coli* preferred codons. It is probable that this deviation is reducing expression level of the *C. parvum* DHFR in the *E. coli*. The low expression level may be part of the reason for the difficulty in purifying this protein. Arthur Baca in Wim Hol's laboratory (University of Washington) designed a plasmid, RIG, that contains the coding sequences for *E. coli* tRNA's AGA (Arg) and ATA (Ile), and GGA (Gly). These codons are rare in *E. coli* but used heavily in protozoa, including the *C. parvum* DHFR (Table 10). Cotransforming the RIG plasmid with the DHFR plasmid could allow the cells to translate more protein, making it easier to purify.

Table 10. Comparison of codon preferences in *E. coli* and *C. parvum* DHFR for the tRNA codons found on the RIG plasmid.

Codon	<i>E. coli</i> (# / 1000)	<i>C. parvum</i> DHFR-TS (# / 1000)
AGA	0.00	33.5
ATA	0.15	50
GGA	0.44	20

The RIG plasmid was cotransformed into *E. coli* BL21 cells with the *C. parvum* DHFR plasmid. The crude extract prepared from these cells yielded 0.08 U/mg, better than the yield without the RIG plasmid (0.06 U/mg) and almost at the

same level as the DHFR-TS (0.09 U/mg). The *C. parvum* DHFR is nearly the same size as the *E. coli* DHFR on an SDS-PAGE gel. Thus, the extract was tested with TMP and NCI 114923 to verify that the activity was *C. parvum* DHFR and not *E. coli* DHFR. *E. coli* DHFR is very sensitive to TMP and NCI 114923, while *C. parvum* is slightly sensitive and not sensitive, respectively. The activity in the crude extract agreed with drug sensitivities expected for the heterologous *C. parvum* DHFR.

Cotransformed *E. coli* were induced and the lysate was purified on the MTX column. This column was washed gently and a strong elution buffer used. This time several fractions contained DHFR activity. The yield of protein from the column was 1.15 mg of protein and 7.6 U of activity. While I recovered the same amount of protein as for the DHFR-TS, I had only half as much activity. In addition, I noticed that recovery from the Sephadex G-15 columns (used to remove the DHF used in elution) was considerably poorer for the *C. parvum* DHFR than the DHFR-TS.

CHAPTER SECTION: *IN VITRO* ASSAYS OF PURIFIED *C. PARVUM* DHFR AND DHFR-TS

The first step in evaluating the purified *C. parvum* proteins was to determine the kinetic properties of each enzyme. The K_m of DHF, the K_m of the cofactor (NADPH), and the maximum velocity (V_{max}) values for each form of the enzyme were determined using the *in vitro* biochemical assay, described in detail in chapter 4 (Sirawaraporn et al., 1993). These data are summarized in Table 11.

Table 11: Kinetics of the purified *C. parvum* DHFR and DHFR-TS. The data shown is the average +/- the standard deviation.

	<i>C. parvum</i> DHFR		<i>C. parvum</i> DHFR-TS	
	K_m (μ M)	V_{max} (U/mg)	K_m (μ M)	V_{max} (U/mg)
DHF	3.0 +/- 1.8 n=3	2.9 +/- 1.1 n=3	4.7 +/- 3.6 n=7	2.4 +/- 0.5 n=7
NADPH	23.0 +/- 1.4 n=3	3.5 +/- 1.3 n=3	8.3 +/- 3.5 n=5	2.3 +/- 0.3 n=5

The *C. parvum* DHFR showed very poor stability *in vitro*. While the DHFR-TS enzyme had good stability and lost little activity over the course of a month at 4°C, the DHFR enzyme lost activity during the course of an afternoon. As a result, on occasion the V_{max} value was very low, indicating that much of the enzyme was no longer active. Data from preparations with low V_{max} values were not used in the calculations shown in Table 11. The results tabulated in Table 11 indicate that the two forms of the enzyme, DHFR and DHFR-TS, do not have significantly different affinities for the natural substrate, DHF. The affinities for the cofactor NADPH, however, are not identical between the two forms. The DHFR domain alone had a lower affinity for NADPH and required a higher concentration of the cofactor for half maximal velocity (K_m). The V_{max} is the maximal rate at which the reaction can proceed. The V_{max} values calculated for the DHFR and the DHFR-TS were in reasonable agreement. In addition, the V_{max} values calculated from the DHF and NADPH kinetics are indistinguishable, giving further confidence to the calculations.

Next, the relative affinity of TMX for the two forms of the enzyme was determined. The IC_{50} for the *C. parvum* DHFR-TS was 3.4×10^{-8} M (n=3); slightly

higher than the value obtained by John Vasquez in his *in vitro* assays (4×10^{-9} M). Dr. Vasquez conducted his *in vitro* assays at 37°C whereas the results shown here were measured at room temperature. The temperature difference may explain the variance. The IC_{50} obtained for the *C. parvum* DHFR domain alone was 1.9×10^{-7} M (n=3); 6-fold higher than for DHFR-TS. A similarly high IC_{50} (4×10^{-7} M) was calculated using the crude extract from the DHFR strain, indicating that the purification procedure did not result in an alteration of affinity.

The inhibition of the DHFR and DHFR-TS enzymes by sulfanilamide was also determined. Both the DHFR and DHFR-TS enzymes showed modest sensitivity to sulfanilamide *in vitro*. The degree of inhibition varied somewhat among experiments but the pattern of sensitivity was consistent for both versions of the enzyme. At the highest and lowest concentrations, both enzymes showed insensitivity to sulfanilamide, but at intermediate concentrations, the enzymes were partially inhibited (Figure 26). Although the variability of the data precluded a solid conclusion, the DHFR domain alone seemed to show a peak of sensitivity at 1 mM sulfanilamide, while the DHFR-TS was maximally sensitive at 5 mM.

The interactions between the DHFR, TMX and sulfanilamide when both drugs are present concurrently was also an important issue. The modest effect of sulfanilamide made it impossible to determine an IC_{50} value, so isobolograms could not be constructed. Nonetheless, comparison of the TMX/sulfanilamide data with the single drug data did reveal a pattern. Sample data are shown in Tables 12 and 13 and the conclusions are shown in Table 14. Although sulfanilamide could inhibit DHFR directly, this occurred only when TMX was present at a low concentration. With a higher TMX concentration, the inhibition generally was equivalent to TMX alone, suggesting that the TMX has a higher affinity for the enzyme and successfully competed with the sulfanilamide in the binding site. In Table 12, the DHFR domain alone showed a lower affinity for TMX, so even at 1×10^{-7} M, inhibition intermediate

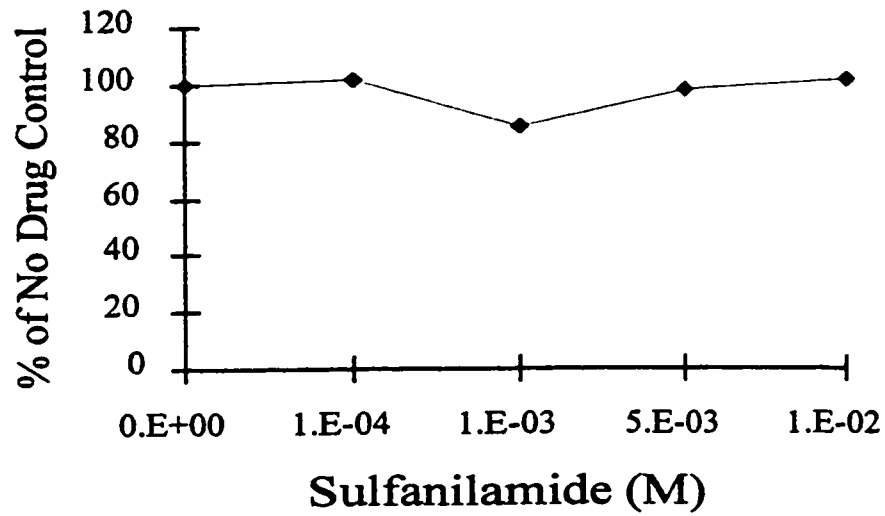
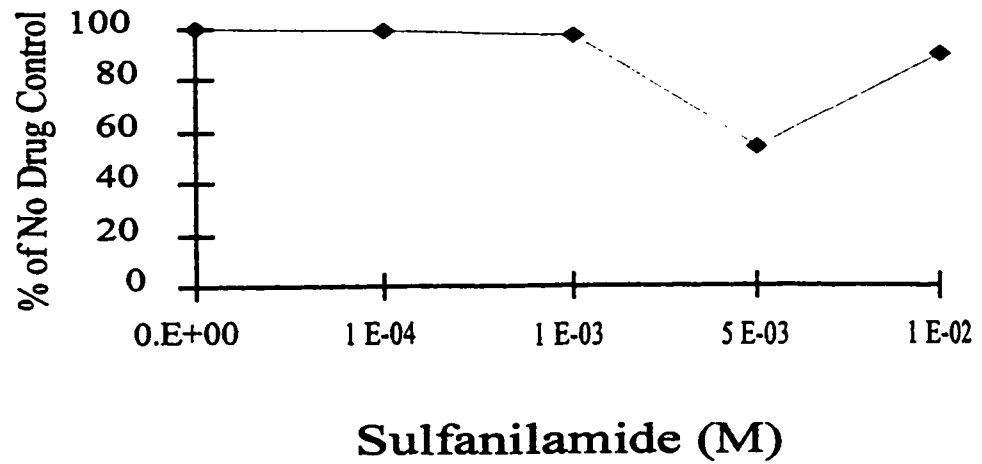
A*C. parvum* DHFR**B***C. parvum* DHFR-TS

Figure 26: In vitro sensitivity of purified *C. parvum* enzymes to sulfanilamide. A) DHFR domain alone B) DHFR-TS

between that of TMX or sulfanilamide alone was seen.

Table 12: Representative data of TMX and sulfanilamide *in vitro* inhibition of the *C. parvum* DHFR.

Sulfanilamide (M)	TMX (M)	% of No Drug Control	Sensitivity of Combination
0	0	100.0	
0	1E-9	96.7	
1E-3	0	84.9	
1E-3	1E-9	79.2	~sulfa alone
0	1E-8	65.0	
1E-3	0	84.9	
1E-3	1E-8	83.0	~sulfa alone
0	1E-7	55.0	
1E-3	0	84.9	
1E-3	1E-7	62.3	intermediate

The DHFR-TS was more sensitive to TMX and at 1×10^{-9} M, some inhibition of the enzyme was already seen. Thus when sulfanilamide was added, the combination gave an inhibition close to that for TMX alone. Thus, no synergism between the two drugs was observed.

Table 13: Representative data of TMX and sulfanilamide *in vitro* inhibition of the *C. parvum* DHFR-TS.

Sulfanilamide (M)	TMX (M)	% of No Drug Control	Sensitivity of Combo.
0	0	100.0	
0	1E-9	93.2	
5E-3	0	53.8	
5E-3	1E-9	87.9	~TMX alone
0	1E-8	81.6	
5E-3	0	53.8	
1E-3	1E-8	76.0	~TMX alone
0	1E-7	35.6	
5E-3	0	53.8	
1E-3	1E-7	26.8	~ TMX alone

Table 14: Summary of TMX and sulfanilamide interactions with *C. parvum* DHFR and DHFR-TS.

[TMX]	[Sulfanilamide]	Inhibition
low	low	none
low	high	= sulfanilamide
mid	high	intermediate
high	low	= TMX
high	high	= TMX

CHAPTER SECTION: DISCUSSION

The observation that the yeast expressing the *C. parvum* DHFR domain alone were more sensitive to sulfanilamide was very surprising. One explanation for this observation is that the DHFR yeast strain possesses a lower level of DHFR function, perhaps due to a lower steady state level of enzyme and less efficient complementation of the *dfp1* phenotype. A lower steady state of DHFR enzyme results in a change in the shape of the Michaelis-Menten curve (Figure 27). More substrate is required to achieve the same rate of product formation (velocity) obtained with the higher enzyme concentration. But inhibition of DHPS with sulfanilamide reduces the pool of available substrate for DHFR. The red line in Figure 27 represents a hypothetical threshold; a velocity below the threshold produces too little product to allow the cells to survive and grow. The blue line represents the substrate concentration in the absence of drug. Both the low and high enzyme concentration produce enough product to maintain the cells. The green line represents the substrate concentration in the presence of a given concentration of sulfanilamide. At this concentration, the high concentration of enzyme is able to keep the cells alive, but the product resulting from the cells with a low concentration of enzyme falls below the threshold and the cells die. Thus, the DHFR domain alone reaction is already partially crippled due to the lower concentration of enzyme and is very sensitive to decreases in the substrate pool.

The above argument suggests that trimetrexate sensitivity as well would be different for the DHFR and DHFR-TS strains of yeast. The trimetrexate sensitivity of the two strains, however, was very similar. Since trimetrexate binds nearly stoichiometrically to DHFR enzymes, the fact that both strains show the same sensitivity to the drug suggests that they have similar levels of DHFR expression (discussed more thoroughly in chapter one). Hence, according to these data,

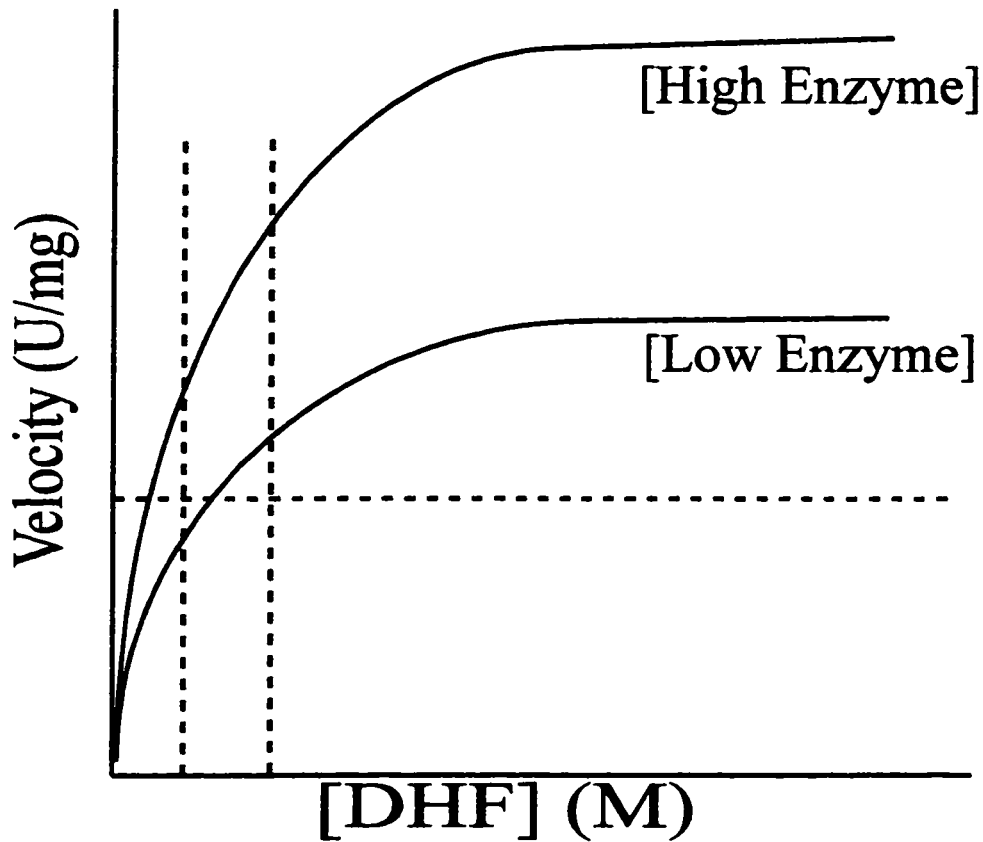


Figure 27: Velocity dependence on enzyme concentration. The dashed red line represents a hypothetical threshold below which the amount of product formed is insufficient to maintain the cells. The dashed blue line represents the amount of substrate and corresponding velocity in the absence of inhibitor. The dashed green line represents the substrate concentration and velocity of the reaction in the presence of a given amount of inhibitor. Note that the velocity of the reaction with the low concentration of enzyme falls below the threshold while the high concentration does not.

expression level did not seem to explain the observed difference in sulfanilamide sensitivity. Work with the purified enzymes, however, suggested that this conclusion is faulty (see below).

The lack of synergy between sulfanilamide and TMX observed for the *C. parvum* DHFR yeast was also very surprising. The experiment with the human DHFR demonstrated that a single domain protein is able to show synergy in this system. Comparison of the strains dependent on the single and two domain *P. falciparum* enzymes showed that the lack of synergy was related to the absence of the TS domain from the normally bifunctional protein. It may be that the DHFR domain does not fold completely correctly without the TS domain, altering the binding pocket. The *C. parvum in vitro* data supported this hypothesis. Both the K_m of NADPH and the IC_{50} for TMX are somewhat higher for the DHFR domain alone. Whether these differences affect the mechanism of synergy is unclear.

The *in vitro* assays revealed that the DHFR domain alone had a lower affinity for NADPH and TMX than the DHFR-TS, but similar affinity for DHF. The fact that DHF binds normally suggests that TMX, a DHF analog, would also bind normally, but this was not the case. Perhaps misfolding of the enzyme due to the absence of TS has altered the spatial relationship of the DHF and NADPH binding pockets.

The V_{max} values of the two forms of the enzyme were similar. However, this similarity is misleading. The units of V_{max} are Units/mg of protein. A unit is a measure of the amount of product the enzyme generates per unit time. The DHFR domain alone is smaller; thus there are more enzyme molecules per milligram than the DHFR-TS. Therefore, a milligram of DHFR should be able to produce more product than a milligram of DHFR-TS. This is not the case, revealing that the DHFR domain alone enzyme is not as efficient an enzyme as the DHFR-TS form.

The *P. falciparum* DHFR and DHFR-TS comparison did not reveal as many differences as I observed with the *C. parvum* enzymes (Sirawaraporn et al., 1993). The K_m for DHF was somewhat higher for the DHFR domain alone, but the K_m for NADPH and the efficiency of the enzymes were the same. The drug sensitivity to pyrimethamine, the antimalaria drug, was the same for both forms of the enzyme as well. There was a significant difference in degree of synergy observed in the yeast dependent upon *P. falciparum* enzymes, however, and that suggests the two forms of the enzyme may be more different than is apparent from the biochemical data.

Significant difficulty was encountered purifying the enzyme that comprised the DHFR domain alone. The expression level in *E. coli* was lower than the DHFR-TS but that alone is not sufficient to explain all the difficulties. The *in vitro* data showed that DHFR alone had a lower affinity for TMX and this difference is likely to be the case for the closely related compound, MTX. Thus, it appears that the enzyme does not bind to the MTX affinity column as strongly as the DHFR-TS does. Additionally, the enzyme may be aggregating, reducing the yield. The *P. falciparum* DHFR domain alone is known to form inclusion bodies and precipitation has been a persistent problem in several projects designed to purify large amounts of the protein. The *C. parvum* enzyme may have produced similar difficulties that could not be detected because there of lower protein levels at the outset. Added to these problems, the *C. parvum* DHFR enzyme is very unstable, no doubt contributing to the poor yield.

Although the RIG plasmid improved the yield of *C. parvum* DHFR sufficiently to allow the purification of the protein, the yield was still not impressive. Even with the RIG plasmid, there was insufficient expression to see a band on an SDS-PAGE of the extract, either in the soluble or pellet fraction. The instability and possible misfolding of the protein may explain this observation.

The pattern of sulfanilamide sensitivity was extremely puzzling. Higher concentrations produced less inhibition than intermediate concentrations. This may be an artifact due to precipitation of the drug; in some cases, the highest concentration was 10 mM and sulfanilamide crystals were observed in the reaction. Due to crystallization, the actual concentration of drug in the reaction is unknown and the data from that very high concentration sample untrustworthy. In other experiments, however, a lack of inhibition was seen at 5 and 1 mM (no visible crystals), inhibition at 0.1 mM, and decreasing inhibition at lower concentrations (data not shown). It seems unlikely that precipitation can explain the observation in that particular experiment.

Although the pattern of inhibition was reproducible for sulfanilamide alone, the degree of inhibition was not. When testing the two drugs concurrently on purified enzyme, I observed a similar inconsistency in the degree of inhibition (TMX alone inhibition was consistent). A pattern did emerge: direct inhibition of DHFR or DHFR-TS by sulfanilamide occurred only when the TMX concentration was too low to inhibit by itself. At higher TMX concentrations, TMX apparently successfully competes with sulfanilamide for binding in the active site.

The *in vitro* data partially explain the characteristics of the yeast expressing the *C. parvum* enzymes. In the yeast experiments, cells reliant on DHFR show the same IC_{50} for TMX as the yeast dependent on DHFR-TS. The IC_{50} value assumes a large number of factors: enzyme accessibility, enzyme activity, penetration of the drug and overall robustness of cell growth. The data on the purified enzymes shows that the two enzymes differ in several important properties. I propose that the expression level of DHFR domain alone is lower, either due to instability or improper folding. Therefore there is less enzyme present so the yeast are more sensitive to growth inhibition. The affinity of the enzyme for the drug, however, is lower than the DHFR-TS. Thus, the lowered concentration of enzyme combined with the decreased

affinity results in a similar IC_{50} value to that observed in the yeast expressing DHFR-TS.

The yeast have an endogenous TS enzyme and cells expressing DHFR-TS have two copies of thymidylate synthase. One hypothesis is that the extra TS is regenerating DHF more quickly, making the yeast less sensitive to the decrease in DHF produced as a result of sulfanilamide inhibition. However, the human and *P. carinii* DHFR yeast, lacking the extra TS, show similar sensitivity to sulfanilamide as the *C. parvum* DHFR-TS. Alternatively, a lower steady state level of *C. parvum* DHFR in the yeast relative to DHFR-TS may be the cause of the increased sensitivity to sulfanilamide (see above and Figure 27). The instability of the DHFR domain alone likely reduces the steady state level. The TMX susceptibility does not reveal this lower level because the DHFR is less sensitive to the drug. Another possibility is that the DHPS enzyme is downregulated in response to the low level of DHFR since producing large amounts of DHF is wasteful if it cannot be reduced.

The explanation for the lack of synergy of sulfanilamide and TMX in the yeast is still elusive. The *in vitro* data suggest that synergy is not the result of both drugs binding to DHFR. In the presence of both drugs, the inhibition was similar to that with TMX alone. These data do not support the hypothesis that synergy is the result of dual inhibition of one enzyme and thus indirectly supports the hypothesis of inhibition of sequential enzymes in a pathway. Additionally, physiological levels of sulfa drugs never reach the 10^{-3} M range, the amount required *in vitro* to inhibit the DHFR, as this is near the limit of solubility for these drugs. The peak serum level reported by the manufacturer for sulfadoxine is $1.6 - 2.5 \times 10^{-4}$ $\mu\text{g/ml}$ (PDR, 1990). Thus, clearly any physiological effect of sulfa drugs is on the DHPS, not on the DHFR.

An alternative mechanism for the mechanism of synergy in the folate pathway has been proposed (W.M. Watkins, personal communication). It has been shown that the DHPS enzyme can incorporate sulfa drugs into a product (Roland *et al.*, 1979). The hypothesis suggests that the abnormal product formed is used by DHFS to form an abnormal version of DHF. This abnormal DHF in some way inhibits the activity of DHFR in addition to the inhibition by TMX, resulting in synergism. However, one could predict that the abnormal DHF and TMX would both bind in the active site of the enzyme. Presumably only one compound can bind to a particular site at a time, so the inhibitors would compete for the binding pocket and the one with better affinity would bind. DHFR inhibitors are competitive drugs and an excess of DHF lowers the degree of inhibition by the drug. Therefore, if the abnormal DHF cannot bind to the active site, the TMX would have less competition for the active site and a higher percentage of inhibitory molecules would be bound to the enzyme. The outcome of this rationale is comparable to the standard explanation for synergy: the inhibition of DHPS results in less DHF to compete with TMX for the active site.

The comparison of the DHFR and DHFR-TS versions of the *C. parvum* enzyme revealed several things. The binding affinity of the two enzymes for the cofactor and the inhibitor TMX were not identical, suggesting that the binding sites are not identical in conformation. The V_{\max} value for the DHFR domain alone showed that it is a less efficient enzyme than its bifunctional counterpart. The expression in yeast also demonstrated, by the lack of synergy, that the DHFR domain is not functioning as expected. Taken together, these results reveal that the DHFR domain alone of *C. parvum* is not functionally equivalent to the natural bifunctional DHFR-TS form of the enzyme. *C. parvum* is fairly closely related to *P. falciparum* and the malarial DHFR domain alone shows a similar lack of expected synergy in the yeast. This suggests that the *P. falciparum* DHFR may not be functionally equivalent to its

DFHR-TS either. Thus, the study of that DHFR domain alone may yield misleading results and should be used with caution.

CHAPTER 3: CONCLUSIONS

The initial goal of this project was to develop a system in a model organism to rapidly identify potential lead drugs for treating Cryptosporidiosis. The system has demonstrated the capacity to detect selective and effective inhibitors and has been used to identify several interesting compounds out of the forty-three that have been tested to date. Because each drug can be tested quickly, hundreds can easily be tested each year. The voluminous data produced will be a boon to medicinal chemists who can compare the chemical structures to the degree of inhibitory activity in order to discern the shape and properties of the enzyme active site. The information can be used to model the structure of the *C. parvum* DHFR and rationally design better inhibitors. Plus, data for each compound will be collected for the control DHFR enzymes (e.g. *Plasmodium falciparum* DHFR). As these DHFR enzymes originate from human pathogens, this information will also be valuable. In addition, the assay may identify compounds of potential clinical use that have already been synthesized but had not been previously tested. This model system approach can easily be extended to DHFR enzymes from other organisms that are difficult or hazardous to cultivate in the laboratory.

This model system also lends itself to the study of expression difficulties of heterologous genes. Each species of DHFR is apparently expressed at a somewhat different level even though the promoter sequences are identical. The various DHFR sequences can be analyzed and mutagenized to search for determinants that result in altered expression level. Possibilities include fortuitous degradation or stability signals that may alter mRNA or protein stability. An example is the *P. falciparum* topoisomerase II coding region that contains many sequences that function as transcription termination signals in yeast, though obviously not in the native organism (Sibley et al., 1997).

The assay allows for identification of compounds that inhibit the yeast by a non-DHFR mechanism. These compounds may be of interest for treating fungal infections or for identifying new drug targets. A drug target identified in yeast may have an ortholog in pathogenic organisms that could be exploited for chemotherapy.

The purpose of the bifunctional DHFR-TS enzymes in protozoa is believed to be improved efficiency of the pathway (Elcock *et al.*, 1996; Knighton *et al.*, 1994) but *in vitro* experiments have not previously detected any significant differences between the DHFR-TS and the DHFR alone (Sirawaraporn *et al.*, 1993). Expression of the monofunctional and bifunctional enzymes in yeast demonstrated that a functional difference does exist between the two forms. The advantage of bifunctionality can be studied in this system. Along those lines, the lack of synergy exhibited by the single domain protein can be further examined. The protein may not fold properly without the TS domain. Fusion proteins linking the *C. parvum* DHFR domain and the yeast TS domain or an unrelated protein domain may help answer these questions. The fusion of the human TS to the human DHFR may provide interesting results as well. What happens to the function of each of those domains?

One hypothesis to explain the sulfanilamide sensitivity of the yeast expressing the *C. parvum* DHFR domain alone is that the single domain does not interact with the yeast TS properly. Cotransformation into yeast of the *C. parvum* DHFR domain and the *C. parvum* or yeast TS domain as separate entities would test this hypothesis. If the sensitivity to sulfanilamide decreased or the synergy returned in the presence of a second separate yeast TS, the experiment would argue that an increase in TS activity likely explains the sulfanilamide phenotype observed with the *C. parvum* DHFR-TS expressing yeast. If, however, the second yeast TS has no effect on the lack of synergism observed with the yeast expressing the *C. parvum* DHFR domain alone, then TS copy number is likely not the explanation for the sulfanilamide sensitivity differences between the *C. parvum* DHFR and DHFR-TS expressing yeast.

On the other hand, if expression of the *C. parvum* TS as a separate entity in conjunction with the *C. parvum* DHFR results in synergism between TMX and sulfanilamide, then the result would argue that the DHFR domain alone can function properly but cannot interact with the yeast TS properly. In this case, proper heterologous DHFR function would be observed only when the heterologous TS is present as well so that correct protein-protein interactions can occur.

Although the human and yeast DHFR and TS enzymes are not naturally bifunctional, they may interact directly *in vivo* through protein-protein interactions. The yeast protein STE5 acts in the pheromone response pathway as a scaffold upon which several kinases assemble (Herskowitz, 1995). These MAPK (mitogen activated protein kinases) proteins act sequentially in the response to pheromone. The folate pathway may have a protein of similar function that improves the efficiency of the pathway. A scaffold would keep the sequential enzymes of the pathway in one location so that products could easily shuttle to the next enzyme. Coimmunoprecipitation and two hybrid experiments could be used to search for and identify this hypothetical protein. A scaffold protein could explain our observations: some heterologous proteins may not assemble with the other yeast components properly.

Saccharomyces cerevisiae is an excellent organism for the study of heterologous genes. It is eukaryotic, has a compact genome that has been completely sequenced, is easy to culture, and many clever techniques have been developed to manipulate the organism. For instance, permeability of the cells to some of the test compounds (Chapter 1) may prove to be an obstacle. This problem can be overcome by introducing mutations in one or more of several genes that have been identified which alter the permeability of yeast. For instance, ERG6 participates in the synthesis of the membrane lipid ergosterol, PDR1 and PDR3 (Nitiss and Wang, 1988; Nitiss, 1994) are involved in membrane transport, and a mutation in CAM1 allows entry of

cAMP (Pillai *et al.*, 1993) and other compounds. The introduction of specific mutations in this organism is straightforward and well characterized (Guthrie and Fink, 1991). In addition to creating mutations in the host strain, mutations can be generated in the heterologous sequence in order to study motifs or structure/function relationships. The yeast two-hybrid and related screens allow the identification of protein-protein, protein-DNA, and protein-RNA interactions (Chien *et al.*, 1991; SenGupta *et al.*, 1996). Yeast provide the opportunity to address questions on heterologous proteins that cannot be answered in the native organism.

CHAPTER 4: MATERIALS AND METHODS

CHAPTER SECTION: BACTERIAL AND YEAST CULTURE

CHAPTER SUBSECTION: STRAINS

The strain of *E. coli* used for plasmid propagation was DH5 α . The *Saccharomyces cerevisiae* strains TH1 (Mat a *ura3-52 leu2-3.112 trp1 tup1*) and TH5 (Mat a *ura3-52 leu2-3.112 trp1 tup1 dfr1::URA3*) were kindly provided by Tun Huang (Huang et al., 1992). TH5 must be maintained in the presence of adenine, histidine, methionine, and dTMP. The heterologous DHFR enzymes were expressed from a yeast shuttle plasmid derived from pRS314 (Sikorski and Hieter, 1989; Wooden et al., 1997). These constructs were transformed into strain TH5 to generate the strains listed in Table 15. All strains are haploid.

Table 15: Plasmids used in the yeast assays.

Strain	DHFR Origin	Promoter	Source
Yeast	<i>Saccharomyces cerevisiae</i>	600 bp	(Wooden et al., 1997)
PyrS	<i>P. falciparum</i> , Pyr sensitive	600 bp	(Wooden et al., 1997)
PyrR	<i>P. falciparum</i> , Pyr resistant	600 bp	(Wooden et al., 1997)
Human	Human	450 bp	this work
hCp D-TS	<i>C. p.</i> , human isol.; DHFR-TS	450 bp	this work
hCp D	<i>C. p.</i> , human isol.; DHFR	450 bp	this work
bCp D-TS	<i>C. p.</i> , bovine isol.; DHFR-TS	450 bp	this work
T.g.	<i>Toxoplasma gondii</i>	600 bp	Mary Reynolds
P.c.	<i>Pneumocystis carinii</i>	450 bp	this work

E. coli were grown in LB media and on LB plates containing antibiotic. Ampicillin was used at 100 µg/ml, kanamycin at 50 µg/ml, and chloramphenicol at 25 µg/ml. Yeast were grown in YEPD liquid media and on C and D plates (Guthrie and Fink, 1991). YEPD is rich media made from yeast extract that contains dextrose as the carbon source. D plates are made from YEPD and C plates are made from defined synthetic complete media that can be formulated to lack a specific nutrient such as an amino acid.

CHAPTER SUBSECTION: TRANSFORMATIONS

E. coli transformations were performed using standard calcium chloride and heat shock protocols (Sambrook *et al.*, 1989). Yeast transformations were performed using a high efficiency lithium acetate protocol (Ito *et al.*, 1983) or a Yeast Transformation Kit (Zymo Research, Orange, CA). Transformed cells were plated on plates containing complete synthetic media lacking tryptophan to select for the plasmid. In some cases, dTMP (100 µg/ml) (Sigma, St. Louis, MO) was added to the plates so that the DHFR was not required to be active.

CHAPTER SUBSECTION: PLASMID CONSTRUCTION

The parent vector, pEH2, was derived from pRS314 (Sikorski and Hieter, 1989) and is shown in Figure 28. The vector has the following features: an *E. coli* origin for bacterial replication, an ampicillin resistance gene for bacterial selection, a centromere sequence for yeast mitotic segregation, an autonomous replication sequence (ARS) for yeast replication, and a *TRP1* marker for yeast selection. It also has a 600 bp fragment from the region directly 5' of the yeast DHFR gene and a 400 bp fragment from the region directly 3' of the yeast DHFR gene. These fragments had been cloned into the multiple cloning site by Jason Wooden and confer promoter and termination activity, respectively. In contrast to the previously

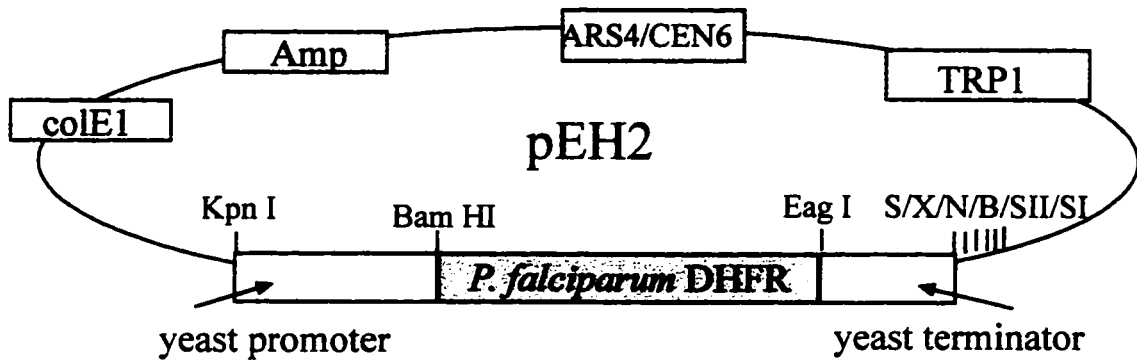


Figure 28: Map of the yeast expression vector. The plasmids constructed in this work were based on pEH2. The *P. falciparum* DHFR sequence was removed by digestion with Bam HI and Eag I and another sequence inserted in its place. pEH2 differs from pTrp (Wooden *et al*, 1997) only in that an Eag I site in the middle of the *P. falciparum* DHFR and a Bam HI site 3' of the terminator sequence were removed. S, Spe I; X, Xba I; N, Nco I; B, BstXI; SII, Sac II; SI, Sac I.

reported construct (Wooden et al., 1997), two restriction sites have been eliminated from pEH2: the duplicate Bam HI and Eag I sites 3' of the terminator have been removed for ease of cloning (Eleanor Hankins, personal communication).

The *C. parvum* and human DHFR sequences were obtained from John Vasquez (Vasquez et al., 1996). The *P. carinii* DHFR sequence was provided by the AIDS Research and Reference Reagent Program and the *T. gondii* by Mary Reynolds in David Roos' laboratory (University of Pennsylvania).

The plasmid pEH2 contains the *Plasmodium falciparum* (*P.f.*) DHFR gene between the 5' promoter sequence and the 3' terminator sequence. The *P.f.* sequence can be removed by digestion of the plasmid with Bam HI (5' end) and Eag I (3' end). The plasmid was digested with Bam HI and Eag I (overnight at 30°C), then the fragments were treated with Calf Intestinal Phosphatase (one hour at 37°C) to remove the terminal phosphates. This prevents religation of the vector without insert. The band was excised from the gel and the DNA was recovered by centrifugation through polyester fiber as follows: a hole was poked in the bottom of a 0.6 ml centrifuge tube and the tube stuffed about half-full with craft polyester fiber. The lid was removed and the tube placed inside a 1.5 ml tube. The gel slice was placed on top of the fiber and the apparatus centrifuged for several minutes at 3000 rpm. The DNA in 1X TAE is recovered in the 1.5 ml tube and frozen for future use.

In order to insert the heterologous DHFR genes into pEH2, Bam HI and Eag I restriction sites were engineered onto the ends of the DHFR using polymerase chain reaction (PCR). Primers were manufactured by Life Technologies (Grand Island, NY) and the sequences are listed in Table 16. The upstream primer contained homology to the 5' end of the DHFR coding sequence and a Bam HI site with six additional bases 5' of the site to ensure that the restriction enzyme had enough

Table 16: PCR Primers

Primer name	Specificity	Primer Sequence
Sibley 110	5' of <i>C.p.</i> DHFR-TS bovine isolate, Bam HI site	AGGAGAGGATCCCATGAGTAAA AAGAACGTTT
Sibley 111	3' of <i>C.p.</i> DHFR bovine isolate, Eag I site	CGGGGCCGTTAATTGACCTCTTA CAGGG
Sibley 112	3' of <i>C.p.</i> DHFR-TS human isolate, Eag I site	GATTATACCGGCCCGGTCCATTTT ATACCGCCATG
Sibley 113	3' of <i>C.p.</i> DHFR-TS bovine isolate, Eag I site	GCCGGCCGTGGATAATTTAAAAG TAATAG
Sibley 114	3' of <i>C.p.</i> DHFR human isolate, Eag I site	CGATCGCGGCCGTTAATTGACCT CTGGCAGGG
Sibley 125	5' of human DHFR, Bam HI site	CTATATGGATCCCATGGTTGGTT CGCTAAACTGC
Sibley 126	3' of human DHFR, Eag I site	CGGGCCACGGCCGTATTAATCAT TCTTCTCATATAC
Sibley 129	5' of <i>P.c.</i> DHFR, Bam HI site	CGGCGCGGATCCGATGAATCAG CAAAAGTCTTTAAC
Sibley 130	3' of <i>P.c.</i> DHFR, Eag I site	CGCGTGCGGCCGTATAAATCTC TTGTCCACATTTT
Sibley 142	5' of <i>S.c.</i> DHFR promoter, Xho I site	CGGACTCGAGCTATAGGAATCGT CACTC
Sibley 145	5' of <i>C.p.</i> DHFR-TS human isolate, Bam HI site	AGGAGAGGATCCCATGAGTGAA AAGAACGTTT
Sibley 169	sequencing primer for 5' of <i>C.p.</i> TS	GTGACCCTGTCAGAGGTC

sequence to bind to the DNA. Two downstream primers were designed for the *C. parvum* human isolate: one that amplified from within the junction region so that the

product includes the *C. parvum* DHFR only and another that amplified from just beyond the stop codon, so that the product includes the entire *C. parvum* DHFR-TS coding sequence. Each downstream primer contains an Eag I site at its 5' end with the six additional bases for improved restriction digestion. The vector terminator sequence contains a stop codon, so the DHFR alone protein will be properly terminated.

Reactions were run on a DNA Engine PTC-200 (MJ Research, Watertown, MA). The standard final concentrations in the reactions were: each primer 1 μ M, DNA 10 ng, Replitherm polymerase buffer 1X, dNTP's 0.2 mM, Replitherm polymerase 0.3 U. The $MgCl_2$ concentrations varied for each primer set. The standard cycling profile was: 1) 94°C 2:30 min. 2) 94°C :30 min 3) 52°C :30 min 4) 72°C :30 min 5) go to 2, 29 times 6) 72°C 2:30 min. 7) 4 °C. Changes made for amplification of each DHFR coding sequence are listed in Table 17.

PCR products and vector were digested to completion for at least two hours at 37°C with Bam HI and Eag I (New England Biolabs, Beverly, MA) or overnight at 30°C. The PCR product was purified using a Wizard PCR column (Promega Corp., Madison, WI). Vector and insert were then mixed with T4 ligase (New England Biolabs) and incubated overnight at 16°C. The ligation reaction was then transformed into DH5 α *E. coli*. DNA was prepared from several colonies by boiling miniprep (Sambrook et al., 1989) and checked by restriction mapping to verify the identity of the insert.

Table 17: PCR cycling conditions

Primers	Cycling Changes from Standard	Changes from Standard
Sibley 110 and 111	none	MgCl ₂ 1.0 mM
Sibley 110 and 113	none	MgCl ₂ 1.0 mM
Sibley 145 and 112	initial 94°C 2:00, no step 6	MgSO ₄ 2 mM, Vent pol., 0.4 µM of each
Sibley 145 and 114	initial 94 °C 2:00, no step 6	MgSO ₄ 2 mM, Vent pol., 0.4 µM of each
Sibley 125 and 126	initial 94°C 1:00, first two cycles annealed at 50°C, rest at 54°C, final extension for	0.5 mM MgCl ₂ , 0.08 mM dNTP's
Sibley 129 and 130	initial 94°C 2:00, final extension for 3:00	1.5 mM MgCl ₂ , 0.15 mM dNTP's

CHAPTER SUBSECTION: PROMOTER MUTAGENESIS

The 600 bp yeast DHFR promoter (Wooden et al., 1997) was mutagenized by error-prone PCR (Zhou et al., 1991). The buffer was composed of 7 mM MgCl₂, 50 mM KCl, 10 mM Tris-Cl, and 0.01% gelatin. dCTP and dTTP were used at 1 mM, dATT and dGTP were used at 0.2 mM. Five units of Taq polymerase and 0.5 mM MnCl₂ were used. The PCR run was 30 cycles of 94°C 1 min, 45°C 1 min, 72°C 1 min. Primers Sibley 69 and 89 were used at the final concentration of 30 pmoles. Ten ng of pTB3 DNA was used as template in each amplification reaction. PTB3 vector and the mutagenized PCR product were digested with Bam HI and Kpn I and purified as described in plasmid construction. Ligation was as described above,

but the products were transformed directly into TH5 yeast. Colonies were patched onto rich media and tested for drug sensitivity by replica plating onto rich plates containing 1×10^{-5} M trimetrexate. Candidate colonies were further characterized by spoke assay and liquid IC_{50} .

The *C. parvum* and *P. carinii* coding sequences were transferred to the plasmid with the truncated promoter chosen for further work (pTB4) by digestion with Bam HI and Eag I to remove the existing human DHFR coding sequence and ligation of the *C. parvum* and *P. carinii* coding sequences in its place. The *T. gondii* plasmid retained the original promoter.

The plasmid pTB7 contains the coding sequence for the *C. parvum* DHFR from the human isolate. This was known to contain a point mutation due to a fault in primer design. The sequence was re-cloned and designated pTB9.

Table 18: Plasmids Generated During this Work

<u>Plasmid</u>	<u>Plasmid Identity</u>	<u>Comments</u>
pTB1	<i>C.p.</i> DHFR, human isolate	600 bp promoter, low sensitivity
pTB2	<i>C.p.</i> DHFR-TS, human isolate	600 bp promoter, low sensitivity
pTB3	Human DHFR	600 bp promoter, low sensitivity
pTB4	Human DHFR	450 bp promoter
pTB5	<i>P.c.</i> DHFR	no promoter, pRS414 plasmid backbone
pTB6	<i>P. c.</i> DHFR	450 bp promoter
pTB7	<i>C.p.</i> DHFR, human isolate, known point mutation at codon	450 bp promoter
pTB8	<i>C.p.</i> DHFR, bovine isolate	450 bp promoter
pTB9	<i>C.p.</i> DHFR, human isolate	450 bp promoter
pTB10	<i>C.p.</i> DHFR-TS, human isolate	450 bp promoter
pTB11	<i>C.p.</i> DHFR, bovine isolate	450 bp promoter, restriction analysis suggests questionable
pTB12	<i>C.p.</i> DHFR-TS, bovine isolate	450 bp promoter
pTB13	<i>T.g.</i> DHFR	no promoter, pRS414 plasmid backbone
pTB14	<i>T.g.</i> DHFR M2M3 mutant	no promoter, pRS414 plasmid backbone
pTB15	<i>C.p.</i> DHFR, human isolate	pET-9d plasmid

CHAPTER SUBSECTION: SEQUENCE ANALYSIS

The mutagenized promoter and each insert were sequenced. Two cycle sequencing kits were used: initially the original Dye Terminator kit was used, later sequencing reactions were performed using the BigDye™ kit (Perkin-Elmer, Foster City, CA). Cycling parameters were: 1) 94°C 30 seconds 2) 50°C 15 seconds 3) 60°C 4 minutes for 26 cycles. A ramp was added between cycles for the BigDye kit of 0.8°C/second to prevent the temperature from changing too rapidly.

The sequence for the mutagenized promoter is shown in Chapter 1. The sequence of the human DHFR matched the published sequence (Genbank accession U00140). The *P. carinii* DHFR contains five point mutations from the published sequence (Genbank accession M26495, M26496). Two of the mutations are silent and the other three are missense. Position +57 contains a C instead of a T and codes for a Thr as opposed to the published Ile. DHFR proteins vary widely from species to species making alignment difficult and imprecise, but according to one alignment (Vasquez et al., 1996), this change is in a conserved codon. However, the DHFR complements very well in the yeast system, so the mutation has apparently not compromised function. The second missense mutation is at nucleotide position 125 and changes a T to a C, Phe to Leu. This position contains a Leu in the *Leishmania major* DHFR sequence and may be an unimportant change. The third mutation is at position 127 and changes a T to a G, Val to Ala. According to the alignment, this position is highly variable across species and is likely to be unimportant. Five is a very high number of point mutations to be introduced by PCR into a 550 bp sequence. I suspect that the sequence we obtained from the AIDS Research and Reference Reagent Program already contained these changes.

The *C. parvum* human isolate DHFR contains one point mutation in codon three, changing it from Glu to Lys. Lys is the third codon in the bovine isolate

as well and is likely to be an irrelevant change. The *C. parvum* human isolate DHFR-TS contains one point mutation in the DHFR that is silent (+440, T→C) and another in the junction region that changes a Ile to Val (+604, A→G). The sequence of the junction region is highly variable among species and is thought to be unimportant with respect to function.

When the bovine isolate DHFR-TS was cloned, the C-terminal portion of the TS domain was not recovered (Vasquez et al., 1996). The authors used the TS domain from the human isolate to replace the missing sequence. The published sequences (accession U41365 and U41366), however, show polymorphisms between the C-terminal portion of the human and bovine isolates of the TS domain. The sequence analysis of the clones reported here showed that the C-terminal domain of the bovine isolate does indeed match the human isolate. The DHFR, junction region, and N-terminal portion of the TS of the *C. parvum* bovine isolate match the published sequence.

CHAPTER SUBSECTION: PLASMID RECOVERY

To recover plasmids from the yeast, either a Smash and Grab (Hoffman and Winston, 1987) or a Zymoprep (Zymo Research, Orange, CA) was performed. A Smash and Grab uses glass beads and vortexing to physically disrupt the cells, followed by phenol/chloroform separation. A Zymoprep uses the enzyme Zymolyase to disrupt the cell wall, followed by cell lysis using buffers. The recovered DNA, including both yeast genomic and plasmid DNA, is then transformed into DH5 α *E. coli*. Plasmid was recovered from the transformed *E. coli*.

CHAPTER SUBSECTION: COMPOUNDS

Trimetrexate and the NCI compounds were obtained through Mohammed Nasr at the National Cancer Institute. The Dana-Farber compounds were

obtained from Andre Rosowski (Dana-Farber Cancer Institute and Harvard Medical School) and the WRAIR compounds were obtained through Lt. Col. John Forney, PH.D. Sulfanilamide was purchased from Sigma (St. Louis, MO). All compounds were dissolved in DMSO (Sigma St. Louis, MO) and the concentration of DMSO in the yeast assays was less than 1% to avoid interference of the solvent with cell growth.

CHAPTER SUBSECTION: SPOKE ASSAY

The strains listed in Table 1 were streaked onto a YEPD yeast plate using the narrow side of a sterile toothpick (Figure 29). The yeast were streaked from the center of the plate towards the periphery. The plate was grown for two days at 30°C, then replica plated to a fresh plate. This new plate was then replica plated again onto several fresh plates that contained 1 mM sulfanilamide. This double replica plating reduces the background and improves the resolution of the assay. Ten µl of concentrated drug solution (10 mM in DMSO) was placed in the center of the plate and allowed to soak into the media. The pipet tip was pressed into the agar to mark the center of the drug spot. The plates were incubated at 30°C for two days before scoring. Trimetrexate was used on one plate in each assay set as a control. One plate contained sulfanilamide only. The last plate in each experiment contained no drug at all to ensure that cells were transferred throughout the experiment. To score the plates, a ruler was used to measure the "kill zone": the region from the pipet tip mark to the beginning of growth for each strain. Each drug was tested three times and the distances averaged.

CHAPTER SUBSECTION: IC₅₀ ASSAY

A saturated culture of each strain was grown in YEPD liquid media from a colony and stored at 4°C. A series of dilutions from the saturated culture was made into fresh YEPD and grown overnight. The concentration of each dilution was

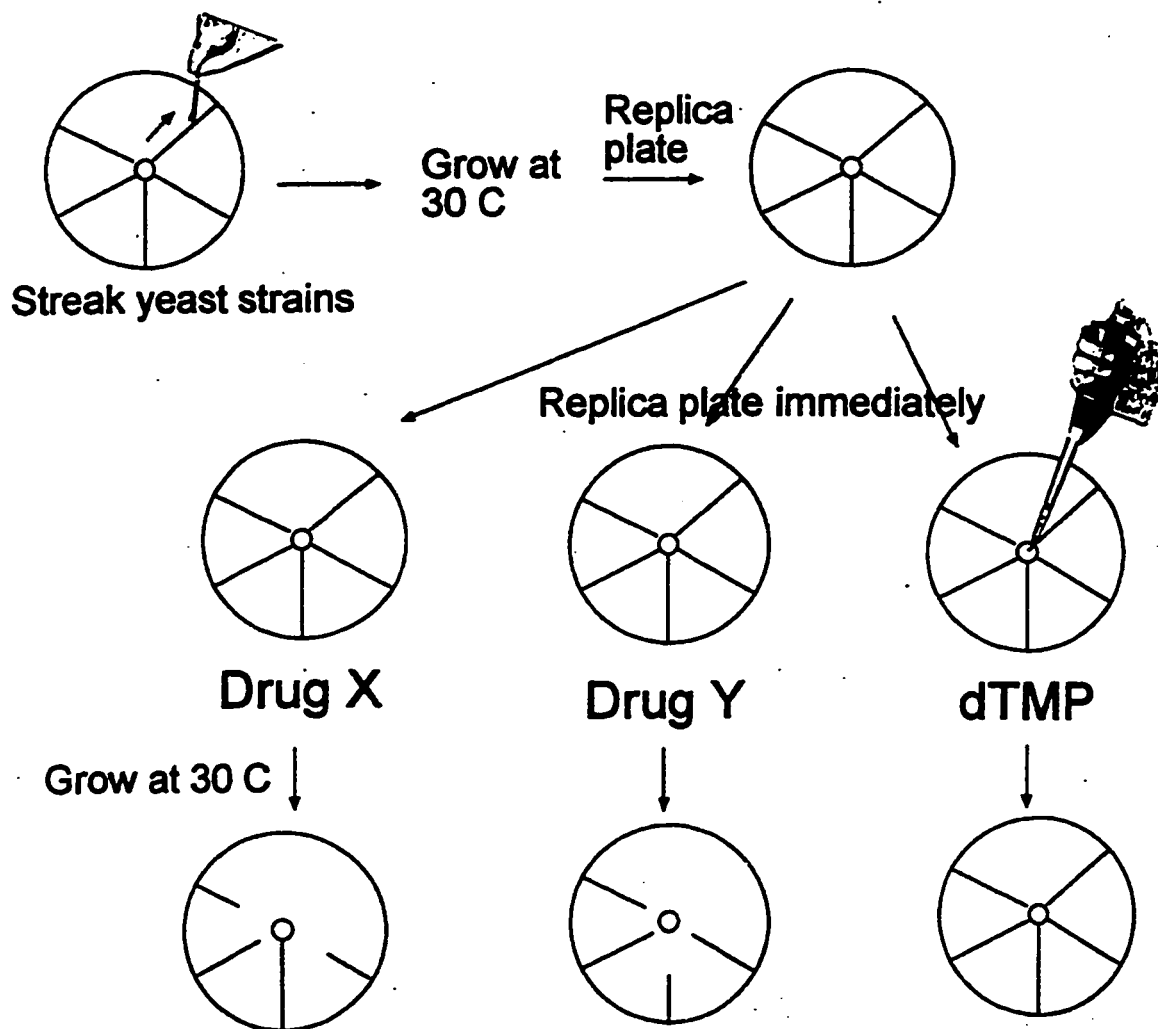


Figure 29: Spoke assay for testing yeast strain drug sensitivity. Each strain is streaked on a fresh D plate and allowed to grow for two days. The master plate is replica plated to a fresh plate; that plate is then replica plated to a series of fresh plates. Ten microliters of fresh drug is placed in the center of each plate and allowed to diffuse through the media. The final plate receives nothing or solvent as a control for uninhibited growth.

determined by optical density (OD) at 660 nm on a spectrophotometer (Spectronic 1001, Bausch & Lomb). For each strain, a culture in log phase ($0.5 - 2 \times 10^7$ cells/ml) was selected for use in the experiment. The cells were diluted in media containing 1mM sulfanilamide (final concentration) to 3.5×10^4 cells/ml and 0.8 ml aliquots were distributed to wells in a deep-well (2 ml) 96 well plate. Drug dilutions were made into YEPD media and 200 μ l was added to the wells to generate the final concentrations listed in the results. Each drug concentration was assayed in duplicate for each strain. The plates were incubated on a 30°C shaker for 24 hours. 200 μ l of each well was transferred to a 96-well assay plate and the A_{650} was read on a plate reader (Molecular Dynamics, Sunnyvale, CA). Three wells containing media alone were used as a blank. The "no drug" wells (with 1mM sulfanilamide and DMSO, however) were set as 100% growth and the OD's of the various drug dilutions were divided by the control to determine the percentage of no drug control growth. The IC_{50} was calculated using the two drug dilutions that resulted in percentage of no drug control growth flanking the 50% mark. The formula used was $y = mx + b$ where $y = 50$ (%) and m and b are the slope and y-intercept calculated from the two flanking drug dilutions. Solving for x yields the IC_{50} .

CHAPTER SUBSECTION: COMPLEMENTATION TESTS

Transformants expressing the heterologous DHFR's were patched onto rich media plates plus dTMP, grown for three days, and double replica plated onto rich media plates lacking dTMP and synthetic media plates lacking adenine, histidine, or methionine. Growth on all of these plates indicated that the heterologous DHFR was complementing the *dhfr1* disruption. All of the DHFR sequences were able to complement the yeast *dhfr1* disruption. In the same experiment, the transformants were replica plated onto synthetic media lacking tryptophan, leucine, or uracil to verify the identity of the yeast strain.

CHAPTER SECTION: IN VITRO ASSAYS

CHAPTER SUBSECTION: YEAST PROTEIN EXTRACTS

Yeast extracts were prepared using a modification of the procedure listed in Current Protocols (Ausubel, 1988). Yeast cells were grown to mid-log phase and centrifuged for 5 minutes at 3000 rpm (Beckman TJ-6) in preweighed tubes. The media was removed and the tubes reweighed to determine the weight of the cell pellets. The cells were resuspended in 3 volumes of cold water and centrifuged for 5 min. at 3K rpm (Beckman TJ-6). The pellet was then resuspended in 2 volumes of cold lysis buffer plus inhibitors (20 mM Tris-Cl pH 7.9, 10 mM MgCl₂, 1 mM EDTA, 5 % glycerol, 1 mM DTT, 0.3 M (NH₄)₂SO₄, 200 µg/ml aprotinin, 100 µg/ml pepstatin A, 720 µg/ml E-64, , 1 µg/ml leupeptin, 250 µg/ml antipain, 10 mM benzamidine, 10 mM sodium metabisulfite, 1 mM PMSF) and transferred to a smaller tube. Cold glass beads were added so that half of the liquid is filled with beads. The tubes were vortexed for 30 seconds, then left on ice for 2 minutes. The vortexing step was repeated 3 or more times. Lysis was monitored microscopically using trypan blue staining. Supernatants were collected using a gel loading tip (narrow opening to partially eliminate bead interference) then one volume of fresh disruption buffer was added to the beads, mixed, removed, and pooled with first supernatants. The supernatants were centrifuged for 30 minutes at 12,000 x g at 4°C, then transferred to a new tube. Glycerol was added to 20% prior to freezing at -70°C (Western analysis samples). Enzyme assay samples were not frozen.

CHAPTER SUBSECTION: WESTERN ANALYSIS

Twenty µl of each yeast extract and varying amounts of purified *P. falciparum* DHFR protein (a gift from Jason Wooden) were loaded onto a 10 % SDS-PAGE gel. The proteins were fractionated on an 8 x 10 cm gel (Hoefer Scientific

Instruments, San Francisco, CA) and electroblotted (Bio-Rad, Cambridge, MA) to PVDF membranes (Millipore, Bedford, Mass.). The membranes were blocked with 5% blotto (nonfat dry milk in 1X TBST (10 mM Tris-Cl pH 6.7, 150 mM NaCl, 0.05 % Tween-20). After blocking, the membranes were incubated overnight at 4°C with antibodies directed against the *P. falciparum* DHFR suspended in 5% blotto. The membranes were washed twice for seven minutes each with 1X TBST, then incubated for one hour at room temperature with secondary antibody in 5% blotto. The secondary antibody was goat anti-rabbit-specific coupled to horseradish peroxidase (Santa Cruz Biotechnology, Santa Cruz, CA). The primary antibody was used at a dilution of 1:250 and the secondary at 1:500. The blot was then washed for four times for five minutes each with 1X TBST. Detection was with SuperSignal (Pierce Chemical Co, Rockford, IL) chemiluminescence according to manufacturer's instructions and the signal was recorded on Reflection film (NEN, Boston, MA).

CHAPTER SUBSECTION: *E. COLI* OVEREXPRESSION AND PROTEIN EXTRACTS

For overexpression of protein, the *E. coli* strain BL-21 (λ DE3) was used as a host strain. Cells carrying the pET plasmid were grown overnight in LB media and kanamycin (50 μ g/ml) in a 37°C shaking incubator. Media for cells carrying the RIG as well as the pET plasmid also contained chloramphenicol (25 μ g/ml) to select for that plasmid. The overnight culture was diluted approximately 1:100 into 0.5- 1.0 L of fresh LB media containing kanamycin and chloramphenicol (if applicable). That culture was shaken at 37°C for several hours until the A_{600} was between 0.500 and 0.600. IPTG was added to the media to a final concentration of 1 mM. The culture was further incubated for 3 to 4 hours. The culture was then centrifuged (15 minutes, 10K rpm), washed with 1X PBS, re-centrifuged, and the dry pellet frozen overnight at -70°C.

The frozen pellet was resuspended at room temperature using 15 ml of lysis buffer/gram of cell pellet. Lysis buffer consisted of 50 mM Tris-HCl pH 7.4, 75 mM β -mercaptoethanol, 1 mM EDTA, 0.17 mg/ml PMSF, 0.16 mg/ml benzamidine-HCl, 1 μ g/ml leupeptin, 1 μ g/ml pepstatin A, 1 μ g/ml aprotinin, and 0.2 mg/ml lysozyme. After the pellet was resuspended, it was stirred at 4°C until the solution was viscous. Then $MgCl_2$ was added to a final concentration of 10 mM and DNase was added to 10 μ g/ml. This was stirred at room temperature until the solution was no longer viscous. The solution was pelleted by centrifugation for 15 minutes at 10K. The supernatant was removed to a clean tube and used for enzyme assays or column purification. If the solution was insufficiently clarified, it was re-centrifuged to prevent clogging of the column. If the extract was not used immediately, glycerol to 20% was added prior to freezing at -70°C.

CHAPTER SUBSECTION: *IN VITRO* DHFR ACTIVITY ASSAYS

DHF was prepared by Jason Wooden by the method of (Friedkin *et al.*, 1962). Shortly before use, a frozen aliquot of DHF was thawed, centrifuged for one minute at >10K rpm, and the β -mercaptoethanol removed from the pellet. NaOH (0.1 N) was added to the pelleted DHF until no particulates were visible. A 1:10,000 dilution (in water) of the DHF was measured on the spectrophotometer (Spectronic 1001, Bausch & Lomb) at 282 nm. The concentration of DHF was calculated as follows: $(A_{282} \times 10,000)/28,400 = \text{molar DHF}$. 28,400 is the extinction coefficient for DHF. A 7.5 mM DHF solution was then prepared in water.

Also shortly before use, a 7.5 mM solution of NADPH (6.25 mg/ml) was prepared by solution in water. Both the DHF and the NADPH were kept on ice. The buffer was prepared the day of use as well and consists of 50 mM TES (N-tris[Hydroxymethyl]methyl-2-aminoethanesulfonic acid), 1 mM EDTA, 75 mM β -mercaptoethanol, and 1 mg/ml BSA.

The enzyme assays were conducted using a spectrophotometer set at 340 nm. NADPH absorbs at 340 nm, but NADP does not. Thus as NADPH is used in the reaction, the A_{340} falls proportionately. A 2 ml quartz cuvette (1 cm path length) was filled with 1 ml of assay buffer and the instrument blanked. Then 10 μ l of 7.5 mM NADPH was added, mixed and the A_{340} recorded. If the A_{340} was not between 0.350 and 0.450, fresh NADPH was prepared. Then 10 μ l of 7.5 mM DHF was added, mixed, and the A_{340} recorded. Five minutes later, the A_{340} was recorded again. This process was repeated and the average ΔA_{340} (five minute A_{340} - 0 minute A_{340}) was taken as background. For the samples, 1 ml of buffer, 10 μ l of DHF, 10 μ l of NADPH, and sample were mixed and readings taken at 0 and 5 minutes. In later experiments, readings were taken every fifteen or thirty seconds in addition to the endpoints. These data were analyzed by plotting the A_{340} versus time and the slope from the linear portion of the curve was used as the $\Delta A_{340}/\text{minute}$. The control DHFR used in these assays was commercially purified bovine DHFR (Sigma, St. Louis, MO). Five microliters of a 1:10 dilution was used in the reaction volume and the U/mg calculated to verify that the assay was working properly. A unit is defined as the amount of enzyme required to produce 1 μ mol of product per minute at room temperature. U/mg was calculated as follows: $(\Delta A_{340}/\text{min} \times \text{total assay volume}) / (12.3 \times \text{sample volume}) = \text{U/ml}$; $(\text{U/ml}) / \text{sample protein concentration} = \text{U/mg}$. The extinction coefficient for NADPH and DHF together is 12.3. Sample volumes varied for the test DHFR enzymes, depending on the amount of activity in the sample.

For drug inhibition assays, the NADPH, sample, and drug were added to the buffer, mixed and incubated for five minutes. The reaction was started by addition of DHF. The IC_{50} was calculated as described above. Kinetics assays were conducted in similar fashion to the standard protocol except that the amount of NADPH or DHF was varied between 0.5 μ M and 75 μ M. The kinetics data were analyzed by a Hanes-Woolf plot (Segel, 1975): plotting the substrate concentration

(DHF or NADPH) versus the substrate concentration divided by the velocity (U/mg). This method of analyzing the data is reported to be more accurate than a Lineweaver-Burk analysis (Dowd and Riggs, 1965). The regression line generated for a Lineweaver-Burk plot is weighted heavily by a few points at low substrate concentration. This weighting can lower the accuracy. A Hanes-Woolf plot allows the data points to be more evenly distributed.

CHAPTER SUBSECTION: OPTIMIZATION OF ENZYME ACTIVITY IN EXTRACTS

A crude extract of TH5 yeast gave 0.7 mU/mg of activity that can be accounted for by other reductases. TH1 gave 1.7 mU/mg of activity; 0.001 U/mg after subtracting TH5. An extract volume of 100 μ l (in a one ml reaction) had to be used to get a reliable measurement of the DHFR activity in TH1. Extracts prepared from yeast expressing the *P. falciparum* DHFR expressed from the usual Cen plasmid (one copy per cell) and from a 2 μ m plasmid (high copy number/higher expression level) were tested and no activity over background was detected any in either of the strains. Thus, these yeast do not produce enough DHFR for *in vitro* assay to detect in crude extracts. A crude extract of TH1 was purified over the MTX affinity column, but no detectable protein was recovered.

Since DHFR activity could not be recovered from the yeast expressing the heterologous enzyme, overexpression of the enzyme in *E. coli* was used instead. The *E. coli* pET plasmid series is designed for inducible overexpression of proteins. John Vasquez originally provided the *C. parvum* DHFR-TS on a pET-9d plasmid in the BL21 (λ DE3) strain of *E. coli* (Vasquez et al., 1996). Significant enzyme activity was detected in the induced *E. coli* extract (0.09 U/mg) and when purified over the MTX affinity column yielded 0.99 mg of protein and 16 U of activity.

I replaced the DHFR-TS in the pET vector with the DHFR domain alone generated by PCR and transformed the construct into the BL21 *E. coli*. Cells (500 ml) were induced, extracted, and loaded onto a MTX column. Activity was detected in the crude extract (0.06 U/mg), but none in the fractions. The protein was binding to the column but not being recovered. The column was washed less stringently in buffer with no NaCl (versus 0.5 M NaCl) and eluted using a stronger elution buffer: 4 mM DHF and 0.5 M NaCl versus 2 mM DHF and no NaCl. I still recovered no activity. The RIG plasmid was cotransformed into BL21 cells with the *C. parvum* DHFR plasmid. The crude extract prepared from these cells gave 0.08 U/mg, better than without the RIG plasmid and almost as much as the DHFR-TS. Cotransformed *E. coli* were induced and the lysate was purified on the MTX column. This column was washed gently (0.1 M NaCl) and a strong elution buffer used (4 mM DHF, no NaCl). This time, several fractions contained DHFR activity. The yield of protein from the column was 1.15 mg of protein and 7.6 U of activity.

CHAPTER SUBSECTION: METHOTREXATE AFFINITY COLUMN PURIFICATION

MTX affinity resin (Sigma, St. Louis, MO) (approximately 2.5 ml packed) was allowed to settle in a glass column and washed with column buffer (20 mM TES pH 7.0, 1 mM EDTA, 75 μ M β -mercaptoethanol). The column was then washed with 20 column volumes of 1 mg/ml of BSA in column buffer to eliminate non-specific binding. The column was subsequently washed with 0.5 M NaCl in column buffer followed with 20 column volumes of 2 mM DHF in column buffer. The column was then washed with 0.5 M NaCl in column buffer, 0.2 M NaCl in column buffer.

For *C. parvum* DHFR-TS, the extract was loaded on the column after the 0.2 M NaCl wash step. For *C. parvum* DHFR, the column was equilibrated with no-salt column buffer before the extract was loaded. The extract was cycled two to

three times over the column, which was then washed with 50 volumes. The DHFR-TS was washed with 0.5 M NaCl in column buffer, while the DHFR domain alone was washed with 0.1 M NaCl in column buffer. The column was equilibrated with no-salt column buffer before approximately 10 ml of elution buffer was run over the column. The elution buffer consisted of no-salt column buffer plus 2 mM (DHFR-TS) or 4 mM (DHFR) fresh DHF. The column was left overnight and 2 ml fractions taken the next morning using the approximately 20 ml of elution buffer. All steps were conducted at 4°C and all solutions contained 75 mM β -mercaptoethanol. Each form of the enzyme was purified two separate times.

Prior to use in the *in vitro* assays, the DHF used in the elution buffer had to be removed from the purified DHFR preparations. This was accomplished using Sephadex G-15 resin (Sigma, St. Louis, MO). A small amount of glass wool was placed in the bottom of a 1 ml tuberculin syringe and swelled G-15 resin was allowed to settle in the syringe barrel up to the 1 ml mark. The column was equilibrated with assay buffer without BSA and 250 μ l of DHFR solution was placed on top of the resin, followed by more assay buffer. 100 μ l fractions were taken from the bottom of the syringe and 5 μ l aliquots were tested in a 2.5 minute DHFR assay. Fractions containing activity were pooled, a total protein assay was performed, and the pool used for *in vitro* assay.

BIBLIOGRAPHY

- Anonymous. (1993a). *Cryptosporidium parvum*. In Animal Health Newsletter: United States Dept. of Agriculture, Wisconsin Dept. of Agriculture, Trade & Consumer Protection).
- Anonymous. (1993b). *Cryptosporidium* is common in dairy calves. In Animal Health Newsletter: United States Dept. of Agriculture, Wisconsin Dept. of Agriculture, Trade & Consumer Protection).
- Anonymous (1997). Outbreaks of *Escherichia coli* O157:H7 infection and cryptosporidiosis associated with drinking unpasteurized apple cider—Connecticut and New York, October 1996. MMWR Morb Mortal Wkly Rep 46, 4-8.
- Ausubel, F. M. (1988). Current protocols in molecular biology (New York: Published by Greene Pub. Associates and Wiley-Interscience : J. Wiley).
- Berenbaum, M. C. (1978). A method for testing for synergy with any number of agents. J Infect Dis 137, 122-30.
- Black, M. L. (1963). Journal of Medicinal Chemistry 6, 145-153.
- Blakley, R. L. (1995). Eukaryotic Dihydrofolate Reductase, Volume 70, A. Meister, ed.: John Wiley & Sons).
- Camenisch, G., Folkers, G., and van de Waterbeemd, H. (1996). Review of theoretical passive drug absorption models: historical background, recent developments and limitations. Pharm Acta Helv 71, 309-27.

- CDC. (1997). . In American Society of Tropical Medicine and Hygiene (Lake Buena Vista, FL.
- Cella, R., Carbonera, D., Orsi, R., Ferri, G., and Iadarola, P. (1991). Proteolytic and partial sequencing studies of the bifunctional dihydrofolate reductase-thymidylate synthase from *Daucus carota*. *Plant Mol Biol* 16, 975-82.
- Chien, C. T., Bartel, P. L., Sternglanz, R., and Fields, S. (1991). The two-hybrid system: a method to identify and clone genes for proteins that interact with a protein of interest. *Proc Natl Acad Sci U S A* 88, 9578-82.
- Clarke, J. J. (1895). A study of coccidia in mice. *J. Microscop Soc* 37, 277-302.
- Colebunders, R., Francis, H., Mann, J. M., Bila, K. M., Izaley, L., Kimputu, L., Behets, F., Van der Groen, G., Quinn, T. C., Curran, J. W., and et al. (1987). Persistent diarrhea, strongly associated with HIV infection in Kinshasa, Zaire. *Am J Gastroenterol* 82, 859-64.
- Colonna, W. J., Gentile, J. M., and Magee, P. T. (1977). Inhibitor by sulfanilamide of sporulation in *Saccharomyces cerevisiae*. *Can J Microbiol* 23, 659-71.
- Cowman, A. F., Morry, M. J., Biggs, B. A., Cross, G. A., and Foote, S. J. (1988). Amino acid changes linked to pyrimethamine resistance in the dihydrofolate reductase-thymidylate synthase gene of *Plasmodium falciparum*. *Proc Natl Acad Sci U S A* 85, 9109-13.
- Current, W. L. (1989). *Cryptosporidium* spp. In *Parasitic infections in the compromised host*, P. D. Walzer and R. M. Genta, eds. (New York: Marcel Dekker), pp. 281-341.

- Despommier, D. D., and Karapelou, J. W. (1987). *Parasite life cycles* (New York: Springer-Verlag).
- Dowd, J. E., and Riggs, D. S. (1965). A comparison of estimates of Michaelis-Menten kinetic constants from various linear transformation. *Journal of Biological Chemistry* 240, 863-869.
- Dubey, J. P., Speer, C. A., and Fayer, R. (1990). *Cryptosporidiosis of man and animals* (Boca Raton, Fla.: CRC Press).
- Elcock, A. H., Potter, M. J., Matthews, D. A., Knighton, D. R., and McCammon, J. A. (1996). Electrostatic channeling in the bifunctional enzyme dihydrofolate reductase-thymidylate synthase. *J Mol Biol* 262, 370-4.
- Friedkin, M., Crawford, E. J., and Misra, D. (1962). *Fed. Proc. Fed. Am. Soc. Exp. Biol.* 21, 176.
- Grindley, G., Moran, R., Werkheiser, W. C. (1975). *Drug Design, Volume 5*, E. J. Ariens, ed. (New York: Academic Press).
- Guerrant, R. L. (1997). Cryptosporidiosis: an emerging, highly infectious threat. *Emerging Infectious Diseases* 3, 51-7.
- Guthrie, C., and Fink, G. R. (1991). *Guide to yeast genetics and molecular biology* (San Diego: Academic Press).
- Harp, J. A., Jardon, P., Atwill, E. R., Zylstra, M., Checelsky, S., Goff, J. P., and De Simone, C. (1996). Field testing of prophylactic measures against *Cryptosporidium parvum* infection in calves in a California dairy herd. *Am J Vet Res* 57, 1586-8.

- Hellard, M. E., Sinclair, M. I., Streeton, C. L., and Fairley, C. K. (1997). Drinking water and microbiological pathogens--issues and challenges for the year 2000. *Journal Of Public Health Medicine* 19, 129-31.
- Herskowitz, I. (1995). MAP kinase pathways in yeast: for mating and more. *Cell* 80, 187-97.
- Hewlett, P. S. (1969). Measurement of the potencies of drug mixtures. *Biometrics* 25, 477-87.
- Hoepelman, I. M. (1996). Human cryptosporidiosis. *International Journal Of Std and Aids* 7 Suppl 1, 28-33.
- Hoffman, C. S., and Winston, F. (1987). A ten-minute DNA preparation from yeast efficiently releases autonomous plasmids for transformation of *Escherichia coli*. *Gene* 57, 267-72.
- Huang, T., Barclay, B. J., Kalman, T. I., von Borstel, R. C., and Hastings, P. J. (1992). The phenotype of a dihydrofolate reductase mutant of *Saccharomyces cerevisiae*. *Gene* 121, 167-71.
- Ito, H., Fukuda, Y., Murata, K., and Kimura, A. (1983). Transformation of intact yeast cells treated with alkali cations. *Journal of Bacteriology* 153, 163-168.
- Ivanetich, K. M., and Santi, D. V. (1990). Bifunctional thymidylate synthase-dihydrofolate reductase in protozoa. *Faseb J* 4, 1591-7.
- Jokipii, L., and Jokipii, A. M. (1986). Timing of symptoms and oocyst excretion in human cryptosporidiosis. *New England Journal Of Medicine* 315, 1643-7.
- Knighton, D. R., Kan, C. C., Howland, E., Janson, C. A., Hostomska, Z., Welsh, K. M., and Matthews, D. A. (1994). Structure of and kinetic channelling in

bifunctional dihydrofolate reductase-thymidylate synthase. *Nat Struct Biol* 1, 186-94.

Koch, K. L., Phillips, D. J., Aber, R. C., and Current, W. L. (1985). Cryptosporidiosis in hospital personnel. Evidence for person-to-person transmission. *Ann Intern Med* 102, 593-6.

Kurland, C. G. (1991). Codon bias and gene expression. *FEBS Lett* 285, 165-9.

Kurland, C. G. (1993). Major codon preference: theme and variations. *Biochem Soc Trans* 21, 841-6.

Laughon, B. E., Druckman, D. A., Vernon, A., Quinn, T. C., Polk, B. F., Modlin, J. F., Yolken, R. H., and Bartlett, J. G. (1988). Prevalence of enteric pathogens in homosexual men with and without acquired immunodeficiency syndrome. *Gastroenterology* 94, 984-93.

Lazar, G., Zhang, H., and Goodman, H. M. (1993). The origin of the bifunctional dihydrofolate reductase-thymidylate synthase isogenes of *Arabidopsis thaliana*. *Plant J* 3, 657-68.

LeChevallier, M. W., and Moser, R. H. (1993). Monitoring *Giardia* and *Cryptosporidium* in the American Water System.: American Water Works Service Co.).

LeChevallier, M. W., Norton, W. D., and Lee, R. G. (1991). Occurrence of *Giardia* and *Cryptosporidium* spp. in surface water supplies [published erratum appears in *Appl Environ Microbiol* 1992 Feb;58(2):780]. *Appl Environ Microbiol* 57, 2610-6.

- Lemeteil, D., Roussel, F., Favennec, L., Ballet, J. J., and Brasseur, P. (1993). Assessment of candidate anticryptosporidial agents in an immunosuppressed rat model. *J Infect Dis* 167, 766-8.
- Lin, J. T., and Bertino, J. R. (1987). Trimetrexate: a second generation folate antagonist in clinical trial. *J Clin Oncol* 5, 2032-40.
- Little, J. G., and Haynes, R. H. (1979). Isolation and characterization of yeast mutants auxotrophic for 2'- deoxythymidine 5'-monophosphate. *Mol Gen Genet* 168, 141-51.
- MacKenzie, W. R., Hoxie, N. J., Proctor, M. E., Gradus, M. S., Blair, K. A., Peterson, D. E., Kazmierczak, J. J., Addiss, D. G., Fox, K. R., Rose, J. B., and et al. (1994). A massive outbreak in Milwaukee of cryptosporidium infection transmitted through the public water supply [published erratum appears in *N Engl J Med* 1994 Oct 13;331(15):1035] [see comments]. *N Engl J Med* 331, 161-7.
- Marshall, M. M., Naumovitz, D., Ortega, Y., and Sterling, C. R. (1997). Waterborne protozoan pathogens. *Clinical Microbiology Reviews* 10, 67-85.
- McDonald, V., Stables, R., Warhurst, D. C., Barer, M. R., Blewett, D. A., Chapman, H. D., Connolly, G. M., Chiodini, P. L., and McAdam, K. P. (1990). In vitro cultivation of *Cryptosporidium parvum* and screening for anticryptosporidial drugs. *Antimicrob Agents Chemother* 34, 1498-500.
- Meisel, J. L., Perera, D. R., Meligro, C., and Rubin, C. E. (1976). Overwhelming watery diarrhea associated with a cryptosporidium in an immunosuppressed patient. *Gastroenterology* 70, 1156-60.

- Miyajima, A., Miyajima, I., Arai, K., and Arai, N. (1984). Expression of plasmid R388-encoded type II dihydrofolate reductase as a dominant selective marker in *Saccharomyces cerevisiae*. *Mol Cell Biol* 4, 407-14.
- Mumberg, D., Muller, R., and Funk, M. (1995). Yeast vectors for the controlled expression of heterologous proteins in different genetic backgrounds. *Gene* 156, 119-22.
- Myers, C. E., Lippman, M. E., Elliot, H. M., and Chabner, B. A. (1975). Competitive protein binding assay for methotrexate. *Proc Natl Acad Sci U S A* 72, 3683-6.
- Nime, F. A., Burek, J. D., Page, D. L., Holscher, M. A., and Yardley, J. H. (1976). Acute enterocolitis in a human being infected with the protozoan *Cryptosporidium*. *Gastroenterology* 70, 592-8.
- Nitiss, J., and Wang, J. C. (1988). DNA topoisomerase-targeting antitumor drugs can be studied in yeast. *Proc Natl Acad Sci U S A* 85, 7501-5.
- Nitiss, J. L. (1994). Using yeast to study resistance to topoisomerase II-targeting drugs. *Cancer Chemother Pharmacol* 34, S6-13.
- O'Donoghue, P. J. (1985). *Cryptosporidium* infections in man, animals, birds and fish. *Australian Veterinary Journal* 62, 253-8.
- Ortega, Y. R., Roxas, C. R., Gilman, R. H., Miller, N. J., Cabrera, L., Taquiri, C., and Sterling, C. R. (1997). Isolation of *Cryptosporidium parvum* and *Cyclospora cayetanensis* from vegetables collected in markets of an endemic region in Peru. *Am J Trop Med Hyg* 57, 683-6.
- PDR. (1990). Physicians' desk reference : PDR, Volume issue. (Oradell, N.J.: Medical Economics Co.).

- Peterson, D. S., Walliker, D., and Wellems, T. E. (1988). Evidence that a point mutation in dihydrofolate reductase-thymidylate synthase confers resistance to pyrimethamine in *falciparum* malaria. *Proc Natl Acad Sci U S A* 85, 9114-8.
- Pillai, R., Kytle, K., Reyes, A., and Colicelli, J. (1993). Use of a yeast expression system for the isolation and analysis of drug- resistant mutants of a mammalian phosphodiesterase. *Proc Natl Acad Sci U S A* 90, 11970-4.
- Poe, M. (1976). Antibacterial synergism: a proposal for chemotherapeutic potentiation between trimethoprim and sulfamethoxazole. *Science* 194, 533-5.
- Prapunwattana, P., Sirawaraporn, W., Yuthavong, Y., and Santi, D. V. (1996). Chemical synthesis of the *Plasmodium falciparum* dihydrofolate reductase-thymidylate synthase gene. *Mol Biochem Parasitol* 83, 93-106.
- Roland, S., Ferone, R., Harvey, R. J., Styles, V. L., and Morrison, R. W. (1979). The characteristics and significance of sulfonamides as substrates for *Escherichia coli* dihydropteroate synthase. *J Biol Chem* 254, 10337-45.
- Rose, J. B. (1997). Environmental ecology of *Cryptosporidium* and public health implications. *Annu Rev Public Health* 18, 135-61.
- Rubin, R. J., Reynard, A., Handschumacher, R. E. (1964). An Analysis of the Lack of Drug Synergism during Sequential Blockade of *de Novo* Pyrimidine Biosynthesis. *Cancer Research* 24, 1002-1007.
- Sambrook, J., Maniatis, T., and Fritsch, E. F. (1989). *Molecular cloning : a laboratory manual*, 2nd Edition (Cold Spring Harbor, N.Y.: Cold Spring Harbor Laboratory).
- Segel, J. H. (1975). *Enzyme Kinetics* (New York: John Wiley and Sons).

- SenGupta, D. J., Zhang, B., Kraemer, B., Pochart, P., Fields, S., and Wickens, M. (1996). A three-hybrid system to detect RNA-protein interactions in vivo. *Proc Natl Acad Sci U S A* 93, 8496-501.
- Sherwood, D., Angus, K. W., Snodgrass, D. R., and Tzipori, S. (1982). Experimental cryptosporidiosis in laboratory mice. *Infect Immun* 38, 471-5.
- Sibley, C. H., Brophy, V. H., Cheesman, S., Hamilton, K. L., Hankins, E. G., Wooden, J. M., and Kilbey, B. (1997). Yeast as a model system to study drugs effective against apicomplexan proteins. *Methods* 13, 190-207.
- Sikorski, R. S., and Hieter, P. (1989). A system of shuttle vectors and yeast host strains designed for efficient manipulation of DNA in *Saccharomyces cerevisiae*. *Genetics* 122, 19-27.
- Sims, P., Wang, P., and Hyde, J. E. (1998). On 'the efficacy of antifolate antimalarial combinations in Africa'. *Parasitology Today* 14, 136-137.
- Sirawaraporn, W., Prapunwattana, P., Sirawaraporn, R., Yuthavong, Y., and Santi, D. V. (1993). The dihydrofolate reductase domain of *Plasmodium falciparum* thymidylate synthase-dihydrofolate reductase. Gene synthesis, expression, and anti-folate-resistant mutants. *J Biol Chem* 268, 21637-44.
- Sirawaraporn, W., Sirawaraporn, R., Cowman, A. F., Yuthavong, Y., and Santi, D. V. (1990). Heterologous expression of active thymidylate synthase-dihydrofolate reductase from *Plasmodium falciparum*. *Biochemistry* 29, 10779-85.
- Sirotnak, F. M. (1984). *Folate antagonists as therapeutic agents* (New York: Academic Press).

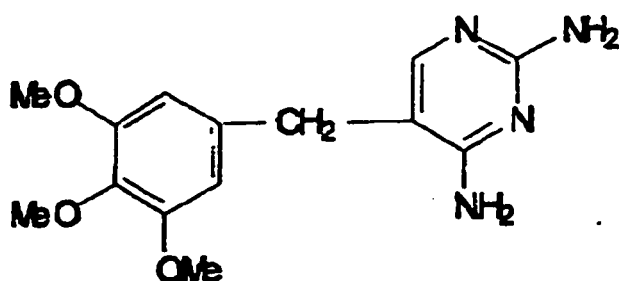
- Stokstad, E. L., and Jukes, T. H. (1987). Sulfonamides and folic acid antagonists: a historical review. *J Nutr* 117, 1335-41.
- Trumbly, R. J. (1992). Glucose repression in the yeast *Saccharomyces cerevisiae*. *Mol Microbiol* 6, 15-21.
- Tyzzer, E. E. (1907). A sporozoan found in the peptic glands of the common mouse. *Proc Soc Exp Biol Med* 5, 12-13.
- Ungar, B. L., Gilman, R. H., Lanata, C. F., and Perez-Schael, I. (1988). Seroepidemiology of *Cryptosporidium* infection in two Latin American populations. *J Infect Dis* 157, 551-6.
- Ungar, B. L., Mulligan, M., and Nutman, T. B. (1989). Serologic evidence of *Cryptosporidium* infection in US volunteers before and during Peace Corps service in Africa. *Arch Intern Med* 149, 894-7.
- Vasquez, J. R., Gooze, L., Kim, K., Gut, J., Petersen, C., and Nelson, R. G. (1996). Potential antifolate resistance determinants and genotypic variation in the bifunctional dihydrofolate reductase-thymidylate synthase gene from human and bovine isolates of *Cryptosporidium parvum*. *Molecular and Biochemical Parasitology* 79, 153-65.
- Watkins, W. M., Mberu, E. K., Winstanley, P. A., and Plowe, C. V. (1997). The efficacy of antifolate antimalarial combinations in Africa: A predictive model based on pharmacodynamic and pharmacokinetic analyses. *Parasitology Today* 13, 459-464.
- Webb, J. L. (1963). *Enzyme and Metabolic Inhibitors, Volume 1* (New York: Academic Press).

- Welch, A. D. (1983). Folic acid: discovery and the exciting first decade. *Perspect Biol Med* 27, 64-75.
- Wooden, J. M., Hartwell, L. H., Vasquez, B., and Sibley, C. H. (1997). Analysis in yeast of antimalaria drugs that target the dihydrofolate reductase of *Plasmodium falciparum*. *Mol Biochem Parasitol* 85, 25-40.
- Woods, K. M., Nesterenko, M. V., and Upton, S. J. (1995). Development of a microtitre ELISA to quantify development of *Cryptosporidium parvum* in vitro. *FEMS Microbiol Lett* 128, 89-94.
- Woods, K. M., Nesterenko, M. V., and Upton, S. J. (1996). Efficacy of 101 antimicrobials and other agents on the development of *Cryptosporidium parvum* in vitro. *Ann Trop Med Parasitol* 90, 603-15.
- Yang, S., Healey, M. C., Du, C., and Zhang, J. (1996). Complete development of *Cryptosporidium parvum* in bovine fallopian tube epithelial cells. *Infect Immun* 64, 349-54.
- Zhou, Y. H., Zhang, X. P., and Ebright, R. H. (1991). Random mutagenesis of gene-sized DNA molecules by use of PCR with Taq DNA polymerase. *Nucleic Acids Res* 19, 6052.
- Zolg, J. W., Plitt, J. R., Chen, G. X., and Palmer, S. (1989). Point mutations in the dihydrofolate reductase-thymidylate synthase gene as the molecular basis for pyrimethamine resistance in *Plasmodium falciparum*. *Mol Biochem Parasitol* 36, 253-62.

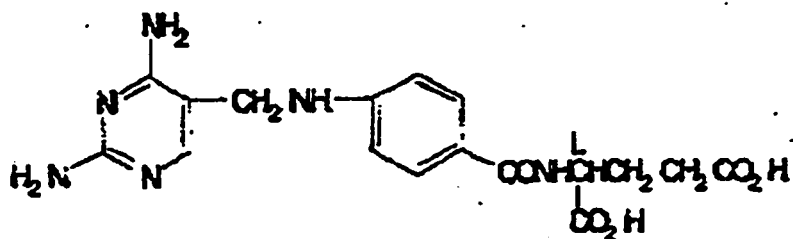
APPENDIX A: CHEMICAL STRUCTURES OF TEST COMPOUNDS

National Cancer Institute Compounds

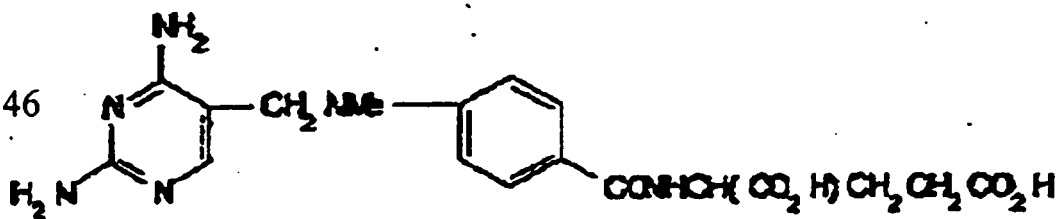
106568



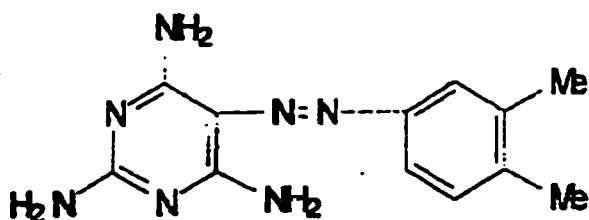
112421



121146

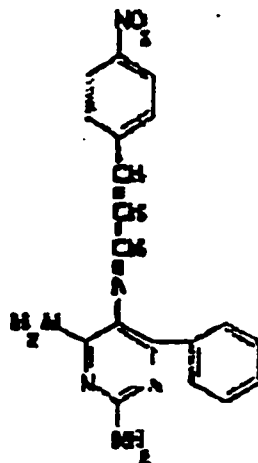


117288

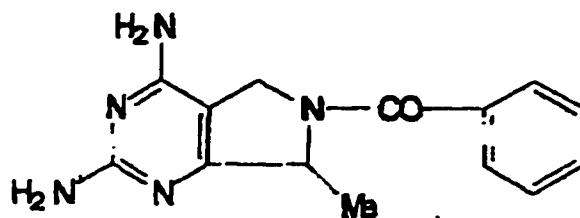


126

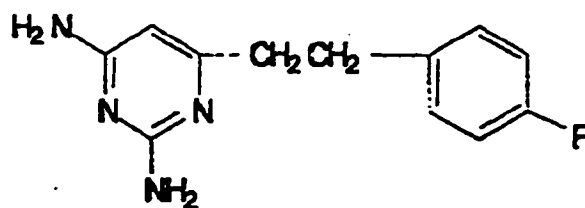
104126



107242



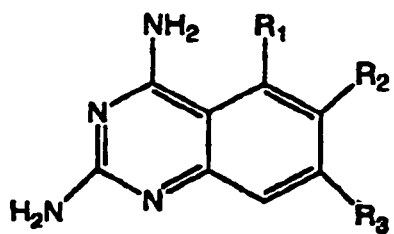
61670



Structures Unavailable:

3081
47532
77028
104133
127916
529861

Dana-Farber Compounds



PY359

R1 = H

R2 = Cl

R3 = H

PY361

R1 = MeO

R2 = H

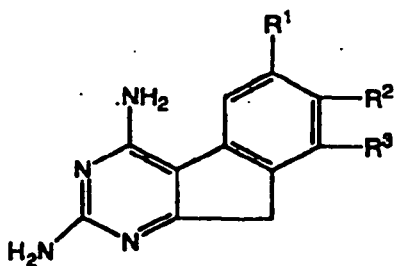
R3 = H

PY365

R1 = EtO

R2 = H

R3 = H

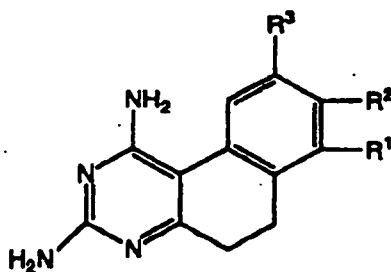


PY460

R1 = H

R2 = MeO

R3 = MeO



PY461

R1 = MeO

R2 = H

R3 = H

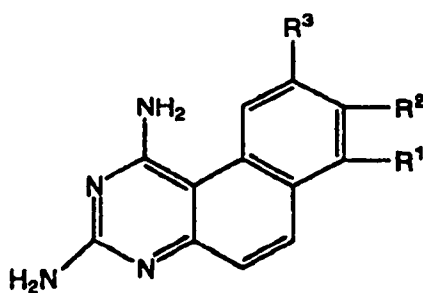
PY468

R1 = H

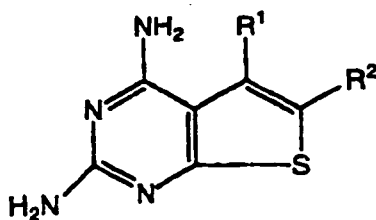
R2 = Cl

R3 = H

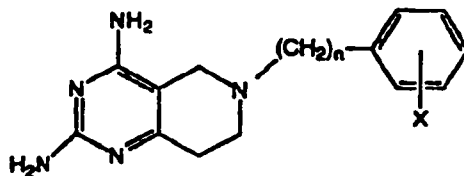
128



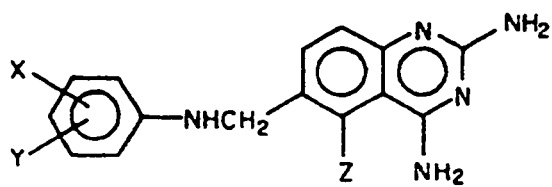
PY488	R1 = H	R2 = Br	R3 = H
PY489	R1 = H	R2 = Cl	R3 = H
PY490	R1 = H	R2 = H	R3 = Cl
PY497	R1 = H	R2 = H	R3 = MeO



PY821	R1 = Me	R2 = 3,4-Cl ₂ C ₆ H ₃
PY823	R1 = Me	R2 = 3,4-Cl ₂ C ₆ H ₃
PY826	R1 = 4-ClC ₆ H ₃	R2 = Me
PY833	R1 = 4-ClC ₆ H ₃	R2 = EtO
PY841	R1 = Me	R2 = 3,4,5-(MeO) ₃ C ₆ H ₂
PY842	R1 = Me	R2 = 3,4,5-(MeO) ₃ C ₆ H ₂ CH ₂
PY888	R1 = 3,4,5-(MeO) ₃ C ₆ H ₂ NHCH ₂	R2 = H
PY890	R1 = 3,4,5-(MeO) ₃ C ₆ H ₂ N(Me)CH ₂	R2 = H



PY875	n = 1	X = 3,4,5-(MeO) ₃
-------	-------	------------------------------



PY896	X,Y = 3,4-(MeO) ₃	Z = H
PY898	X,Y = H	Z = H
PY899	X,Y = 3,4,5-(MeO) ₃	Z = H

APPENDIX B: EXPRESSION OF CD14 CORRECTS THE SLOW RESPONSE TO
LIPOPOLYSACCHARIDE IN THE 1B8 MUTANT OF THE B CELL LYMPHOMA

70Z/3

ORIGINAL PAPER

Victoria Hertle Brophy · Carol Hopkins Sibley

Expression of CD14 corrects the slow response to lipopolysaccharide in the 1B8 mutant of the B cell lymphoma 70Z/3

Received: 3 June 1997 / Revised: 26 June 1997

Abstract B cells and macrophages both activate NF- κ B/Rel in response to lipopolysaccharide (LPS), but differ in sensitivity to LPS and in downstream genes that are activated. CD14 is a high-affinity receptor for LPS found on macrophages, but not B cells. We expressed human CD14 (hCD14) in the mouse B lymphoma, 70Z/3, and a mutant, 1B8, which responds slowly to LPS, to test whether expression of hCD14 could correct or bypass the defect in 1B8 cells. We compared the timing and extent of known responses to LPS in 70Z/3 cells and the 1B8 mutants. The hCD14⁺ 1B8 and 70Z/3 cells responded more rapidly and were sensitive to 100-fold lower levels of LPS than their untransfected counterparts. Degradation of the I κ B- α and - β molecules and translocation of the NF- κ B/Rel complexes into the nucleus were more rapid and the steady-state levels of *Igk* mRNA and mIgM on the cell surface were markedly increased in cells that expressed hCD14. The LPS response of the hCD14⁺ 1B8 and 70Z/3 cells showed subtle differences. In the 1B8 hCD14 cells, the p50/p50 complexes were never abundant in nuclear extracts, and degradation of I κ B- β was slower than in hCD14 70Z/3 cells. This partial correction of the 1B8 phenotype suggests that the defective component in 1B8 participates in the CD14 signaling pathway and could include the B-cell LPS receptor itself.

Key words NF- κ B/Rel · Signal transduction · Endotoxin · LPS · CD14

Introduction

The pathways by which extracellular molecules stimulate changes in transcription have been intensively studied in recent years. Genetic analysis has played a prominent role in the definition of many signal transduction pathways. We employed this approach to begin to dissect the complex

network by which cells in the mammalian immune system respond to stress, a network that centers on activation of the nuclear factor kappa B/Rel (NF- κ B/Rel) family of transcription factors (Bal 1986; Sen and Baltimore 1986; Ulevitch et al. 1996).

NF- κ B/Rel molecules comprise a diverse family of heterodimeric transcription factors that share a Rel homology domain (reviewed in (Baldwin 1996; Liou and Baltimore 1993; Ulevitch et al. 1996)). The NF- κ B/Rel complexes are ubiquitous, but are particularly prominent in hematopoietic cells. In lymphocytes, monocytes, and macrophages, the NF- κ B/Rel complexes are anchored in the cytoplasm by interaction with members of the inhibitor of kappa B (I κ B) family (Baeuerle and Baltimore 1988; Baldwin 1996; Chen et al. 1995; Palombella et al. 1994). Activation is initiated by phosphorylation (DiDonato et al. 1997; Ghosh and Baltimore 1990; Israel 1997; Schouten et al. 1997), ubiquitination (Thompson et al. 1995), and degradation of the I κ B anchor (Baeuerle and Baltimore 1988), exposing the nuclear localization domain of the NF- κ B/Rel complexes and allowing their active transport into the nucleus. The p50, p65, and Rel subunits form hetero- and homodimers and all bind to sites in nuclear genes that conform to the sequence 5'-GGGRNYYCC-3' and stimulate transcription of linked genes (Baldwin 1996; Liou and Baltimore 1993; Ulevitch et al. 1996). Bacterial lipopolysaccharide (LPS) is a major constituent of the outer membrane of gram-negative bacteria; it is a potent activator of NF- κ B/Rel in hematopoietic cells (Golenbock et al. 1991; Morrison et al. 1994; Morrison and Ryan 1987; Raetz 1990; Rietschel and Brade 1992; Ulevitch et al. 1996). We focused on genetic approaches to begin to dissect this pathway of NF- κ B/Rel activation.

In monocytes and macrophages, as little as 1 ng/ml LPS can activate NF- κ B/Rel and rapidly initiate synthesis of tumor necrosis factor α and interleukin-1 (Baldwin 1996; Beaty et al. 1994; Beg and Baldwin 1994; Raetz et al. 1991). In the B-cell lymphoma, 70Z/3, the unstimulated cells actively transcribe the *mu* heavy chain but *Igk* light chain synthesis is at a very low level (Paige et al. 1978). Treatment of 70Z/3 cells with 1 μ g/ml LPS is required to

V.H. Brophy · C.H. Sibley (✉)
Department of Genetics, Box 357360, University of Washington,
Seattle, WA 98195, USA

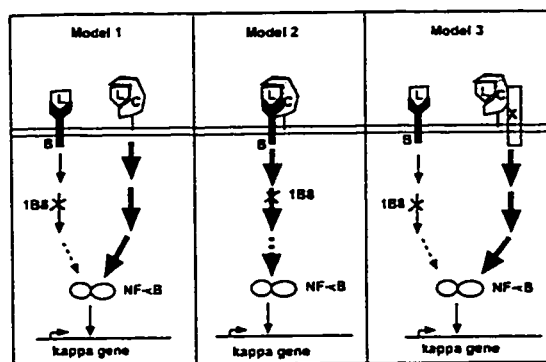


Fig. 1 Models for CD14 signaling in 702/3 cells. B represents the B-cell LPS receptor, L = LPS, C = hCD14, and X = hypothetical transmembrane signaling protein that is not the B-cell LPS receptor. Model 1: CD14 signals through its GPI anchor and the B-cell LPS receptor signals by itself only. Model 2: The B-cell LPS receptor can signal weakly on its own or strongly in concert with CD14. Model 3: The B-cell LPS receptor signals only on its own and CD14 signals through a distinct transmembrane protein

maximally activate NF- κ B/Rel (Mains and Sibley 1982, 1983; Sen and Baltimore 1986), stimulate transcription and translation of *Igk*, and express IgM on the cell surface (Nelson et al. 1984; Paige et al. 1981; Weeks et al. 1984; Weeks and Sibley 1987, 1988). We had previously selected 702/3 cells with defects in their response to LPS to better define the mechanism by which LPS induces transcription of *Igk* (Mains and Sibley 1983; Rhodes et al. 1994; Rooney et al. 1990a, b; Weeks and Sibley 1987). One clone that resulted from this selection was 1B8, a line that responds to LPS far more slowly than the wild type (Mains and Sibley 1983). The defect is manifested in much slower activation of NF- κ B/Rel complexes into the nuclear fraction and a correspondingly slower increase in *Igk* transcription and transport of mIgM to the cell surface (Mains and Sibley 1983; Ostrowski et al. 1991; Rooney et al. 1990).

Although both B cells and macrophages respond to the LPS stimulus by activating NF- κ B/Rel, they differ both in sensitivity to LPS and in the downstream genes that are activated (Baeuerle and Henkel 1994; Baldwin 1996; Chen et al. 1990; Ulevitch et al. 1996). In monocytes and macrophages, but not B cells, a high-affinity LPS receptor has been identified: CD14. This glycosylphosphatidylinositol-linked (GPI) membrane molecule binds LPS complexed to the serum protein LPS-binding protein (LBP) (Raetz et al. 1991; Schumann 1992; Wright et al. 1990). CD14 has been shown to mediate the LPS response (Couturier et al. 1991; Golenbock et al. 1993; Kirkland et al. 1993; Weinstein et al. 1993; Wright et al. 1990), but the signaling pathway that it stimulates has not been completely defined. Three models have been proposed for CD14 action (Fig. 1). In the first model, CD14 signals directly through its GPI anchor. However, a CD14 molecule engineered to be an integral membrane protein was indistinguishable from its lipid-linked counterpart in cell activa-

tion (Lee et al. 1993), rendering this model unlikely. The other two models both postulate that CD14 interacts with a transmembrane protein that accomplishes the signaling. In model 2, the second protein has a low affinity for LPS and can signal weakly by itself, but the signal is strongly augmented when LPS is bound to CD14. In model 3, the second protein can signal only in the presence of LPS-bound CD14. Our goal was to distinguish between these latter two models.

B cells do not express CD14, and despite considerable effort, the LPS receptor has not yet been identified in these cells. When human CD14 (hCD14) was expressed in 702/3 cells, their sensitivity to LPS was dramatically increased. The transfected cells required less than 1 ng/ml to activate a vigorous response to LPS (Lee et al. 1992), demonstrating that the components required for CD14 signaling are expressed in 702/3 B cells. We reasoned that if CD14 signals by a pathway distinct from that normally used by LPS in 702/3 cells, expression of the hCD14 in the mutant might bypass the lesion and rescue the slow response to LPS that defines the 1B8 phenotype (Fig. 1). On the other hand, if the CD14 signals through a transduction pathway that includes the 1B8 defect, the CD14⁺ 1B8 cells should still show a slow activation phenotype. To better understand the signal transduction pathways in the 1B8 mutant cells, we transfected the wild-type and mutant cells with a construct that supports high-level expression of hCD14 and compared the timing and extent of known responses to LPS.

Materials and methods

Cell culture and LPS induction

The mouse B-cell lymphoma 702/3 (Paige et al. 1978), the 702/3 variant 1B8 (Mains and Sibley 1983), and the hCD14-expressing clones were grown in RPMI 1640 supplemented with 3.5% defined fetal calf serum (Hyclone, Logan, Utah), 3.5% fetal clone (Hyclone), 0.3 mg/ml glutamine, 100 units/ml penicillin, 0.1 mg/ml streptomycin, and 5×10^{-5} M 2-mercaptoethanol. Cells were maintained near 1×10^6 cells/ml. The cells were incubated with 1 μ g/ml (unless otherwise stated) of *Salmonella typhosa* 0901 LPS W (StLPS), commercially prepared by the phenol method (Difco, Detroit, Mich.), and samples were taken at various times. After 12 h, the cells were diluted to a density of 5×10^5 cells/ml in RPMI media and additional LPS was added to remain at 1 μ g/ml.

Transfection

Plasmid DNA was isolated from DH5 α *Escherichia coli* using a Qiagen column (Qiagen, Studio City, Calif.). Stable transfection of 702/3 and 1B8 cells was performed by electroporation with a BioRad GenePulser (Hercules, Calif.). Cells (1×10^7) were subjected to electroporation with 25 μ g of pRC/RSV vector or pRC/RSV-hCD14 (a gift from R. Ulevitch) at 400 V and 960 μ farad. The cells were allowed to recover for 24 h in RPMI 1640, then plated in 96-well plates in RPMI 1640 and 1 mg/ml Geneticin (Gibco BRL, Grand Island, N.Y.) to select for transfectants. Wells containing single colonies were isolated and tested for hCD14 expression level by northern analysis and fluorocytometric analysis.

Immunofluorescent staining and flow cytometric analysis

Approximately 1.5×10^6 cells were incubated on ice with a fluorescently labeled antibody directed against the surface protein of interest, then washed with PBS and fixed in 1% paraformaldehyde as described (Rhodes et al. 1994). To determine the amount of IgM on the surface, LPS-stimulated cells were incubated with affinity-purified fluorescein-coupled goat antibodies directed against mouse IgM (Chemicon, El Segundo, Calif.). To determine the level of hCD14 on the surface, untreated cells were stained with the rhodamine-coupled antibody directed against human CD14, MY4 (Coulter, Hialeah, Fla.). The fluorescence of each cell and the mode of the fluorescence in each population were determined on a FACScan instrument using Consort 30 software (Becton and Dickinson, San Jose, Calif.).

Northern blots

Total RNA was isolated by the method of Cox (1968) as described by Labarca and Paigen (1977). Five micrograms of total RNA was separated on a 1.5% agarose 2.2 M formaldehyde gel and blotted to a nylon filter (Hybond-N; Amersham, Arlington Heights, Ill.), which was crosslinked with UV (0.12 J), then baked for 30 min at 80 °C. Filters were incubated in FS [50% formamide, 5× standard sodium citrate (SSC), 10× Denhart's, 0.5% sodium dodecyl sulfate (SDS), and 200 µg/ml denatured salmon sperm DNA] for 2 h at 50 °C. Random-primed probes (Boehringer Mannheim, Indianapolis, Ind.) were synthesized from the *Igk* second exon (p_{rex2}) (Miller et al. 1991) or the hCD14 cDNA clone. Probe was added to the FS to 3×10^6 CPM/ml and the filters were hybridized for 20 h at 50 °C. Following washing (three times at 55 °C in 0.1% SSC and 0.1% SDS for 30 min), the PhosphorImager counts of each band were measured with a Molecular Dynamics PhosphorImager model 400S and analyzed by Molecular Dynamics ImageQuant software. The data were corrected for background radiation and normalized for loading by probing the filter with a random-primed β -actin probe (pActBB) (Miller et al. 1991).

Nuclear protein extraction and electrophoretic mobility shift assay

Extracts were prepared with a modification of the method of Dignam and co-workers (1983). After treatment, 40×10^6 cells were washed once each with 1 ml of phosphate-buffered saline and buffer A (10 mM N-2-hydroxyethylpiperazine-N'-2-ethanesulfonic acid (HEPES), 10 mM KCl, and 1.5 mM MgCl₂; pH 7.9). Cell lysis was evident within 5 min of resuspension on ice in 80 ml of buffer A containing 0.2% NP-40. Nuclei were pelleted by centrifugation (10 min at $14,000 \times g$, 4 °C) and the cytoplasmic fraction (supernatant) was transferred to a new tube, to which 120 µl of buffer D [50 mM KCl, 20 mM HEPES, 0.2 mM ethylenediaminetetraacetate (EDTA), and 20% glycerol, pH 7.9] was added. The nuclear proteins were extracted from the pellet with vigorous mixing in 80 µl of buffer C (420 mM NaCl, 20 mM HEPES, 1.5 mM MgCl₂, 0.2 mM EDTA, and 25% glycerol, pH 7.9) for 10 min (4 °C), followed by centrifugation (10 min at $14,000 \times g$, 4 °C). This supernatant was transferred to a new tube and diluted with 120 µl of buffer D (50 mM KCl, 20 mM HEPES, 0.2 mM EDTA, and 20% glycerol, pH 7.9) and the protein concentration was determined by Coomassie protein assay reagent (Pierce, Rockford, Ill.) and a microtiter plate reader. Dithiothreitol 0.5 mM, 0.5 mM phenylmethylsulfonyl fluoride, and 10 µg/ml of leupeptin were added to both buffers A and C just before use; buffer D contained 0.5 mM dithiothreitol, but only 0.2 mM phenylmethylsulfonyl fluoride. In addition, the following inhibitors were added to buffers A + NP-40 and C: 0.1 mM sodium molybdate, 10 mM β -glycerol phosphate, 10 mM sodium fluoride, 0.1 mM sodium orthovanadate, and 13.84 mg/ml β -nitro-phenylphosphate.

The double-stranded NF- κ B and κ E3 probes were formed by annealing the oligonucleotides 5'TGACAGAGGGACTTTCCGA-GAGGA3' and 5'AAAAATTGTCCTATGTGGTTACAAACCAT3' to their complements. The oligonucleotide probes were end-labeled using [γ -³²P] ATP and T4 Kinase (Gibco BRL). The nuclear protein-DNA probe binding reactions were performed as described previously

(Bomsztyk et al. 1990) with the binding buffer containing 10 mM Tris (hydroxymethyl aminomethane-HCl), 50 mM NaCl, 1 mM EDTA, pH 7.5. Nuclear extracts containing 8 µg of total protein were incubated with radiolabeled probe, 0.0625% NP-40, 0.125 µg/µl poly dI/dC, and 1 mM DTT in the binding buffer for 30 min at room temperature. Nuclear protein-DNA complexes were fractionated on 8×7 cm 6% polyacrylamide gels (0.5× TBE pH 8.3, 50 V, 3 h), dried, and exposed to film. Antibodies directed against p65 (obtained from Karol Bomsztyk) raised to the N-terminal p65 peptide MDDLFLIFP-SEPAQASGPACG were added to the nuclear extracts at the same time as the addition of the probe to supershift the complexes binding to the κ B oligonucleotide.

For presentation, the electrophoretic mobility shift assay (EMSA) films were scanned by a flatbed scanner into Adobe Photoshop, where the images were cropped and the levels adjusted to improve contrast.

Western assays

The cytoplasmic extracts from above were analyzed for I κ B- α and I κ B- β by fractionating 40 µg protein on 10% SDS-polyacrylamide gels. The protein was then electroblotted onto PVDF membrane (Millipore, Bedford, Mass.) and the membrane was blocked with 5% blotto [nonfat dry milk in 1× TBST (10 mM Tris-Cl pH 6.7, 150 mM NaCl, 0.05% Tween-20)]. Following incubation with the primary antibodies against I κ B- α and I κ B- β (1:10 000) the blots were incubated with a goat anti-rabbit-specific secondary antibody coupled to horseradish peroxidase at 1:500 (Amersham, Arlington Heights, Ill.). The proteins were then detected by an enhanced chemiluminescence, modified from Schneppenheim and Rautenberg (1987). Immediately before use, 20 mg of luminol and 5 mg of 4-iodophenol (Sigma, St. Louis, Mo.) were dissolved in 0.5 ml DMSO. Fifty micromolar of Tris-Cl pH 8.5, 12.5 mM NaCl, 62.5 µl H₂O₂ (30%), and H₂O (to bring the volume up to 25 ml) were added to the DMSO and the blot was incubated in the mixture for 90 s and then removed from the reagent and immediately exposed to film. The rabbit polyclonal antisera directed against I κ B α was raised against the C-terminus of the I κ B- α /MAD-3 of human origin (Santa Cruz Biotechnology, Santa Cruz, Calif.). The antibody directed against I κ B- β was a gift from S. Ghosh (Thompson et al. 1995).

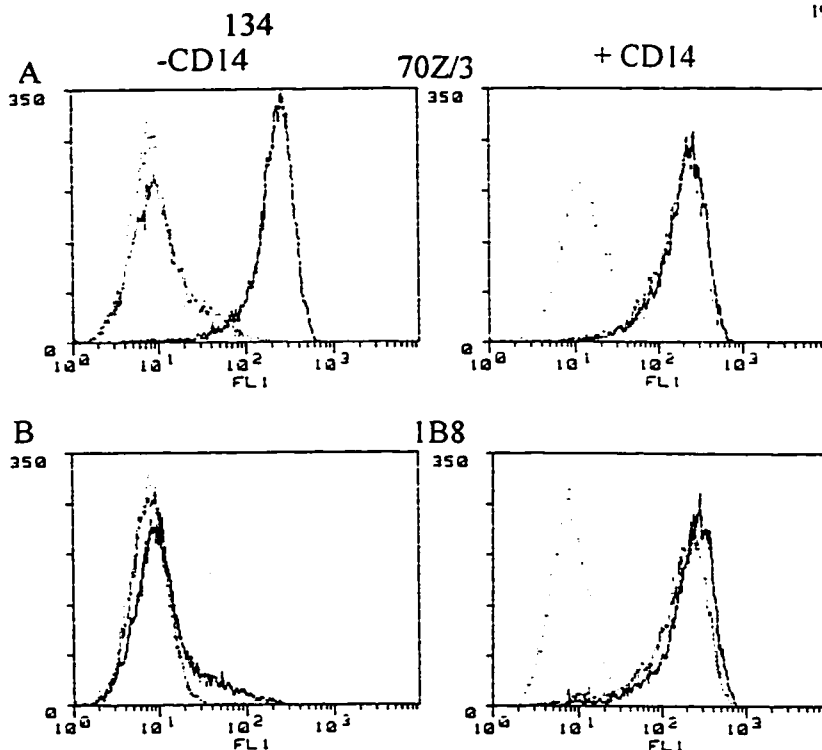
For presentation, the films were scanned by a flatbed scanner into Adobe Photoshop, where the images were cropped and the levels adjusted to improve contrast.

Results

hCD14 expression in 70Z/3 cells increased LPS sensitivity

Expression of human CD14 (hCD14) has been shown previously to increase the sensitivity of 70Z/3 cells to LPS stimulation (Lee et al. 1992). To confirm this observation, we transfected our subline of 70Z/3 with the pRc/RSV hCD14 plasmid (Lee et al. 1992) and several clones that expressed hCD14 were selected for analysis. Equivalent numbers of hCD14+ and CD14- 70Z/3 cells were treated with 10 ng/ml and 1 µg/ml LPS for 24 h and each population was stained with an FITC-labeled antibody directed against mIgM and analyzed in the cytofluorograph. Figure 2A shows that the level of mIgM on the surface of hCD14 70Z/3 cells was equal whether they were treated with low or high levels of LPS, whereas the 70Z/3 cells responded only slightly to 10 ng/ml LPS. These data confirm that CD14 expression in 70Z/3 B cells dramatically increases the sensitivity of the cells to LPS.

Fig. 2 A, B Cytofluorometric analysis of membrane IgM expression. Log of fluorescence intensity is plotted on the X-axis and number of cells is plotted on the Y-axis. A 70Z/3 and 70Z/3 hCD14 cells were stimulated with 10 ng/ml or 1 μ g/ml LPS for 24 h, then stained with an antibody directed against mouse Ig heavy chain *m* μ and analyzed by cytofluorometry. (—) unstimulated, (---) 10 ng/ml, (---) 1 μ g/ml) B 1B8 and 1B8 hCD14 cells were stimulated with 10 ng/ml or 1 μ g/ml LPS for 24 h, then stained as above. (—) unstimulated, (---) 10 ng/ml, (---) 1 μ g/ml)



Expression of hCD14 rescued LPS responsiveness in the 1B8 mutant

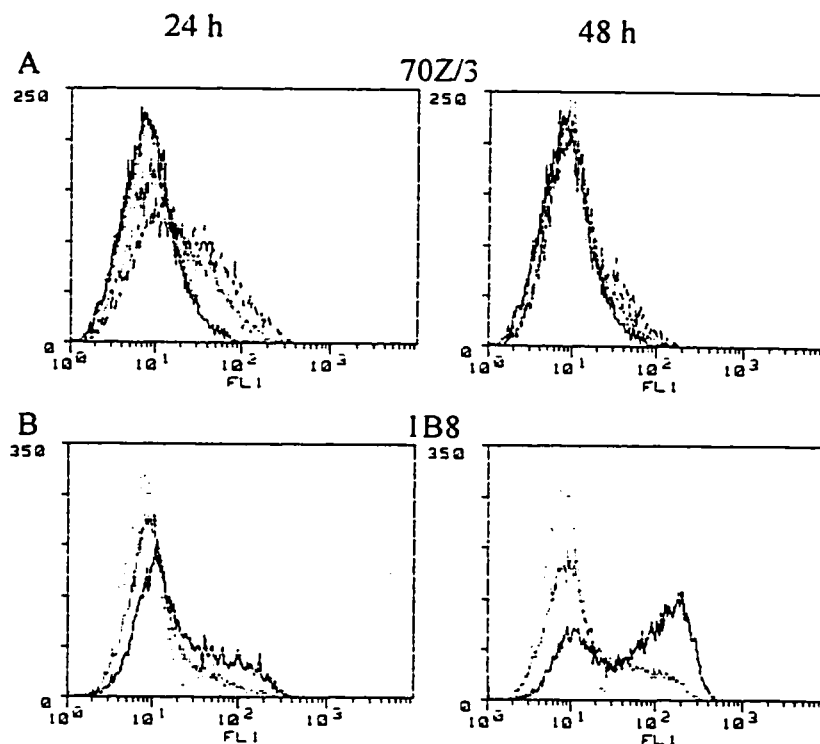
To determine whether expression of hCD14 could restore a wild-type response to LPS in the slow mutant 1B8, the pRc/RSV hCD14 (Lee et al. 1992) was transfected into the mutant cells, and clones were selected as described above. Three clones representing a range of hCD14 expression levels were evaluated to determine whether they now responded as rapidly to LPS treatment as did the wild-type 70Z/3 cells. We treated the 1B8 hCD14 clones with 10 ng/ml or 1 μ g/ml LPS and measured as before the level of expression of mIgM on the surface of each cell in the population. All three clones responded rapidly and robustly to LPS treatment; Fig. 2B shows representative data from one of the clones. In sharp contrast to the 1B8 cells, the 1B8 hCD14 cells had a maximal level of IgM on their surface by 18 h. In addition, these cells responded to 10 ng/ml LPS just as well as the 70Z/3 hCD14 cells. The three 1B8 hCD14 clones were indistinguishable by cytofluorometric and by initial electrophoretic mobility shift assays (EMSA) (described below), so the clone with the highest hCD14 expression was chosen for further analysis. In all cases, target cells were also transfected with pRc/RSV vector alone (Lee et al. 1992) and data not shown). Of course, none of these clones expressed CD14, and their response to LPS was identical to the corresponding untransfected host cells.

The graph depicting the 70Z/3 response to 10 ng/ml LPS resembles the graph for the 1B8 response at 24 h with 1 μ g/ml LPS. However, stimulation of 70Z/3 cells with low doses of LPS for 48 h did not mimic the 1B8 phenotype (Fig. 3A). Thus, the resemblance between the two histograms is superficial.

A higher dose increased the LPS response in 1B8 cells

The correction of the defect in the 1B8 cells by expression of hCD14 could occur by signaling through a CD14 pathway that is distinct from the mutant pathway normally operating in 1B8 cells (Fig. 1, model 3). Alternatively, the two modes of activation might share all of their components, but the ability of the CD14⁺ to capture LPS more efficiently might strongly amplify the usually indolent signal in mutant cells (Fig. 1, model 2). To determine whether an increased signal could overcome the rate-limiting step in 1B8 cells, we stimulated the cells with 1 μ g/ml or 10 μ g/ml LPS for 24 and 48 h. As measured by membrane IgM expression, wild-type 70Z/3 cells responded to the same degree to both 1 μ g/ml and 10 μ g/ml (Sibley et al. 1988). In contrast, 1 μ g/ml LPS did not maximally stimulate the CD14-independent pathway in the 1B8 cells. When treated with 10 μ g/ml LPS, 1B8 cells did increase the amount of mIgM on their surface more rapidly (Fig. 3B).

Fig. 3A, B Cytofluorometric analysis of membrane IgM expression. Log of fluorescence intensity is plotted on the X-axis and number of cells is plotted on the Y-axis. **A** 70Z/3 cells were stimulated for 24 or 48 h with 0, 1, 5, or 10 ng/ml LPS, then stained as above. (— unstimulated, ... 1 ng/ml, - - - 5 ng/ml, 10 ng/ml) **B** IB8 cells were stimulated with 1 μ g/ml and 10 μ g/ml LPS for 24 and 48 h, then stained and analyzed as above. (— unstimulated, 1 μ g/ml - - - 10 μ g/ml)



Kappa protein expression was faster in IB8 hCD14 cells than in IB8 or 70Z/3

Igk gene transcription occurred faster in IB8 hCD14 cells than in IB8 or 70Z/3

A second step in distinguishing the models was to examine in detail the kinetics of activation by LPS in 70Z/3, 70Z/3 hCD14, IB8, and IB8 hCD14 cells. To determine whether the expression of hCD14 had altered the speed, as well as the sensitivity of the LPS response, 70Z/3, IB8, and IB8 hCD14 cells were stimulated with 1 μ g/ml LPS and aliquots were taken at various times after stimulation. The aliquots were promptly stained with FITC antibodies directed against mIgM and the percentage of mIgM⁺ cells determined at the indicated times by fluorometry. The percentage of mIgM⁺ cells was used to compare the responses of each population. Figure 4A shows that the level of mIgM on wild-type cells increased beginning at about 6 h after the initial treatment with LPS but the amount of IgM on the surface of the IB8 cells remained virtually unchanged during the 24 h of the experiment. In contrast, the IB8 hCD14 cells showed increased expression of mIgM by 4 h, 2 h earlier than wild-type 70Z/3 cells, and maintained a higher percentage of fluorescent cells up to 24 h after treatment. Figure 4B tabulates the modal fluorescence of each cell population over the 24-h period sampled. By both measures, the hCD14⁺ cells responded more rapidly to a 1 μ g/ml dose of LPS and were capable of responding to lower levels of LPS.

To determine whether the increase in mIgM was a direct result of an increase in the steady-state level of *Igk* mRNA, 70Z/3, IB8, and IB8 hCD14 cells were stimulated with 1 μ g/ml LPS and aliquots taken at the indicated times. Total RNA was isolated and northern blots prepared and probed to measure the steady-state level of *Igk* and as a control, β -actin mRNA. Figure 5 shows the results from a representative set of blots. The figure was printed to allow visualization of the slight increase in *Igk* mRNA in the IB8 cells. This presentation overexposes the β -actin and *Igk* bands in the other gels. Quantitation plotted in Fig. 5B was determined directly from the northern blots using a phosphor-imager, so this measurement is not affected by the exposure of the film. The steady-state level of *Igk* mRNA increased more rapidly in hCD14 IB8 than in the untransfected 70Z/3 controls. In fact, the steady-state level of *Igk* mRNA was consistently higher in the IB8 hCD14 cells than in 70Z/3 throughout the entire 24 h period of the experiment. As expected, the IB8 cells did not transcribe detectable quantities of *Igk* mRNA until 12 h after LPS treatment, and the level was still very low by 24 h. The kinetics of the increase and magnitude of the mRNA levels correlate with the increased expression of IgM on the surface of the cells. Since the increase in *Igk* mRNA has been shown to result from new transcription in 70Z/3 cells (Nelson et al. 1984),

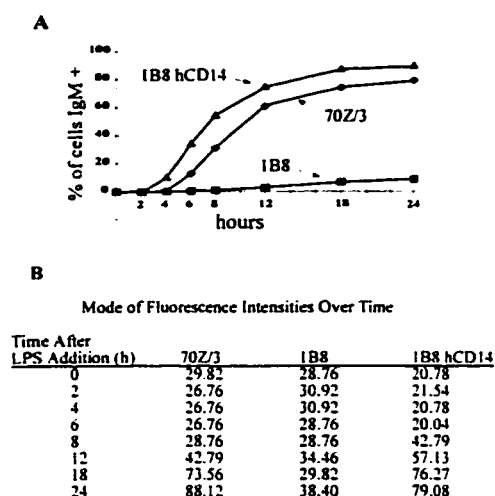


Fig. 4 A, B Time course of membrane IgM expression. A 70Z/3, IB8, and IB8 hCD14 cells were stimulated with 1 μ g/ml LPS; aliquots were taken at various time-points and stained with an antibody directed against mouse Ig heavy chain μ and analyzed by cytofluorometry. The point beyond which 4% of the unstimulated population lay was defined as the threshold and the percentage of cells beyond that point was defined as the fraction positive for mIgM. This mIgM+ fraction was plotted as a function of time. B The mode of the fluorescence for the samples in A

these results suggest that expression of hCD14 in IB8 cells did augment the speed with which LPS stimulated new Igk transcription.

CD14 expression resulted in more rapid nuclear localization of NF- κ B/Rel complexes after LPS stimulation

Translocation of NF- κ B/Rel transcription factors from the cytoplasm to the nucleus is one rapid consequence of LPS treatment in 70Z/3 cells (Sen and Baltimore 1986), and is required for Igk transcription (Rooney et al. 1990). To determine whether NF- κ B/Rel translocation was also occurring more rapidly, hCD14+ and hCD14- 70Z/3 and IB8 cells were treated with 1 μ g/ml LPS for 0, 30 min, 1 h, and 2 h. Nuclear extracts were prepared and the level of NF- κ B/Rel complexes binding specifically to an oligonucleotide containing the κ B site was determined by EMSA. Figure 6A shows that the translocation of NF- κ B/Rel factors occurred much faster in the hCD14+ than in the CD14- cells. The speed of activation in IB8 hCD14 very closely resembled that of 70Z/3 hCD14 and far exceeded the activation observed in IB8 cells. Below each NF- κ B/Rel lane is a second EMSA that measured binding of nuclear factors to κ E3, a constitutive, non-inducible transcription factor (Rhodes et al. 1994). The level of κ E3 was used to judge equivalence of protein concentration and quality of the nuclear extracts.

136

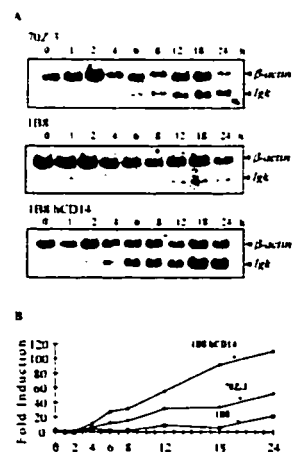


Fig. 5 Analysis of steady state levels of Igk mRNA. 70Z/3, IB8, and IB8 hCD14 cells were stimulated with 1 μ g/ml LPS. Total RNA was prepared from aliquots taken at the indicated timepoints. Northern blots were prepared and the blots were probed using [32 P]-labeled β -actin and Igk mRNA. Each sample was normalized by comparison of the β -actin signal and the fold induction over the unstimulated control was plotted as a function of time

hCD14 expression in IB8 rescued the slow nuclear localization of most, but not all, NF- κ B complexes

Detailed EMSA of 70Z/3 cells reveal several different NF- κ B/Rel complexes, including p50/p65, p65/Rel, and p50/p50 (Liou et al. 1994; Miyamoto et al. 1994). To investigate the composition of the NF- κ B/Rel complexes translocated to the nucleus after LPS stimulation, 70Z/3, 70Z/3 hCD14, IB8, and IB8 hCD14 cells were stimulated with 1 μ g/ml LPS and samples were taken from 0 to 24 h. Figure 6A demonstrates that the mobilization of NF- κ B/Rel complexes into the nuclear fraction was far more rapid in hCD14+ cells. Analysis of extracts taken at longer times (Fig. 6B) revealed that although 70Z/3 took longer to reach its maximum, the levels of the complexes were finally similar to those measured in the hCD14+ cells (the 12 h point was slightly under-loaded). In IB8, levels of the upper band increased slowly but finally reached a level that was indistinguishable from the wild type. The IB8 hCD14 cells, however, reached their maximal level by 1 h (Fig. 6A), far faster than IB8, faster than 70Z/3, and comparable to 70Z/3 hCD14.

Two prominent bands of complexes bind the κ B probe: the upper band mainly composed of p50/p65 heterodimers and the lower band consisting of p50/p50 dimers (Liou et al. 1994; Miyamoto et al. 1994). The level of p50/p50 in the wild-type 70Z/3 cells continued to increase slowly with time so that by 24 h the intensity of the lower band was greater than the upper band (Fig. 6B). Expression of hCD14 in 70Z/3 cells resulted in p50/p50 binding activity that reached its maximum by 4 h after LPS treatment, at a level similar to that observed in 70Z/3 cells. The level of p50/p50 was still increasing by 24 h in the IB8 cells and never

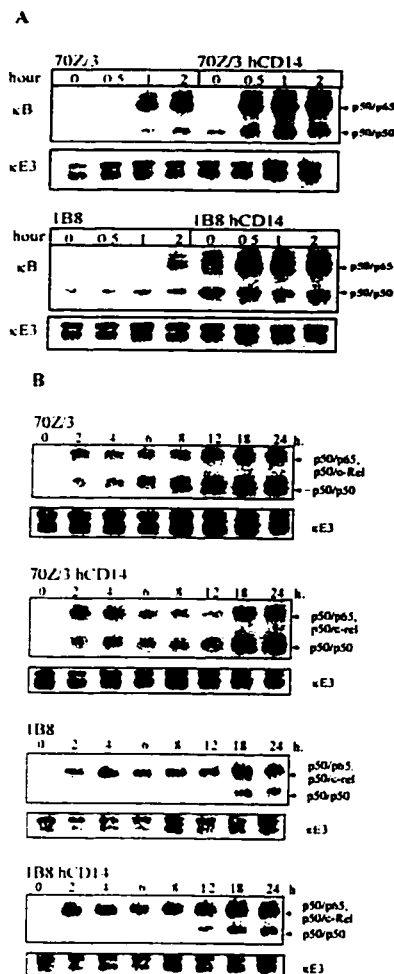


Fig. 6A, B EMSA of NF- κ B complexes in nuclear extracts. 70Z/3, 70Z/3 hCD14, 1B8, and 1B8 hCD14 cells were stimulated with 1 μ g/ml LPS and aliquots were taken at various times. Nuclear extracts were prepared and analyzed by EMSA using a probe containing the Ig κ NF- κ B site. To verify equivalency of quality and total protein, samples were also analyzed by EMSA using a probe containing the κ E3 site which binds a constitutive protein. A 0–2 h of LPS stimulation. B 0–24 h of LPS stimulation

achieved wild-type levels. In contrast to the rapid activation of the other complexes, the p50/p50 EMSA binding activity in 1B8 hCD14 cells was equivalent to that observed in the 1B8 cells; this part of the 1B8 defect was not corrected. This suggests that hCD14 expression does not completely bypass the function that is defective in the 1B8 cells and that the defective component is still an element of the CD14-dependent signaling pathway.

The p50/Rel and p50/p65 complexes are not individually resolved on the standard EMSA. To examine the effect of hCD14 expression on the activation of the p50/Rel, we

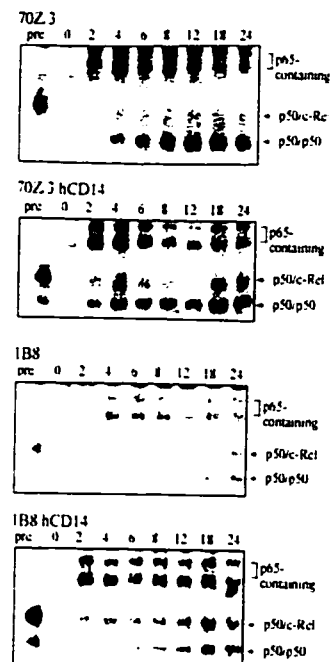


Fig. 7 Supershift EMSA of NF- κ B complexes in nuclear extracts. Nuclear extracts were prepared and analyzed as in Fig. 6 except that an antibody directed against p65 was added to the binding reaction in order to supershift the p65-containing complexes. Lanes marked "pre" received pre-immune serum instead of p65-specific antibody to control for serum effects. Samples were also analyzed by EMSA using a probe containing the κ E3 site which binds a constitutive protein to verify equivalency of quality and total protein. The 70Z/3 \pm gels were run at the same time and have identical exposure times and total protein. The same is true of the 1B8 \pm gels, and the exposure times of the two sets were matched for comparison purposes

treated the binding reactions before the EMSA with a polyclonal antibody directed against p65. All of the NF- κ B/Rel complexes were visible in these super-shifted gels. Figure 7 shows a representative experiment. Analysis of these gels revealed that the 1B8 hCD14 cells localized the p50/p65 and p50/Rel complexes to the nucleus with kinetics equivalent to the 70Z/3 hCD14 cells, but the p50/p50 accumulated far more slowly than in wild type. Quantitative conclusions drawn by comparison between EMSA gels can be misleading due to variations in exposure and signal strength. However, by comparing the strength of different bands within one gel, the distinction becomes clear. In the 70Z/3 cell lines, the p50/p50 band was the most prominent at 24 h. In contrast, both hCD14⁺ and hCD14⁻ 1B8 lines showed equivalent intensities of all bands. In combination with the data in Fig. 6, these data indicate that 1B8 cells have a subtle defect that is revealed by a much lower binding of p50/p50 homodimers to the κ B probe and that the defect is not corrected by hCD14 expression.

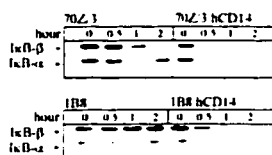


Fig. 8 Analysis of the levels of IκB-α and -β in cytoplasmic extracts. 70Z/3, 70Z/3 hCD14, 1B8, and 1B8 hCD14 cells were stimulated with 1 μg/ml LPS and aliquots were taken at the indicated times. Cytoplasmic extracts were analyzed by western blotting using antibodies directed against IκB-α and IκB-β.

IκB-α and -β degradation occurred more quickly in 1B8 hCD14 than 70Z/3 but more slowly than 70Z/3 hCD14

To examine degradation of the inhibitory IκB proteins, cytoplasmic extracts were prepared at various times after stimulation of the cells with LPS. Those extracts were analyzed by western blots probed with antibodies directed against IκB-α and -β and developed by enhanced chemiluminescence. Although the amount of IκB-α in the 1B8 cell lines appeared to be less than the 70Z/3 lines in this experiment, this was not consistently observed. The blots did consistently show that wild-type 70Z/3 cells degraded nearly all of their IκB-α by 1 h and IκB-β by 2 h, with resynthesis partly restoring the IκB-α by about 2 h. The 70Z/3 hCD14 cells degraded both forms by 30 min and no resynthesis was evident during the 2 h experiment (Fig. 8). The pattern was very different in both lines of 1B8 cells. The 1B8 cells never fully degraded either form of IκB, accounting for the slow nuclear localization of the NF-κB/Rel complexes. On the other hand, the 1B8 hCD14 cells did degrade IκB-α by 30 min, but IκB-β was not completely gone until 1 h after stimulation. The 1B8 hCD14 cells responded faster than 70Z/3 but not as quickly as 70Z/3 hCD14 cells. Thus, when this more sensitive measure was used, it was clear that expression of hCD14 in 1B8 cells has not completely corrected their defect in response to LPS stimulation.

Discussion

The identification of the receptor for LPS and the pathway by which LPS triggers activation of the NF-κB/Rel family of transcription factors in B cells has proved to be a difficult task. The demonstration that CD14 is a high-affinity receptor for LPS on macrophages and monocytes provided one important clue, but B cells do not normally express CD14. One possibility is that the same molecule signals in the absence of CD14 (low sensitivity, as in B cells) and in the presence of CD14 (high sensitivity, as in macrophages and CD14⁺ B cells). On 70Z/3 cells, this second molecular partner could be the B-cell LPS receptor. According to this view, the increased sensitivity in CD14⁺ cells might result from the increased binding of LPS by CD14, and a

cooperative mechanism for signaling through the lower affinity B-cell receptor. Normally in CD14⁺ B cells like 70Z/3 or in macrophages in which the hCD14 molecule is inactivated, the signaling receptor would be limited in sensitivity by its lower capacity for binding LPS. This would be analogous to the situation observed in the nerve growth factor receptor family (Barker and Murphy 1992; Bothwell 1995; Chao and Hempstead 1995). Alternatively, B cells might have a molecular partner distinct from the "normal" B-cell-signaling receptor, one that signals only when it interacts with the LPS-CD14.

Our experiments were designed to distinguish these latter two possibilities. We knew that the 1B8 defect affects the activation pathway upstream of NF-κB/Rel activation (Ostrowski et al. 1991; Rooney et al. 1990). We reasoned that if CD14 functioned mainly as a high-affinity concentration device that signaled through the low-affinity B-cell receptor, the expression of CD14 in the mutant cells should not correct the slow response to LPS. On the other hand, if CD14 interacts with a molecule that responds to LPS only when hCD14 is present, the hCD14 signaling pathway might not include the defective component and the 1B8 defect might be completely bypassed. The fact that expression of hCD14 dramatically augmented the speed of the response to LPS initially seemed to support the idea that the signal transduction bypassed the 1B8 defect. However, several qualitative differences were identified between the hCD14⁺ and hCD14⁻ 1B8 and 70Z/3 cells. For example, the degradation of IκB-β was not fully rescued by the expression of hCD14 in the 1B8 cells. While the degradation was faster than wild type, it did not achieve the speed of a hCD14⁺ wild-type cell. This observation suggests that the signaling component that is mutant in 1B8 cells is also a component of the signaling pathway activated by hCD14.

The diversity of the complexes in the NF-κB/Rel family and differences in the speed and activation of their nuclear localization have made it difficult to assign distinct functions to each complex (Feuillard et al. 1996; Li et al. 1993; Liou et al. 1994; Miyamoto et al. 1994). For this reason, we were especially interested in the possibility that there might be differences in the activation of particular NF-κB/Rel dimers when the 70Z/3 and 1B8 cells were compared with their hCD14⁺ counterparts. The activation of p50/p50 homodimers was the only consistent difference among the various NF-κB/Rel complexes observed in the nuclear fraction. In 70Z/3 cells, this complex was activated slowly during the LPS response, and the expression of hCD14 clearly accelerated this process. In contrast, LPS treatment of either 1B8 or 1B8 hCD14 cells evoked a minimal increase in the number of the p50/p50 complexes measured in the nuclear fraction by the EMSA. The role of the p50/p50 complexes in transcriptional control has been particularly obscure, because the p50 subunit lacks an activation domain (Baldwin 1996; Liou and Baltimore 1993). The fact that vigorous *Igk* transcription was observed in the 1B8 hCD14 cells in the absence of the normal augmentation of p50/p50 suggests that the p50 homodimers are not involved in this facet of the LPS response in 70Z/3 cells. The expression of hCD14 did not change the patterns of the

other three NF- κ B/Rel complexes that we observed after LPS treatment of either hCD14⁺ or hCD14⁺ 70Z/3 and IB8.

Although the defect in the IB8 cells has not yet been identified, we did observe that these cells differ in their dose response to LPS. In wild-type 70Z/3 cells, a maximal response was evoked by treatment with 1 μ g/ml, but the IB8 cells continued to augment their response beyond 1 μ g/ml. This suggests that an amplification of the signal in the normal B cell pathway can partly override the defect in IB8. The hCD14 molecule could rescue the IB8 defect by augmenting the signal and overcoming the rate-limiting step that blocks the response to LPS. If this were the case, then our data support a model in which the hCD14 molecule acts as a high-affinity receptor for LPS, but signals through the same pathway as that normally used by LPS to activate B cells. The subtle qualitative differences between hCD14⁺ IB8 and 70Z/3 cells in the degradation of I κ B and activation of the p50/p50 complexes are also consistent with this model. Our observations are consistent with a defect in one of the kinases that initiate degradation of the I κ B family members (Chen et al. 1996; DiDonato et al. 1997; Israel 1997). Another exciting possibility is that the defect in IB8 could be in the low-affinity B-cell receptor itself. Examination of hCD14⁺ cells for molecules that interact directly with the transfected hCD14 and comparison of cell surface molecules on the IB8 cells that bind LPS poorly in relation to the comparable molecule in wild-type 70Z/3 might be a productive route for finally identifying the LPS receptor in B cells.

As our understanding of intracellular signaling has matured, it has become clear that we are not examining linear pathways, but complex interacting networks. The diversity of the NF- κ B/Rel family members and their activation patterns provide an excellent example of this complexity. Analysis of a well-defined input and the comparison of responses in mutant and normally responsive cells is one approach that can begin to allow us to unravel this network.

Acknowledgments We would like to thank Dr. Jjiang-Dwan Lee and Dr. Richard Ulevitch for providing the pRc/RSV hCD14 construct, Dr. Jean Campbell for her technical assistance, and Dr. Karol Bomsztyk for his thoughtful review and suggestions for improvements in the manuscript. We also thank Dr. Sankar Ghosh and Dr. Karol Bomsztyk for providing the I κ B- β and p65 antibodies, respectively. V.H.B. was supported by NIH training grant GM 67-1173 to the Department of Genetics. The authors will soon stop maintaining the cell lines described in this paper, and would like to distribute them to any researchers who might be interested in using them. The cells can be obtained by contacting C.H.S. at the address indicated.

References

- Bauerle, P. A. and Baltimore, D. I kappa B: a specific inhibitor of the NF-kappa B transcription factor. *Science* 242: 540-546, 1988
- Bauerle, P. A. and Henkel, T. Function and activation of NF-kappa B in the immune system. *Annu Rev Immunol* 12: 141-179, 1994
- Baldwin, A. S., Jr. The NF-kappa B and I kappa B proteins: new discoveries and insights. *Annu Rev Immunol* 14: 649-681, 1996
- Barker, P. A. and Murphy, R. A. The nerve growth factor receptor: a multicomponent system that mediates the actions of the neurotrophin family of proteins. *Mol Cell Biochem* 110: 1-15, 1992
- Beatty, C. D., Franklin, T. L., Uehara, Y., and Wilson, C. B. Lipopolysaccharide-induced cytokine production in human monocytes: role of tyrosine phosphorylation in transmembrane signal transduction. *Eur J Immunol* 24: 1278-1284, 1994
- Beg, A. A. and Baldwin, A. S. Jr. Activation of multiple NF-kappa B/Rel DNA-binding complexes by tumor necrosis factor. *Oncogene* 9: 1487-1492, 1994
- Bomsztyk, K., Toivola, B., Emery, D. W., Rooney, J. W., Dower, S. K., Rachie, N. A. and Sibley, C. H. Role of cAMP in interleukin-1-induced kappa light chain gene expression in murine B cell line. *J Biol Chem* 265: 9413-9417, 1990
- Bothwell, M. Functional interactions of neurotrophins and neurotrophin receptors. *Annu Rev Neurosci* 13: 223-253, 1995
- Chao, M. V. and Hempstead, B. L. p75 and Trk: a two-receptor system. *Trends Neurosci* 18: 321-326, 1995
- Chen, T. Y., Bright, S. W., Pace, J. L., and Russell, S. W. Induction of macrophage-mediated tumor cytotoxicity by a hamster monoclonal antibody with specificity for lipopolysaccharide receptor. *J Immunol* 145: 8-12, 1990
- Chen, Z., Hagler, J., Palombella, V. J., Melandri, F., Scherer, D., Ballard, D., and Maniatis, T. Signal-induced site-specific phosphorylation targets I kappa B alpha to the ubiquitin-proteasome pathway. *Genes Dev* 9: 1586-1597, 1995
- Chen, Z. J., Parent, L., and Maniatis, T. Site-specific phosphorylation of I kappa B alpha by a novel ubiquitination-dependent protein kinase activity. *Cell* 84: 853-862, 1996
- Couturier, C., Haefliger Cavaillon, N., Caroff, M., and Kazatchkine, M. D. Binding sites for endotoxins (lipopolysaccharides) on human monocytes. *J Immunol* 147: 1899-1904, 1991
- Cox, R. A. The use of guanidinium chloride in the isolation of nucleic acids. *Methods Enzymol* 12b: 120-129, 1968
- DiDonato, J. A., Hayakawa, M., Rothwarf, D. M., Zandi, E., and Karin, M. A cytokine-responsive I kappa B kinase that activates the transcription factor NF-kappa B. *Nature* 388: 548-554, 1997
- Dignam, J. D., Lebovitz, R. M., and Roeder, R. G. Accurate transcription initiation by RNA polymerase II in a soluble extract from isolated mammalian nuclei. *Nucleic Acids Res* 11: 1475-1489, 1983
- Feuillard, J., Komer, M., Israel, A., Vassy, J., and Raphael, M. Differential nuclear localization of p50, p52, and RelB proteins in human accessory cells of the immune response in situ. *Eur J Immunol* 26: 2547-2551, 1996
- Ghosh, S. and Baltimore, D. Activation in vitro of NF-kappa B by phosphorylation of its inhibitor I kappa B. *Nature* 344: 678-682, 1990
- Golenbock, D. T., Hampton, R. Y., Qureshi, N., and Takayama, K. Lipid A-like molecules that antagonize the effects of endotoxins on human monocytes. *J Biol Chem* 266: 19490-19498, 1991
- Golenbock, D. T., Liu, Y., Millham, F. H., Freeman, M. W., and Zoeller, R. A. Surface expression of human CD14 in Chinese hamster ovary fibroblasts imparts macrophage-like responsiveness to bacterial endotoxin. *J Biol Chem* 268: 22055-22059, 1993
- Israel, A. Signal transduction - I kappa B kinase all zipped up. *Nature* 388: 519-521, 1997
- Kirkland, T. N., Finley, F., Leturcq, D., Moriarty, A., Lee, J. D., Ulevitch, R. J., and Tobias, P. S. Analysis of lipopolysaccharide binding by CD14. *J Biol Chem* 268: 24818-24823, 1993
- Labarca, C. and Paigen, K. mRNA-directed synthesis of catalytically active mouse beta-glucuronidase in *Xenopus* oocytes. *Proc Natl Acad Sci USA* 74: 4462-4465, 1977
- Lee, J. D., Kato, K., Tobias, P. S., Kirkland, T. N., and Ulevitch, R. J. Transfection of CD14 into 70Z/3 cells dramatically enhances the sensitivity to complexes of lipopolysaccharide (LPS) and LPS binding protein. *J Exp Med* 175: 1697-1705, 1992
- Lee, J. D., Kravchenko, V., Kirkland, T. N., Han, J., Mackman, N., Moriarty, A., Leturcq, D., Tobias, P. S., and Ulevitch, R. J. Glycosyl-phosphatidylinositol-anchored or integral membrane forms of CD14 mediate identical cellular responses to endotoxin. *Proc Natl Acad Sci USA* 90: 9930-9934, 1993

- Li, C. C., Ruscetti, F. W., Rice, N. R., Chen, E., Yang, N. S., Mikovits, J., and Longo, D. L. Differential expression of Rel family members in human T-cell leukemia virus type I-infected cells: transcriptional activation of c-rel by Tax protein. *J Virol* 67: 4205-4213, 1993.
- Liou, H. C., and Baltimore, D. Regulation of the NF-kappa B/rel transcription factor and I kappa B inhibitor system. *Curr Opin Cell Biol* 5: 477-487, 1993.
- Liou, H.-C., Sha, W. C., Scott, M. L., and Baltimore, D. Sequential induction of NF-kB/Rel family proteins during B-cell terminal differentiation. *Mol Cell Biol* 14: 5349-5359, 1994.
- Mains, P. E. and Sibley, C. H. Control of IgM synthesis in the murine pre-B cell line, 70Z/3. *J Immunol* 128: 1664-1670, 1982.
- Mains, P. E. and Sibley, C. H. LPS-nonresponsive variants of mouse B cell lymphoma, 70Z/3: isolation and characterization. *Somatic Cell Genet* 9: 699-720, 1983.
- Miller, C. L., Feldhaus, A. L., Rooney, J. W., Rhodes, L. D., Sibley, C. H., and Singh, H. Regulation and a possible stage-specific function of Oct-2 during pre-B-cell differentiation. *Mol Cell Biol* 11: 4885-4894, 1991.
- Miyamoto, S., Schmitt, M. J., and Verma, I. M. Qualitative changes in the subunit composition of kappa B-binding complexes during murine B-cell differentiation. *Proc Natl Acad Sci USA* 91: 5056-5060, 1994.
- Morrison, D. C., and Ryan, J. L. Endotoxins and disease mechanisms. *Annu Rev Med* 38: 417-432, 1987.
- Morrison, D. C., Dinarello, C. A., Munford, R. S., Natanson, C., Danner, R., Pollack, M., Spitzer, J. J., Ulevitch, R. J., Vogel, S. N., and McSweeney, E. Current status of bacterial endotoxins. *ASM News* 60: 479-484, 1994.
- Nelson, K. J., Mather, E. L., and Perry, R. P. Lipopolysaccharide-induced transcription of the kappa immunoglobulin locus occurs on both alleles and is independent of methylation status. *Nucleic Acids Res* 12: 1911-1923, 1984.
- Ostrowski, J., Sims, J. E., Sibley, C. H., Valentine, M. A., Dower, S. K., Meier, K. E., and Bomsztyk, K. A serine/threonine kinase activity is closely associated with a 65-kDa phosphoprotein specifically recognized by the kappa B enhancer element. *J Biol Chem* 266: 12722-12733, 1991.
- Paige, C. J., Kincade, P. W., and Ralph, P. Murine B cell leukemia line with inducible surface immunoglobulin expression. *J Immunol* 121: 641-647, 1978.
- Paige, C. J., Kincade, P. W., and Ralph, P. Independent control of immunoglobulin heavy and light chain expression in a murine pre-B-cell line. *Nature* 292: 631-633, 1981.
- Palombella, V. J., Rando, O. J., Goldberg, A. L., and Maniatis, T. The ubiquitin-proteasome pathway is required for processing the NF-kappa B1 precursor protein and the activation of NF-kappa B. *Cell* 78: 773-785, 1994.
- Raetz, C. R. Biochemistry of endotoxins. *Annu Rev Biochem* 59: 129-170, 1990.
- Raetz, C. R., Ulevitch, R. J., Wright, S. D., Sibley, C. H., Ding, A., and Nathan, C. F. Gram-negative endotoxin: an extraordinary lipid with profound effects on eukaryotic signal transduction. *FASEB J* 5: 2652-2660, 1991.
- Rhodes, L. D., Paull, A. T., and Sibley, C. H. Two different IFN-gamma nonresponsive variants derived from the B-cell lymphoma 70Z/3. *Immunogenetics* 40: 199-209, 1994.
- Rietschel, E. T. and Brade, H. Bacterial endotoxins. *Sci Am* 267: 54-61, 1992.
- Rooney, J. W., Emery, D. W., and Sibley, C. H. 1.3E2, a variant of the B lymphoma 70Z/3, defective in activation of NF-kappa B and OTF-2. *Immunogenetics* 31: 73-78, 1990a.
- Rooney, J. W., Emery, D. W., and Sibley, C. H. Slow response variant of the B lymphoma 70Z/3 defective in LPS activation of NF-kappa B. *Immunogenetics* 31: 65-72, 1990b.
- Schneppenheim, R. and Rautenberg, P. A luminescence Western blot with enhanced sensitivity for antibodies to human immunodeficiency virus. *Eur J Clin Microbiol* 6: 49-51, 1987.
- Schouten, G. J., Versteeg, A. C. O., Whiteside, S. T., Israel, A., Toebes, M., Dorsman, J. C., van der Eb, A. J., and Zanema, A. I kappa B alpha is a target for the mitogen-activated 90 kDa ribosomal S6 kinase. *EMBO J* 16: 3133-3144, 1997.
- Schumann, R. R. Function of lipopolysaccharide (LPS)-binding protein (LBP) and CD14, the receptor for LPS/LBP complexes: a short review. *Res Immunol* 143: 11-15, 1992.
- Sen, R. and Baltimore, D. Inducibility of kappa immunoglobulin enhancer-binding protein NF-kappa B by a posttranslational mechanism. *Cell* 47: 921-928, 1986.
- Sibley, C. H., Terry, A., and Raetz, C. R. Induction of kappa light chain synthesis in 70Z/3 B lymphoma cells by chemically defined lipid A precursors. *J Biol Chem* 263: 5098-5103, 1988.
- Thompson, J. E., Phillips, R. J., Erdjument-Bromage, H., Tempst, P., and Ghosh, S. I kappa B-beta regulates the persistent response in a biphasic activation of NF-kappa B. *Cell* 80: 573-582, 1995.
- Ulevitch, R. J., Dunn, D. L., Fink, M. P., and Taylor, C. E. Endotoxin-related intracellular pathways: implications for therapeutic intervention. *Shock* 6: 1-2, 1996.
- Weeks, R. S. and Sibley, C. H. Molecular analysis of immunoglobulin expression in variants of murine B lymphoma, 70Z/3. *Somat Cell Mol Genet* 13: 205-219, 1987.
- Weeks, R. S. and Sibley, C. H. Inducible expression of transfected kappa light chains by lipopolysaccharide and IFN-gamma in the murine B lymphoma, 70Z/3. *J Immunol* 140: 1312-1320, 1988.
- Weeks, R. S., Mains, P. E., and Sibley, C. H. Comparison of membrane IgM expression in the murine B cell lymphoma 70Z/3 treated with LPS or supernatant containing T cell factors. *J Immunol* 133: 351-358, 1984.
- Weinstein, S. L., June, C. H., and DeFranco, A. L. Lipopolysaccharide-induced protein tyrosine phosphorylation in human macrophages is mediated by CD14. *J Immunol* 151: 3829-3838, 1993.
- Wright, S. D., Ramos, R. A., Tobias, P. S., Ulevitch, R. J., and Mathison, J. C. CD14, a receptor for complexes of lipopolysaccharide (LPS) and LPS binding protein [see comments]. *Science* 249: 1431-1433, 1990.

VITA

Victoria Hertle Brophy

University of Washington

1998

EDUCATION Ph.D., Genetics, University of Washington, Seattle, WA. (1998)
B.A., Genetics, University of California, Berkeley, CA (1990)

EXPERTISE

Scientific Skills

Protein Analysis: *In vitro* Enzyme Assays, Affinity Chromatography, Immunoprecipitation, *In Vitro* Kinase Assays, Western blots, Electrophoretic Mobility Shift Assays

Cell Culture: Mammalian and Yeast cells

DNA Analysis: PCR, subcloning, DNA cycle sequencing, restriction analysis

RNA Analysis: Northern blots

Computer Skills: Microsoft Windows OS, Macintosh OS, Microsoft Office, Macromedia Freehand, Molecular Dynamics ImageQuant, Internet, Medline/PubMed, minor repairs (PC).

Supervisory Skills

Trained undergraduate students, technicians, and junior graduate students in basic laboratory skills and cell culture. Supervised an undergraduate honors research project and a postbacclaureate volunteer.

Communication Skills

Experienced at giving oral and poster presentations at national and international conferences. Have written several publications.

EXPERIENCE

1993 - present

Graduate research assistant with Dr. Carol Hopkins Sibley, Dept. of Genetics, University of Washington, Seattle, WA. Developed model system in yeast to identify drugs for inhibition of the DHFR of the human parasite *Cryptosporidium parvum*. Purified and characterized kinetic properties of two versions of *C. parvum* DHFR. Studied the signaling pathway involved in murine cell response to lipopolysaccharide.

1990 - 1992

Chemist I/II at Microgenics Corporation, Concord, CA. Developed immunochemistry assays for use in clinical laboratories to monitor ferritin and phenytoin levels.

1989 - 1990

Undergraduate honors research with Dr. Gunther Stent, Dept. of Molecular and Cellular Biology, University of California at Berkeley, Berkeley, CA. Maintained hybridoma cell line and examined the antibodies for reactivity to leech acetylcholine receptor.

6/89 - 8/89

Volunteer with Dr. Mina Bissell, Lawrence Berkeley Laboratory, Berkeley, CA. Stained chick embryo sections for presence of Rous Sarcoma Virus.

1987 - 1990

Lab helper with Dr. Gunther Stent, Dept. of Molecular and Cellular Biology, University of California at Berkeley, Berkeley, CA. Prepared solutions, ordered supplies, maintained leech and turtle colonies, supervised and trained undergraduates.

HONORS

4/93

National Science Foundation Fellowship Honorary Mention

PUBLICATIONS

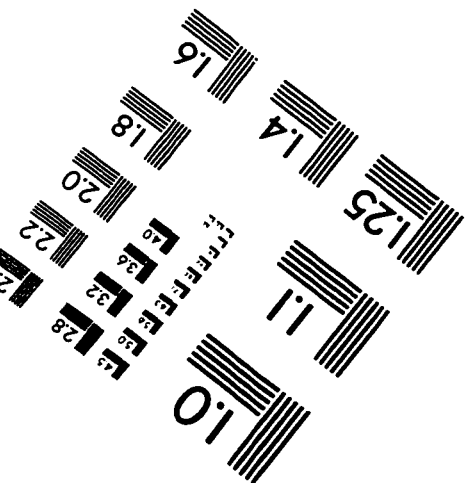
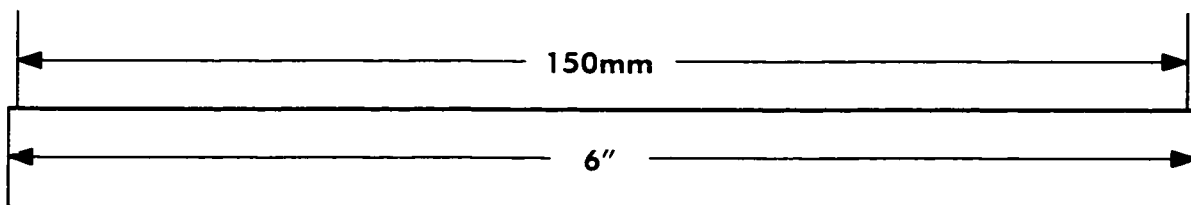
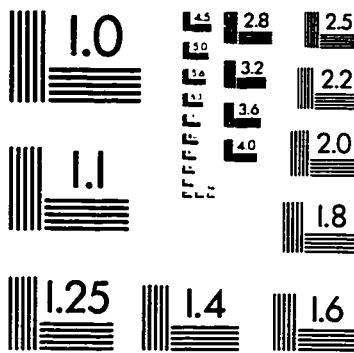
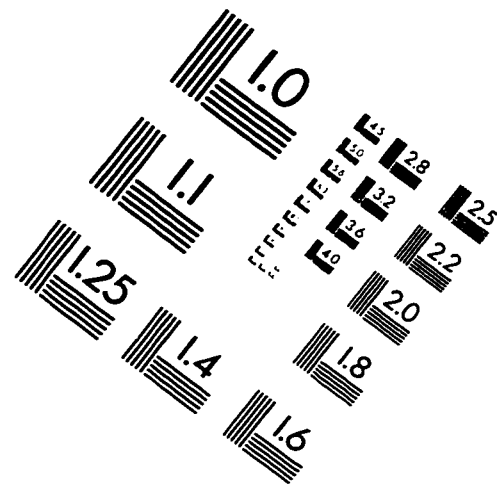
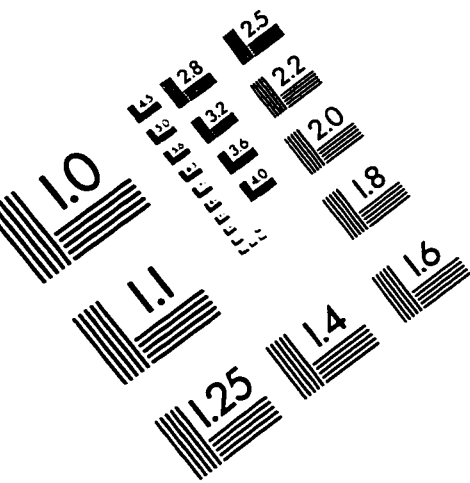
1. Brophy, V. H. and Sibley, C. H. (1998) "Expression of human CD14 rescues LPS response in the 70Z/3 B Lymphoma Mutant 1B8." Immunogenetics 47: 196-205.
2. Sibley, C. H., Brophy, V. H., Cheesman, S., Hamilton, K. L., Hankins, E. G., Wooden, J. M., and Kilbey, B. (1997). "Yeast as a model system to study drugs effective against apicomplexan proteins." Methods 13(2): 190-207.

3. Brophy, V. H., Vasquez, J., Nelson, R. G., Rosowski, A. and Sibley, C. H.. "A rapid screen for inhibitors of the *Cryptosporidium parvum* dihydrofolate reductase (DHFR) by expression in the yeast *Saccharomyces cerevisiae*." Manuscript in preparation.
4. Brophy, V. H. and Sibley, C. H. "Comparison of the *Cryptosporidium parvum* DHFR as a bifunctional and monofunctional enzyme." Manuscript in preparation.
5. Morton, T., Vannucci, S., Murakami, J., Hertle, V., Davoudzadeh, F., Engel, D., Kaspar, P., Coty, W., Loor, R., and Khanna, P.. (1992) "A Homogenous Enzyme Immunoassay for Phenytoin (CEDIA) and Application on the Hitachi 704." Recent Developments in Therapeutic Drug Monitoring and Clinical Toxicology (Irving Sunshine, ed.) Marcel Dekker Inc. Palo Alto.

ABSTRACTS

1. Brophy, V.H. and Sibley, C.H. (1998). "Comparison of *Cryptosporidium parvum* DHFR as a bifunctional and monofunctional enzyme." Oral presentation, Seattle Protozoology Meeting, Seattle, WA.
2. Brophy, V.H., Vasquez, J.R., Nelson, R.G., and Sibley, C.H. (1997). "Expression of *Cryptosporidium parvum* dihydrofolate reductase (DHFR) in the yeast *Saccharomyces cerevisiae*." Poster presentation. Molecular Parasitology Meeting, Woods Hole, MA.
3. Hertle, V.F., Sibley, C.H. (1995). "Expression of human CD14 rescues LPS response in the 70Z/3 B lymphoma mutant 1B8." Poster presentation. International Congress of Immunology Meeting, San Francisco, CA
4. Shindelman, J., Singh, H., Hertle, V., Davoudzadeh, D., Lingenfelter, D., Loor, R., Khanna, P. (1992) "Homogenous enzyme immunoassay for measurement of human ferritin using recombinant enzyme fragments" Poster presentation. American Association of Clinical Chemistry Meeting.

IMAGE EVALUATION TEST TARGET (QA-3)



APPLIED IMAGE, Inc
1653 East Main Street
Rochester, NY 14609 USA
Phone: 716/482-0300
Fax: 716/288-5989

© 1993, Applied Image, Inc., All Rights Reserved

